INTEGRATED IMPACT ASSESSMENT OF CLIMATE CHANGE ON HYDROLOGY OF THE XEDONE RIVER BASIN, LAO PDR

Bounhieng Vilaysane

2015

INTEGRATED IMPACT ASSESSMENT OF CLIMATE CHANGE ON HYDROLOGY OF THE XEDONE RIVER BASIN, LAO PDR

(ラオス国セドン川における水文への気候変化の影響に関する統合的評価手法に関する研究)

by

Bounhieng Vilaysane

A dissertation
Submitted in partial fulfillment of the requirements for the
Degree of Doctor of Engineering

Department of Civil and Earth Resources Engineering
Kyoto University, Japan

December 2015

~ Thank you very much! ~

Acknowledgements

To complete my PhD dissertation, I was most fortunate to count on the help of the many special people I would like to acknowledge.

Firstly, I would like to express my sincere gratitude and appreciation to my supervisor, Professor Kaoru Takara, who accepted me as his student and without him this time in Japan would not be possible. Prof. Takara is a true gentleman and provided me with continuous support, trust a great laboratory and many opportunities for international experience and further learning. He is highly regarded by other lecturers. I also learnt much from his lesson and open mind. In addition, I also extend my gratitude to my sub-supervisors Professor Yasuto Tachikawa and Professor Tetsuya Sumi for their kind suggestions and comments on my research.

I would also like to give my greatest appreciation to Associate Professor Takahiro Sayama for his direct assistance and constructive suggestions and guidance to the improvement of my research. He gave me many suggestions during this research and my laboratory work.

I am also grateful to Associate Professor of GCOE-ARS Ishihara Masahito, Professor Bin He for their help with laboratory work as well as encouragement, and continuous discussions and support during my research. Special mention to Dr. PingPing Luo for the stimulating about the research and for help in every time during my stay in Japan.

I wish to express my thanks to the secretaries of Takara Laboratory and secretaries of the GCOE-ARS program. Highest gratitude is towards Ms Sono Inoue, Ms Yoko Yonekawa, Ms Mayumi Nishimura, Ms Kaori Saidera and Ms Saho Matsuda for their kind and excellent assistance and administrative tasks for me and the other students of Takara Laboratory.

I express my thank to colleagues in my laboratory for helping and grateful friendship during my study: Dr. Apip, Dr. Akpabio Emmanuel Matthew, Dr. Maja Ostric, Dr. Duan Weili, Dr. Nor Eliza Binti Alias, Dr. Teramoto Tomoko, Dr. Dang Quang Khang, Mr. Masato Kato, Mr. Nobuhiko Sawai, Ms. Maya Kusajima, Ms. EunBi Kang, Ms. YongA Shing, Mr. Masaki Azuma, Mr. Toshiharu Sasaki, Mr Shota Kurokawa and Mr. Maochuan Hu, Mr. Han Xue, Mr. Josko Troselj, Mr. Hendy Setiawan, Mr. Pham Van Tien, Mr. Doan Huy Loi, Mr. Adnan Arutyunov, Mr. Tsukawa Goto, Ms Yongxue Shi, Ms. Khai Lin

Chong, Ms. Eva Mia Siska, Mrs. Pham Hong Nga, and Ms Jamila Rafabi.

I would like to express my gratitude to the agencies of which financial support allowed me to conduct this research. The Asian University Network/Southeast Asia Engineering Education Development Network (AUN/SEED-Net) and Japan International Cooperation Agency (JICA), for providing the scholarship for my studies and accommodation in Japan. The GCOE Program "Sustainability/Survivability Science for a Resilient Society Adaptable to Extreme Weather Condition"(GCOE-ARS) for financial support during field research attendances. Acknowledgements are also for the Wakate fund and Kyoto University fund for the internships and international scientific events.

I also would like to thank the Mekong River Commission and the Department Hydrology of Lao PDR for their providing data used in this study, as well as the staff of Water Resource Department of Lao PDR for several generous suggestions and cooperation.

Finally, I would like to thank my family for their always support me during study in Japan. I especially thank my parents, uncles and brothers for offering their invaluable love, encouragement and understanding. That is a significant piece of encouragement from them to make me have been successful in my work.

DPRI, Kyoto University, Uji, December 2015

Abstract

The Xedone River Basin is a sub-basin of the Mekong River Basin. The main agricultural activity of this basin is a rice cropping and vegetables has been growing. Agriculture is the main sector of irrigated area, demand water, increasing due to more active irrigation, also over the year's rapid growth in population, urbanization and changes in economic and social activities have resulted in increased, but the catchment discharge on springs and streams are decreasing day by day. The Xedone River Basin is occasionally inundated because of Typhoon during rainy season. Extreme heavy rainfall has frequently been observed in the area, causing floods in lower Xedone River Basin. Further, the rainfall is much variable in every year but the intensity of rainfall is high. This is very common in the area of southern Laos. Therefore, the main purpose of this thesis is to evaluate the climate change on hydrology of the Xedone River Basin in Lao PDR by using data driven and modeling approaches.

In Chapter 2, the trend of the annual and season precipitation and temperature in the Xedone River Basin, Lao PDR was analyzed by using Mann-Kendall test and Inverse Distance Weighting (IDW) interpolation method in GIS software. The objective of the analysis was to find the impact of climate change and attempt to discuss a relationship with the recent increase of natural disasters. The precipitation increased trend (annual daily maximum etc.) was found in the southeastern part of the Xedone River Basin at Nikhom34 station. The annual decreased trend precipitation associated to drought risk was also found in the middle part of the Xedone River Basin at the LaoNgam station. The results of the analysis provide important information for water resource management in the region.

In Chapter 3, SWAT model was successfully calibrated and validated in the Xedone River Basin by using an application algorithm called SUFI-2. Then the sensitivity analysis of the model showed that the flow is sensitive not only to parameters, but also to the HRU delineation thresholds relate to sub-basin discretization. The results suggested that 230 HRUs are appropriate in the whole basin. The SUFI-2 algorithm performed well adjusted with simulated flows in the Xedone River Basin. The model was calibrated and validated in the two periods respectively: 1993-2000 and 2001-2008. The results of daily simulation values of R^2 and NSE were 0.821 and 0.819 respectively during the calibration period, and 0.732 and 0.707 respectively during the validation period. Results of monthly simulation

R^2 and NSE are 0.927 and 0.925 respectively during the calibration period, and 0.910 and 0.856 respectively during the validation period. The SWAT model produced good simulation results of daily and monthly time steps, which are useful for water resources management in this basin. The calibrated model can be used for further analysis of the effect of climate and land use changes as well as other different management scenarios on river discharge.

In Chapter 4, the calibrated model was run with climate change scenarios proposed by the Mekong River Commission (MRC). The three climate change scenarios were considered for running the model for the period of 1993-2008 with climate change factors of GFDL2030, GISS2030, and IPSL2030 to project surface runoff for the period of year 2030. Different institutes researched climate change factors. With the result of IPSL2030, flows in the dry season (Feb-May) becomes lower than the baseline while in the end of the rainy season is beyond the baseline. The flows of climate change scenarios generated more than 400 m^3/s for months in July, August and September baseline at Souvannakhili station. The reason for the high peak flow during these months that is the southwest monsoon normally affects the catchments from mid of May to early October. It is predominant when atmospheric pressure is low over Laos and causes heavy rainfall. The extreme change was observed with the scenario of GISS 2030, which results in high volume monthly runoff, increase the duration of the high monthly runoff prolongs the high runoff season until the first week of September. The model simulation with the climate change scenarios should be used for better information for future studies.

Overall, this thesis focused on the climate change impacts on hydrology in the Xedone River Basin Lao PDR. After trend analysis of precipitation and temperature in the Xedone River Basin, it carried out calibration and validation of river discharge. So over the subsequent Chapters, the thesis just focused on the climate change scenarios to project surface runoff for the period of year 2030 in the Xedone River Basin. The results obtained in this thesis enhance the knowledge of climate change impacts on hydrology in Lao PDR. Furthermore, research provides useful information for the planning of dam construction and flood disaster risk management, which are vital for the sustainable development of the country.

Contents

List of Tables

List of Figures

Chapter 1 Introduction

1.1 Background

Climate change is one of the most important factors for the available water resources. Water is the most precious and prime natural resource and a major constituent of all known forms of living matter on the planet earth. It is the single most important requirement for life. It is probably the only natural resource to touch all aspects of human civilizations-from agriculture and industrial development to the cultural and religious values embedded in society. Over the year's rapid growth in population, urbanization and industrialization and changes in economic and social activities have resulted in increased and diversified demand of water. As the quantity of available water has remained constant, water has progressively emerged as the most important national and international issues. So there are needed to analyze the climate change and simulate the runoff with reasonable accuracy by data driven and modeling approaches.

The Xedone River Basin is one of the major tributaries of the Mekong River Basin, which has created livelihood and joy to ethnic-tribes of locals for a long time though there is a high rate of poverty in this area. The Xedone River Basin has rich land, water, forest, biodiversity and other natural resource. The use of water, land, forest and related natural resources for economic development are not sustainable due to poor management and inadequate practices. The loss of forest cover has been reported as very high in this basin.

The climate in the area is characterized by two distinct seasons: a rainy season (May to October) and a dry season: (November to April). The area is influenced by the tropical monsoons the south-west monsoon reverses its maximum activity, especially on the windward side. The maximum and minimum temperatures at Khongxedon station are range from 29.8 to 34.8^{o}c and 18 to 25.6^{o}c, respectively (1991-2005) except for Bolaven plateau at the Nikhom34 station ranging from 23.5 to 26.2 ^{o}c and 6.6 to 16.4^{o}c respectively.

The Xedone River Basin is occasionally inundated because of typhoons during rainy seasons. Extremely heavy rainfall is the cause of floods in the lower part of the Xedone River Basin. Furthermore, the intensity of rainfall can be very high. This is very common in the southern part of Laos.

Water resources of the upper portion of the Xedone River Basin in Saravanne province are mainly used for agricultural purposes. Fertilizers and pesticides have contaminated the river, which flows downstream to Champasack Province. In addition, slash-and-burn practices have diminished the forest cover in the basin, resulting in frequent flooding in Champasack during the rainy seasons. Limited livelihood opportunities and poor information among communities have perpetuated these practices.

In the year 2011, Laos experienced two tropical storms, namely Haima and Nock-Ten. On July 30-31, Nock-Ten hit central and southern parts in Lao PDR, the provinces Vientiane, Bolikhamxay, Khammuan, Savannakhet, and Champassak. According to the report prepared by the government of the Lao PDR, (2011), the Xedone catchment was affected by both storms mentioned above. They brought heavy rains, which had caused the rise of water levels of the Xedone River and the Mekong River. As a result, many districts in Champasak Province, located at the mouth of the Xedone River had been significantly affected by floods as shown in **Figure 1.1.**

In the Chammpassak province on the lower of the Xedone River Basin, more than 70,000 residents were affected by flooding caused by the rising levels of the Mekong River and Xedone River. About 15,000 rice farming families have been affected to some degree, with a combined cultivation area of about 18,900 hectares of rice damaged by flooding. It is estimated that at least 13,200 hectares of crops have been destroyed. In addition, 20 irrigated areas and many local roads were damaged, according to our site investigation and other related data (http://laovoices.com/food-water-needed-flood-hit-areas-southern-laos/).

Significant areas of rain-fed and irrigated rice fields are located in these floodplains. The flood control structures such as levees are not available yet in these agricultural areas. For extreme floods, the banks are overstepped and most of the floodplain area on both sides of the Xedone River is under water.

(a) **(b)**

Figure 1.1 Laos experienced two tropical storms Haima and Nock-Ten in 2011 (a) Mekong River was flooding southern part of Lao PDR and (b) Xedone River was flooding in area of Khongsedone district.

The middle and lower parts of the Xedone River Basin is a flat area and a few mountains in the upper part of the basin based on the data collected from the field in Saravan province had an irrigation area of 4,535 ha and 17,294 ha of Champasak province its sources water from Xedone River Basin.

Most of the rice farming area and other agricultural land area of the Xedone River Basin are plain area and located along the Xedone River Basin from middle to downstream of the basin. During dry seasons water resource availability is less in some years and severe drought is seen in the region while during the rainyrainy season this area is under the water.

Water availability is an essential component of welfare and productivity. A developing country like Lao PDR, where agriculture serves as a backbone of the economy, currently Xedone River Basin supplies water to irrigated area of approximately 14,000-15,000 ha in the dry season with the capacity to be increased in the future.

Approximately 423,000 of people live in the basin, and most of them do not have access to adequate supplies of safe water. Therefore, the water availability in this basin at the present and future situation needs to be assessed to ensure the sustainable water resources management and planning.

1.2 Objectives of the Study

The overall goal of this study is to assess the impact of climate change on hydrology of the

Xedone River Basin, Lao PDR; under the current and future condition by using data driven and modeling approaches. The specific objectives are itemized as follows:

1. To analyze the changes of precipitation amounts and temperature in the Xedone River Basin.
2. To test the performance of the SWAT model in the Xedone River Basin.
3. To predict the future discharge under the impact of climate change in the Xedone River Basin.
4. To provide information for sustainable water management and disaster prevention.

1.3 Organization of the Dissertation

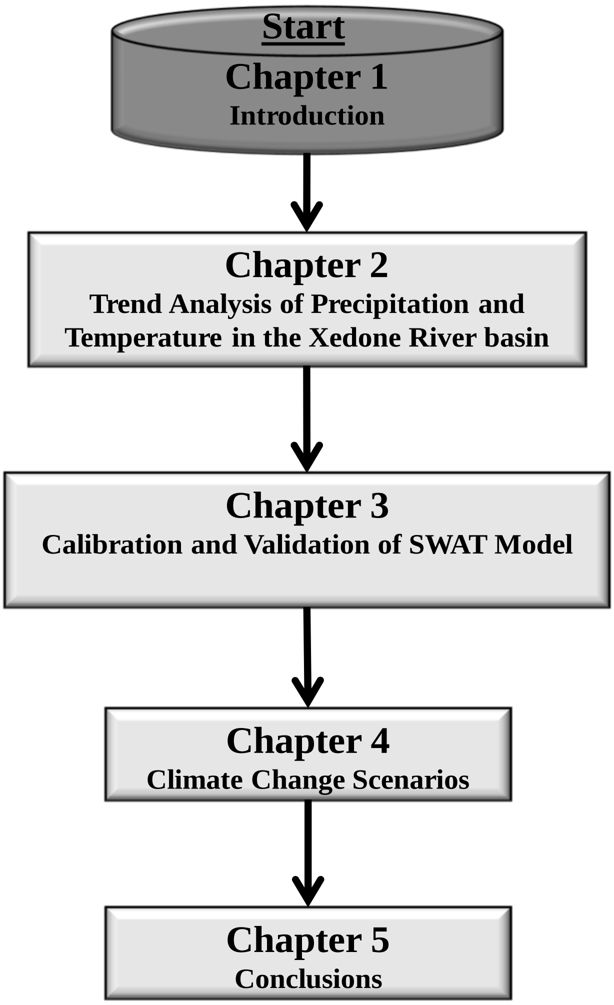

Figure 1.2 Framework of this Ph.D. thesis.

This dissertation consists of five chapters **(Figure 1.1).** A brief explanation of each chapter is outlined as follows:

Chapter 1 presents the background, the study objectives and the Organization of the dissertation.

Chapter 2 characterizes annual and seasonal precipitation trends and annual temperature trends in Xedone River Basin, Lao PDR. The period of precipitation data is 1960-2013 and temperature data is 1990-2012. Trends are analyzed by the Mann-Kendall test and Inverse Distance Weighting (IDW) interpolation method in GIS software. The trend values all of the stations have been plotted on the spatial map. The trend values are classified into three levels: small ($\alpha > 0.05$), middle ($0.01 < \alpha \leq 0.05$) and large ($\alpha \leq 0.01$) level of significance of trends.

Chapter 3 calibrates and validates SWAT model to simulate river discharge in the Xedone River Basin, covering an area of 7,224.61 km^2. The data used to input SWAT model include digital elevation model (DEM), land use, soil type, channel network, observed discharge and weather data. The model is calibrated and validated for two periods: 1993-2000 and 2001-2008, respectively, by using the SUFI-2 technique in this analysis. Result from the calibration model can be baseline data for analyzing the effects of the climate change scenarios 2030 in the next chapter.

Chapter 4 simulates scenarios by using climate change factors obtained from the modeling team of Flood Management and Mitigation Programme (FMMP) and Mekong River Commission (MRC) to the input time series of the SWAT model scenarios. The climate change factors were generated from three global climate models; whose product names are (1) GFDL-cm3-2030, (2) GISS-e2-r-cc2030 and (3) IPSL-cm5a-mr2030. The results of the three climate change scenarios are assessed by running the calibrated model for the period 1993-2008 of Suvanakhili station, and applied by climate change factors of GFDL-cm3-2030, GISS-e2-r-cc2030 and IPSL-cm5a-mr2030, by keeping the DEM, soil map, slope map and land use/cover map and all parameters, to predicted surface runoff for the year 2030.

Chapter 5 summaries the conclusion of this study based on the overall findings presented and discussed in the previous chapters. Some of further concerns and recommendation are described in this chapter.

References

A Report prepared by the Government of Lao PDR, 2011. Typhoon Haima Joint Damage, Losses and Need Assessment. Vientiane, August 29, 2011.

Verona, S., 2008. Lao PDR's country flood report for 2008. National Flood Expert, National Flood Unit, Lao National Mekong Committee Secretariat Water Resources and Environment Administration, Vientiane, Lao PDR.

Chapter 2 Trend Analysis of Precipitation and Temperature in the Xedone River Basin

2.1 Introduction

Precipitation and temperature are the most important driving factors for year-to-year variability in crop production and the available water resources. Stream flow is primarily driven by changes in precipitation (Milliman et al., 2008), which is intimately related to water availability. Furthermore, rain-fed agriculture directly depends on the magnitude and temporal distribution of the rainfall. Increasing temperature and changing patterns of precipitation, are among the many consequences, which are attributed to climate change. Trend analysis in precipitation and temperature time series is one of the interesting research areas in climatology. Many researchers in the world have conducted trend analysis of climate change and variability. Most previous studies concerning long-term climatologic trends have focused on surface precipitation and air temperature. Reviews of relevant recent studies include: for water quality variables (Hirsch et al., 1982; Yu et al., 1993; Luo et al., 2011), for stream flow (Kahya and Kalayci, 2004; Mu et al., 2007; Hamed, 2008; Juahir et al., 2010; Delgado et al., 2011; Tao et al., 2011), and for precipitation and temperature (Su et al., 2005; Longobardi & Villani, 2009; Qin et al., 2010; Wang & Zhang, 2012; Duan et al., 2013; Wu et al., 2013). From these studies, a range of potential climatic impacts on the hydrologic regime for various geographic areas can be hypothesized of climate change in the basin. In this study, the Xedone River Basin, surveys of long-term temperature and precipitation variations, and trends of data continue to go unnoticed despite the fact that the region is suffering from serious environmental, agricultural and water resource issues. The Xenon River Basin is located in the southern part of Lao PDR. In the rainy season, many areas are affected by monsoon (http://reliefweb.int/disasters?country=135#content); precipitation and temperature are one important for sustainable development in Lao PDR. So that, the analysis of the climate change is an important for this basin.

The main objective of this chapter is to analyze the trend of annual and seasonal precipitation, and annual temperature in the Xedone River Basin, which is one of the important sub-basins of the Mekong River Basin. Daily data of precipitation and temperature was obtained from the local staff, Meteorology and Hydrology Department, and the Ministry of Natural Resource and Environment in Lao PDR, all of data is presented in **2.3**. The trends of precipitation and temperature are analyzed by using a non-parametric trend test, Mann-Kendall test. This study uses the daily precipitation data from 7 stations with at least 23 years of the length between 1960-2013 and temperature from 6 stations data for the period of 1990-2012. The study has been conducted to find the evidence of climate change and attempt to discuss relations to the recently increase of natural disasters. The trend results of this study can provide important information for future research on water quality analysis, water management, and dam construction planning.

2.2 Study Area and Data collections

2.2.1 Study Area

(1) Location and General Characteristics

The Xedone River Basin is located in the southern part of Lao People's Democratic Republic PDR, which spans across the Champasack and Saravanne provinces and a small proportion in Savannakhet and Xekong Provinces of southern Lao PDR, as shown in **Figure 2.1.** The study area is located between 15°10'2.858" - 16°11'5.474" North Latitude and 105°35'31.379" - 106°44'51.956" East Longitude, and covers a total area of 7,224.61

km^2 equal to 0.89% out of 809,500 km^2 of the Mekong River Basin area.

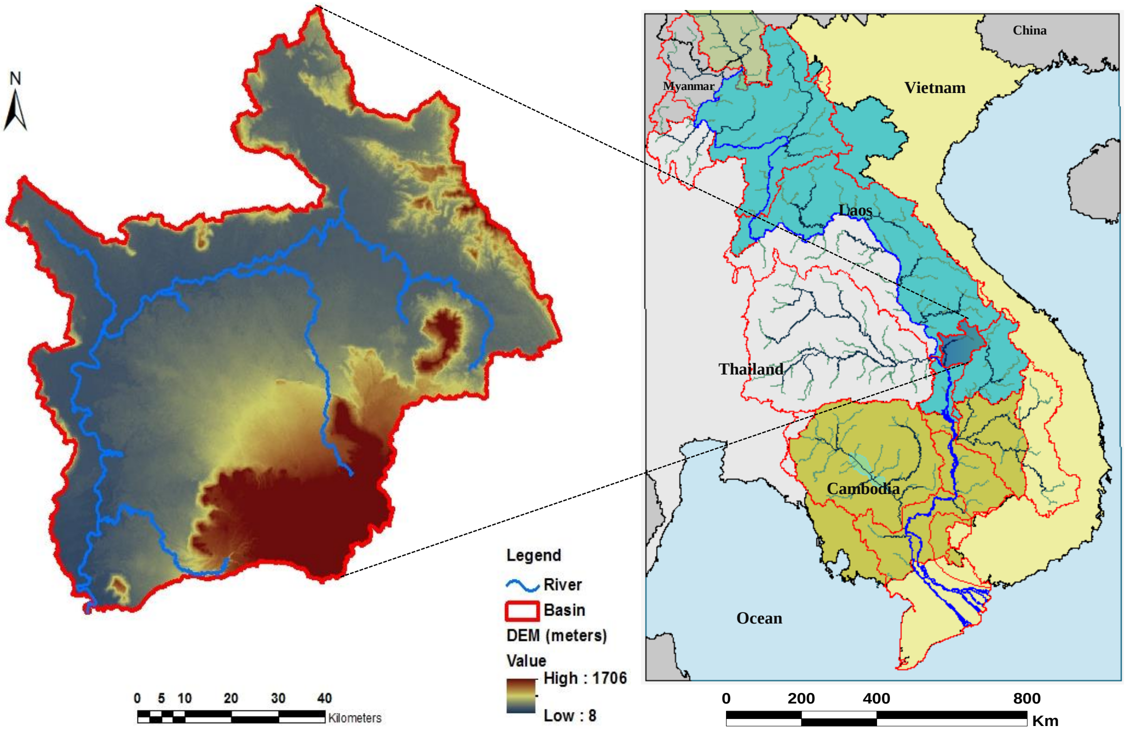

Figure 2.1 Location of Xedone River Basin.

(2) Climate

The climate in the study area is characterized by two distinct seasons: a rainy season (May to October) and a dry season (November to April), as shown in **Figure 2.2**. The annual mean temperature ranges from 15.2 to 32.4°C according to average all of the temperature in the basin. In the mountainous areas, the temperature drops to as low as 0 °C in January and February at night. This area receives about 2070 mm of annual rainfall, during the rainyrainy season which contributes 60-70% of the annual rainfall due to monsoons, tropical cyclones, tropical storms and depressions as described above.

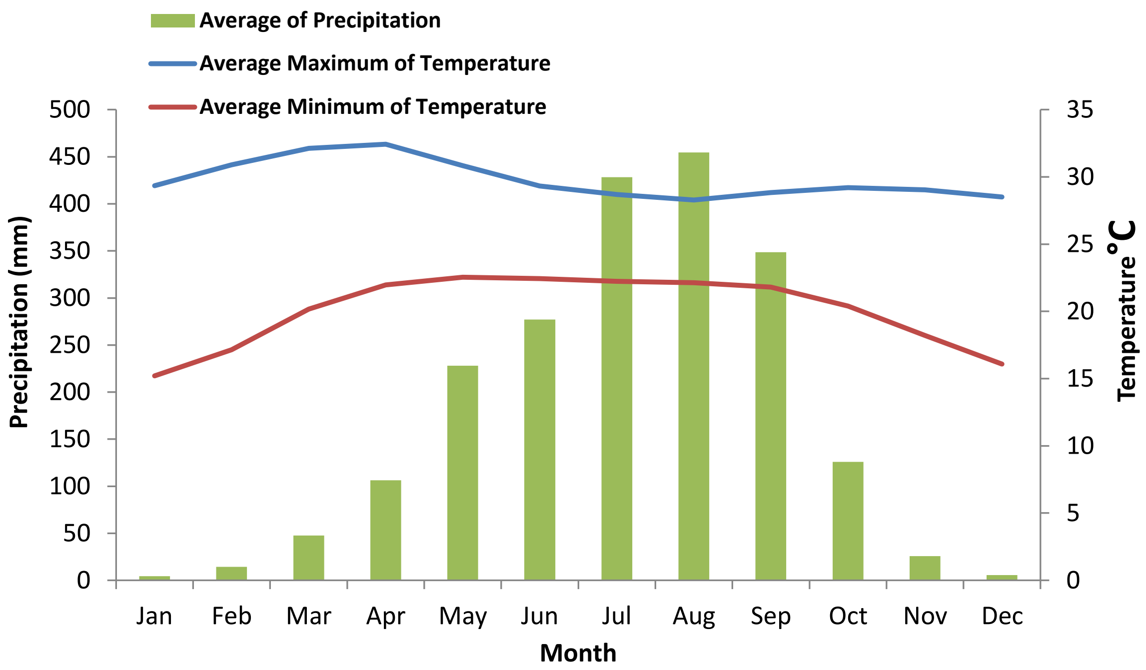

Figure 2.2 Average monthly of precipitation and temperature of the Xedone River Basin.

(3) Topography

The Xedone River Basin has a total length of 240.5 km. The basin originated in the Bolaven Plateau in Thateng District, before flowing through Saravan city, Vapi district before entering the Lower Xedone River Basin floodplains in the areas of Khongxedone and Sanasomboun districts, and the northern border of Pakse District, Champasak Province.

The elevation of the basin ranges from 8 m to 1706 m above the mean sea level MSL as shown in **Figure 2.3**. The elevation of the Bolaven Plateau varies from 800 m to 1706 m above MSL according to the elevation of the basin. The topography of the study area is generally hilly in upstream part, flat land in the middle to downstream. Having sources of water, large middle part is suitable for agriculture and last the lower part is suitable for rice cropping because of available for irrigation water. However, during the dry season, water resources availability is less in the region. The land covers are the vegetables and deciduous trees (46.16%), the agricultural land (14.19 %), the paddy field (17.08%), the shrub land / regrowth (21.21 %), the grassland (1.16 %), the water surface (0.02 %) and the urban area (0.18 %) in this basin that are shown in **chapter 3** in the **Figure 3.3**. Major soil types in this river basin are predominantly Acrisols, Cambisols and Luvisols (sandy, loamy, clay and gravity).

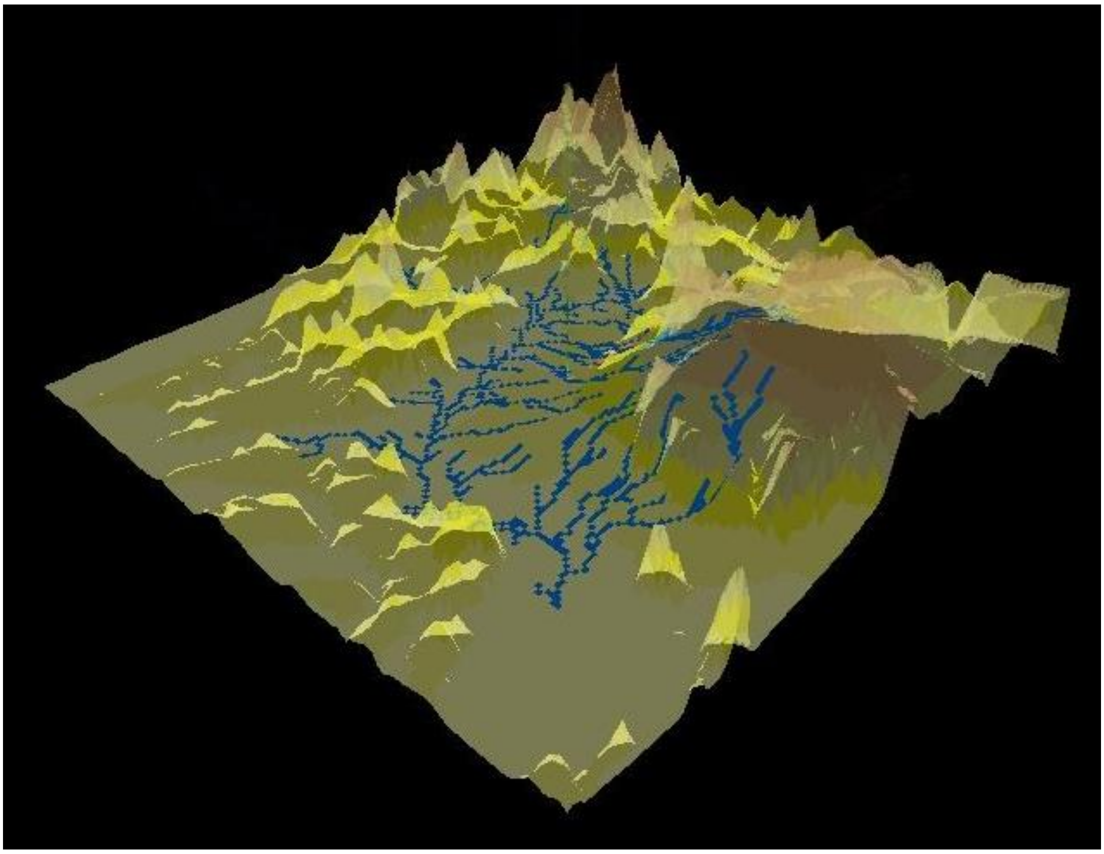

Figure 2.3 Topography of the Xedone River Basin.

2.2.2 Data

(1) Rainfall and Temperature Data

Observed daily precipitation data from seven stations is used for trend analysis. The name of the stations are Khongxedone, Batieng, LaoNgam, Nikhom34, Pakse, Saravan and Selabam. The daily temperature data are also used for the analysis in this study from six stations consists of daily maximum and daily minimum temperature. All of stations, are namely Khongxedone, LaoNigam, Nikhom34, Pakse, Paksong and Saravan. All of the data are obtained from the local staff in Meteorology and Hydrology Department and Ministry of Natural Resource and Environment in Lao PDR. (**Figure 2.4, 2.5** and **Table 2.1).**

Figure 2.4 Pictures of the meteorological station: (a) station site; (b) rain gauge; (c) temperature measurement; (d) relative humidity; (e) evaporation; (f) sunshine hours; (g) discussion with district staff; (h) discussion with local staff and (i) technical staff team of Natural Resource and Environmental Department in Laos.

Table 2.1 Meteorological stations and data periods of Xedone River Basin.

No	Station	Period of data		Latitude	Longitude	Elevation
		Temperature	Precipitation			
1	Khongxedone	1990 - 2012	1960 - 2013	15.611	105.808	128
2	LaoNgam	1990 - 2012	1960 -2013	15.462	106.163	568
3	Pakse	1990 - 2012	1960 - 2013	15.121	105.858	189
4	Saravan	1990 - 2012	1964 - 2013	15.716	106.428	171
5	Nikhom34	1990 - 2012	1972 - 2013	15.175	106.100	890
6	Selabam		1972 - 2013	15.358	105.833	130
7	Batieng		1990 - 2013	15.249	105.931	230
8	Paksong	1990 - 2012		15.178	106.229	1261

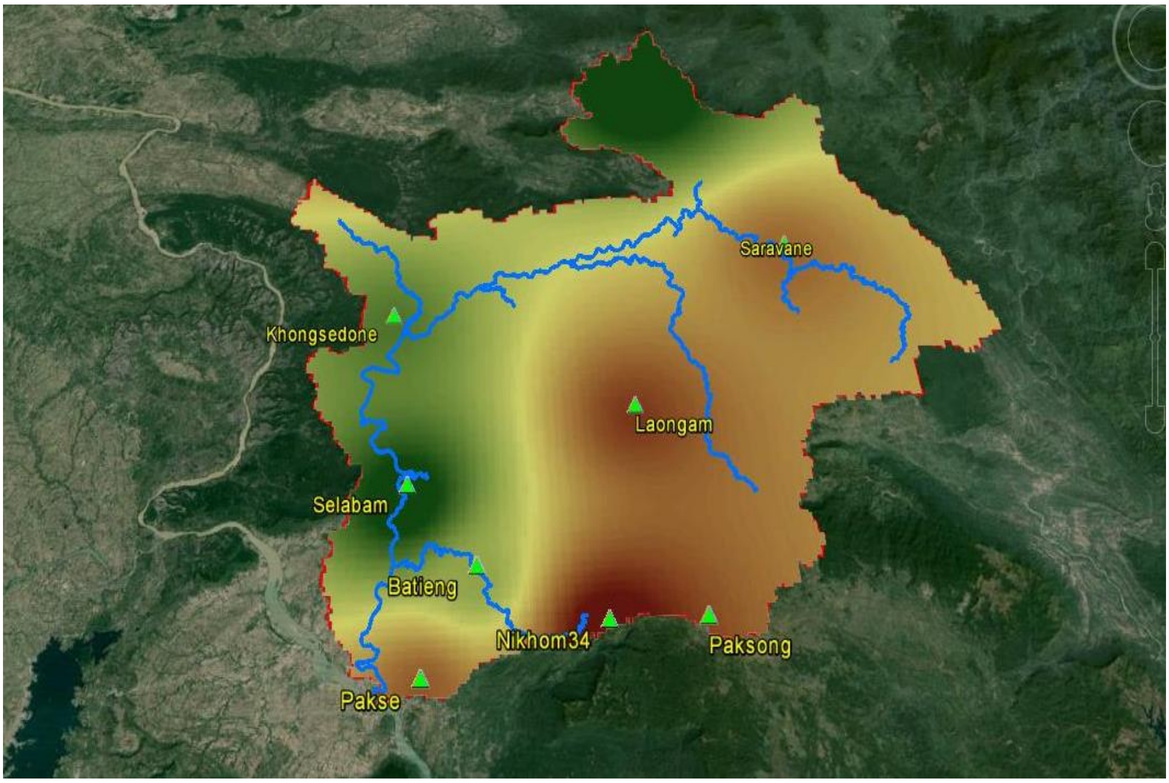

Figure 2.5 Meteorological stations of Xedone River Basin.

(2) Precipitation data for Mann-Kendall Test

The Mann-Kendall test (MKT) is a non-parametric statistical procedure used to test for trends in time-series data. Observed daily precipitation data for the period 1960 to 2013 obtained from local staff of Meteorology and Hydrology Department, Ministry of Natural Resource and Environment in Lao PDR, data were considered for statistical analysis. Spatial distribution of seven precipitation stations is illustrated in **Figure 2.6.** Daily precipitation data obtained were converted to seasonal and annual of each station. Seasons were defined as follows: rainy season (May to October) and dry season (November to April). The data were carefully analyzed for homogeneity and for missing data.

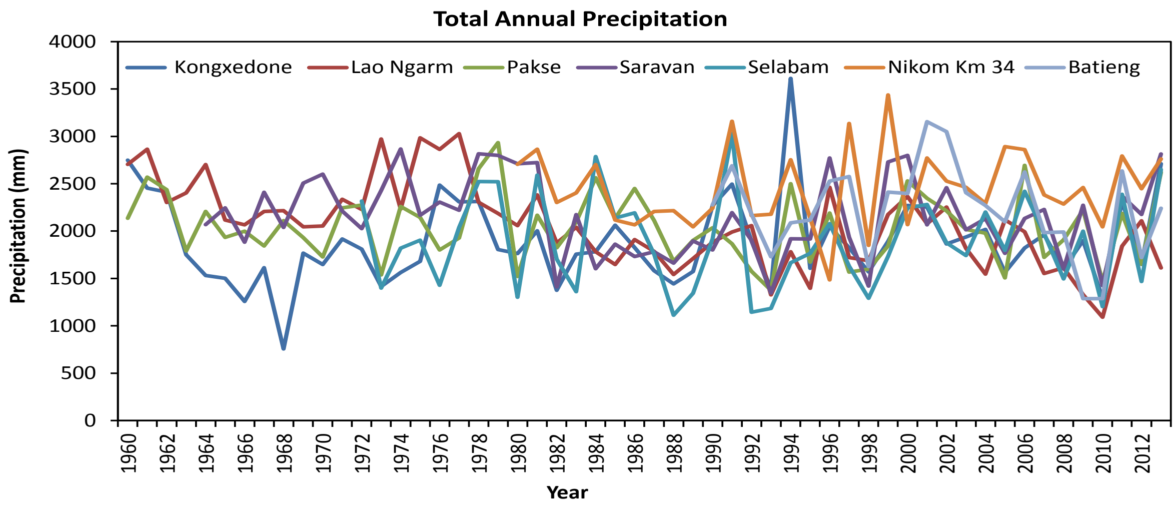
Total Annual Precipitation
Kongxedone
Lao Ngarm
Pakse
Saravan
Selabam
Nikom Km 34
Batieng
Precipitation (mm)
Year

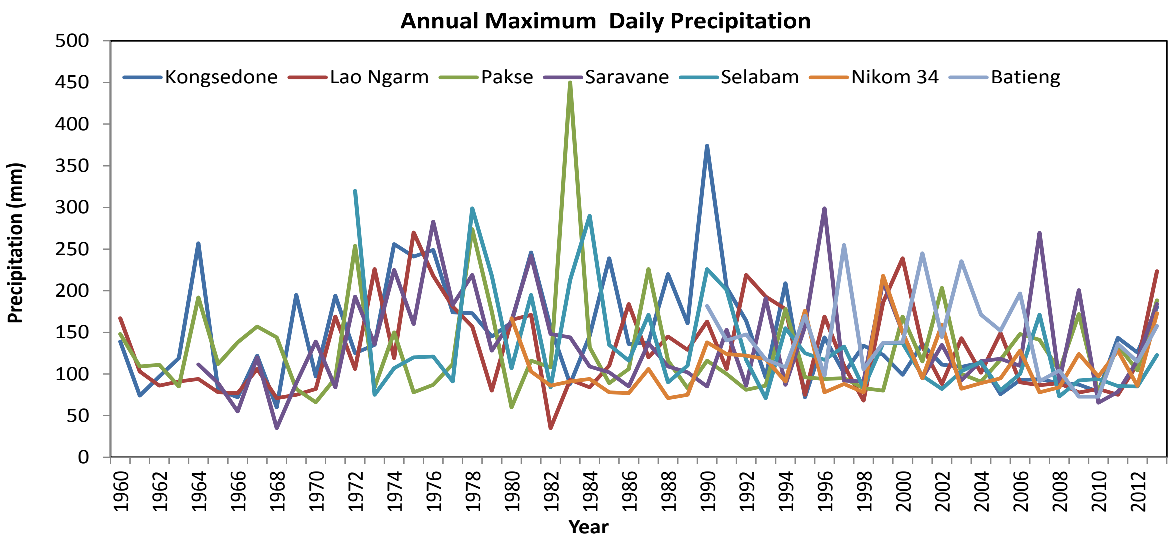
Annual Maximum Daily Precipitation
Kongsedone
Lao Ngarm
Pakse
Saravane
Selabam
Nikom 34
Batieng
Precipitation (mm)
Year

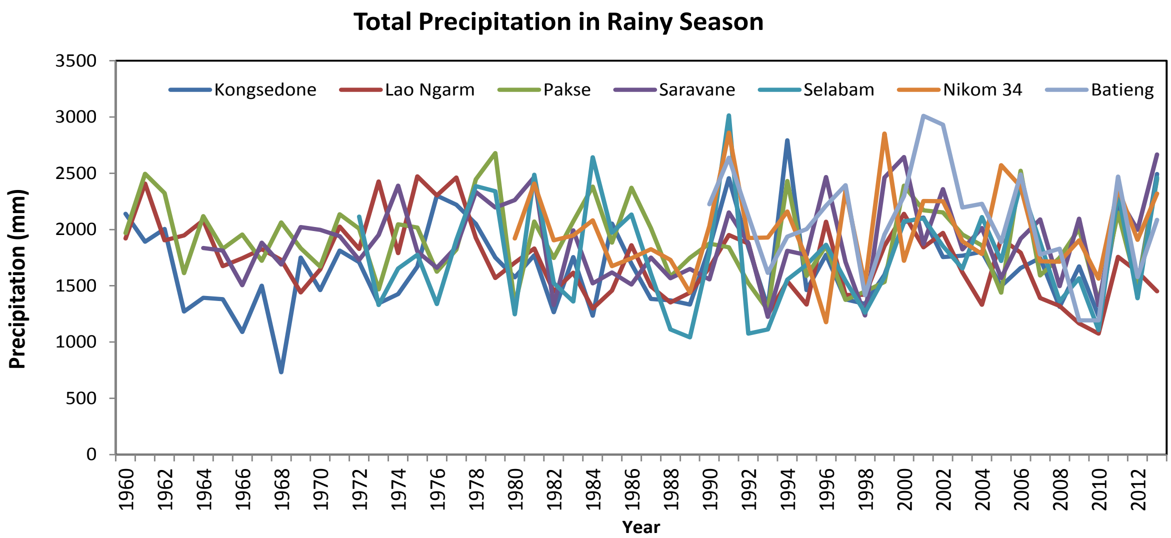
Total Precipitation in Rainy Season
Kongsedone
Lao Ngarm
Pakse
Saravane
Selabam
Nikom 34
Batieng
Precipitation (mm)
Year

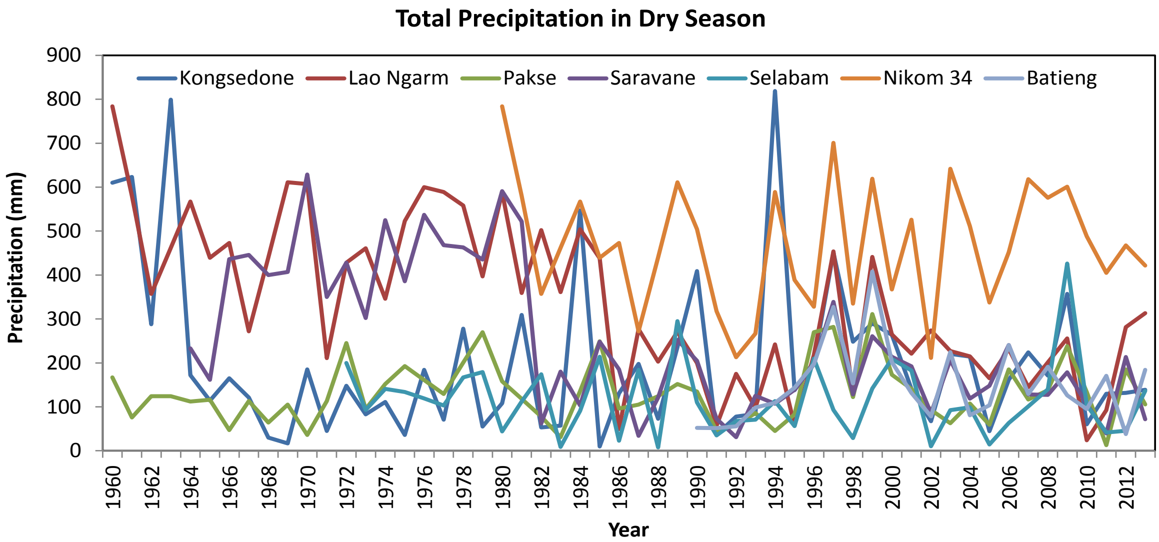

Total Precipitation in Dry Season
Kongsedone
Lao Ngarm
Pakse
Saravane
Selabam
Nikom 34
Batieng
Precipitation (mm)
Year

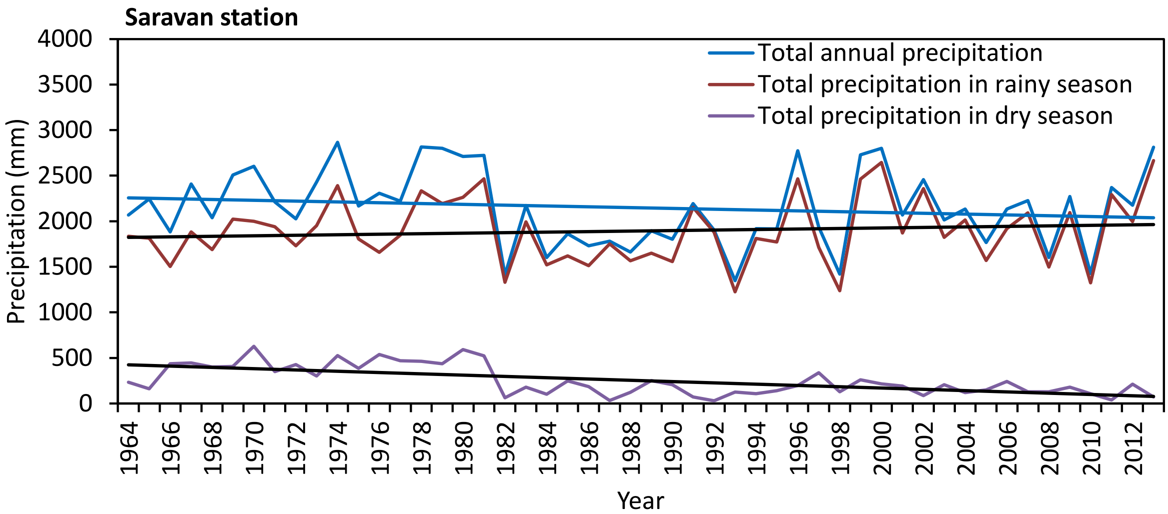

Saravan station
Total annual precipitation
Total precipitation in rainy season
Total precipitation in dry season
Precipitation (mm)
Year

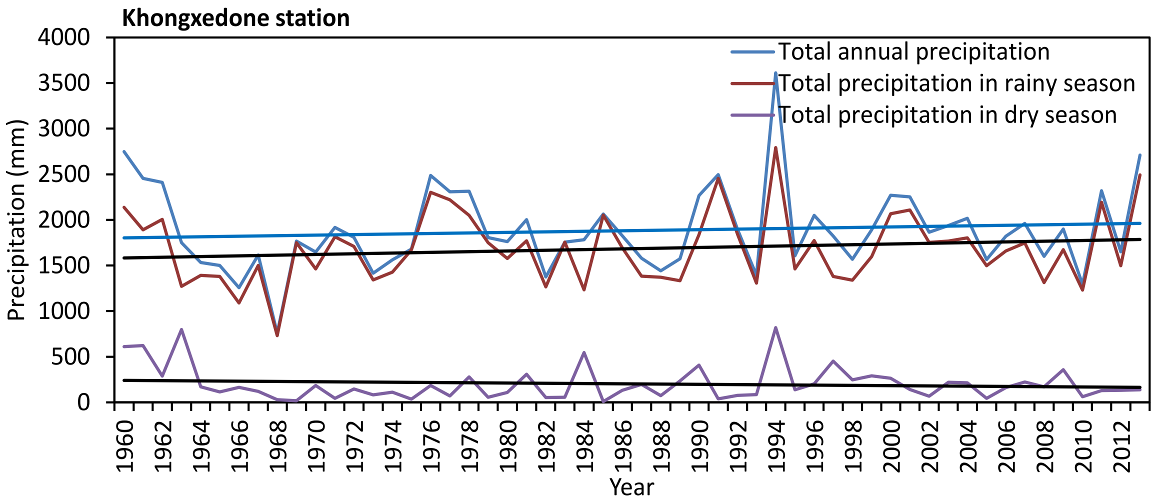

Khongxedone station
Total annual precipitation
Total precipitation in rainy season
Total precipitation in dry season
Precipitation (mm)
Year

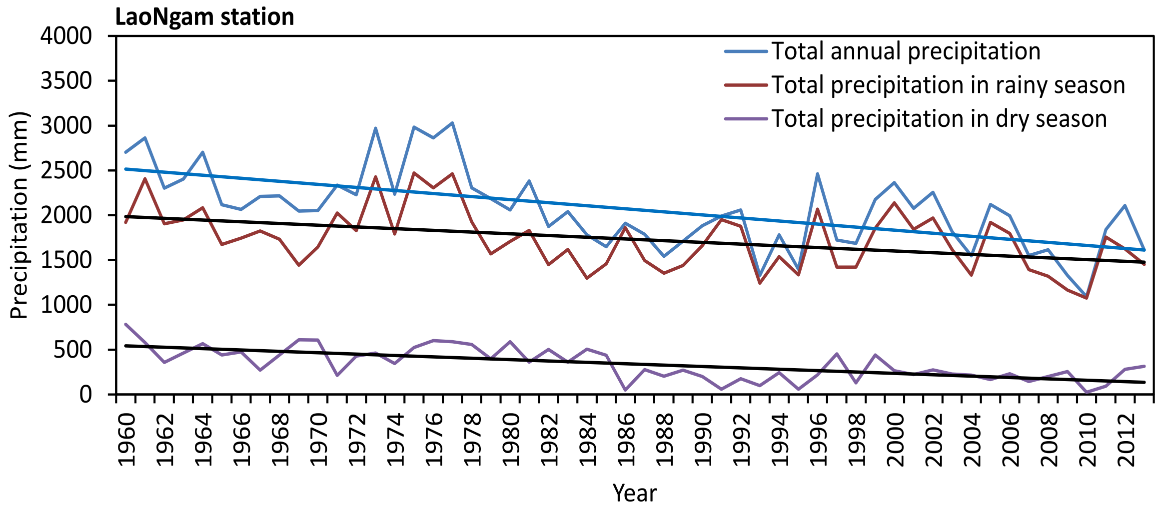
LaoNgam station
Total annual precipitation
Total precipitation in rainy season
Total precipitation in dry season
Precipitation (mm)
Year

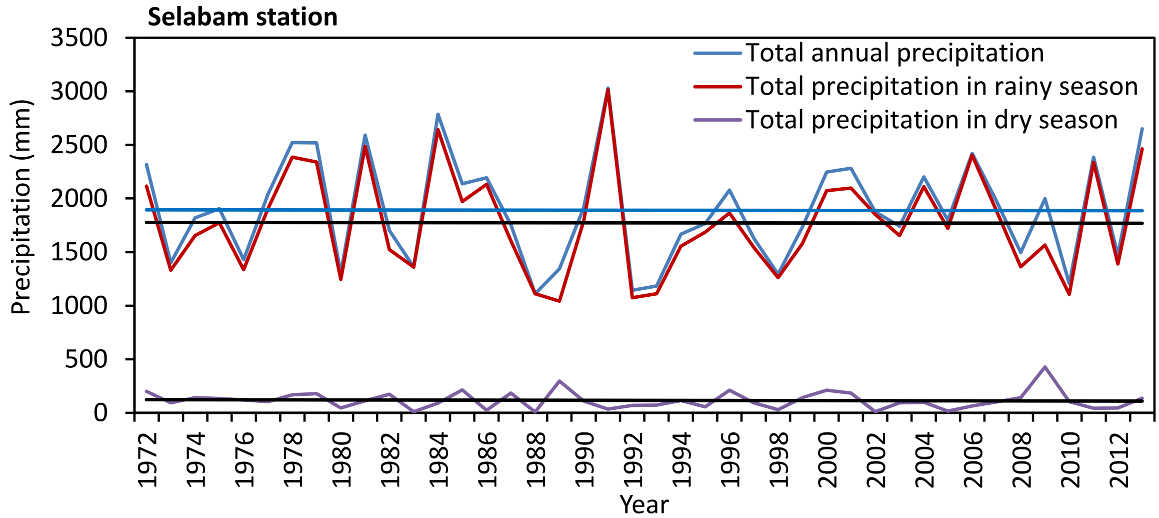
Selabam station
Total annual precipitation
Total precipitation in rainy season
Total precipitation in dry season
Precipitation (mm)
Year

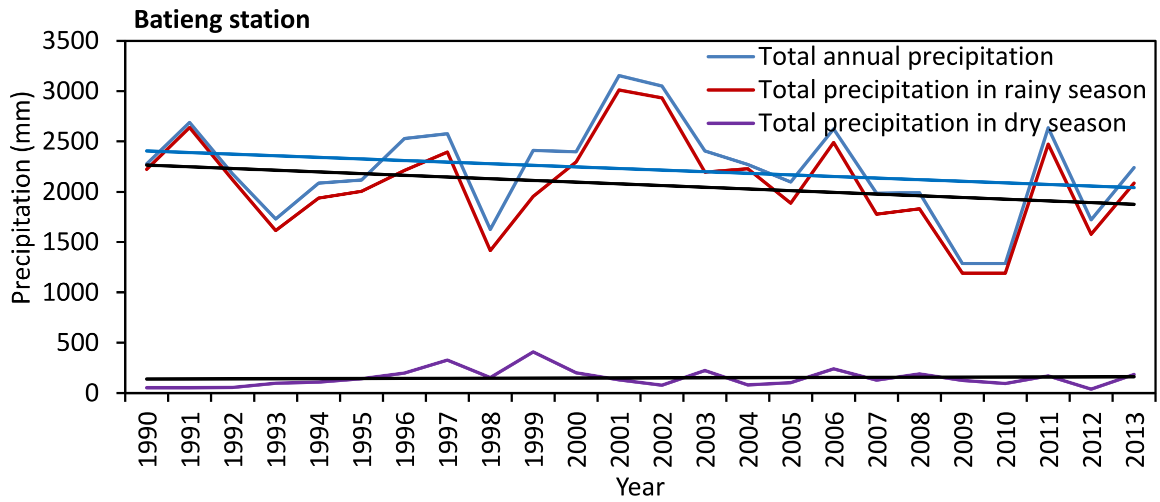
Batieng station
Total annual precipitation
Total precipitation in rainy season
Total precipitation in dry season
Precipitation (mm)
Year

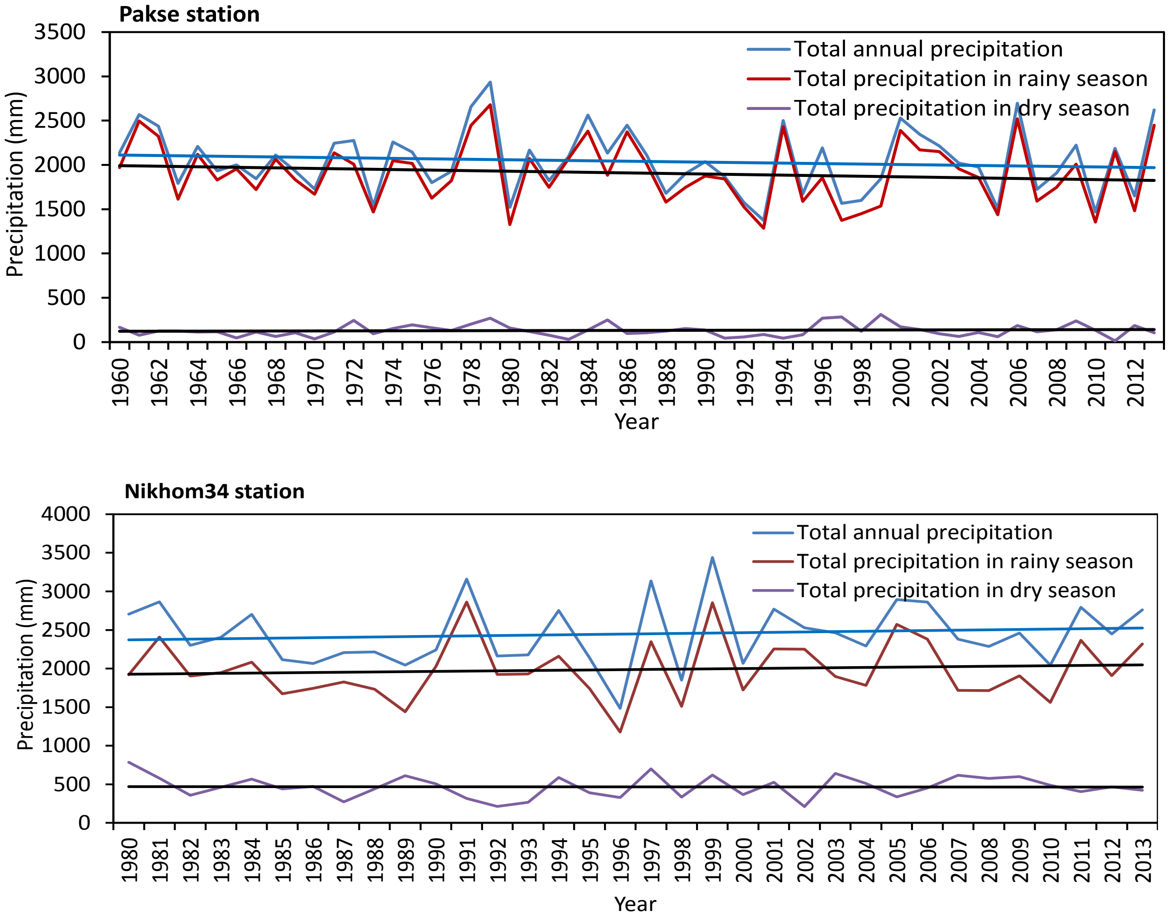

Figure 2.6 Precipitation data of the Xedone River Basin for analysis (total annual precipitation, annual daily maximum, total precipitation in rainy season and total precipitation in dry season).

(3) Temperature data for Mann-Kendall Test

The Mann-Kendall test (MKT) is a non-parametric statistical procedure used to test for trends in time-series data. Observed daily temperature data for the period 1990 to 2012 obtained from local staff in Department of Meteorology and Hydrology, Ministry of Natural Resource and Environment in Lao PDR were considered for statistical analysis. The spatial distribution of six temperature stations is illustrated in **Figure 2.7**. Daily temperature data obtained were converted to annual averages, annual daily maximum and annual daily minimum for each station. The data were carefully analyzed for homogeneity and for missing data.

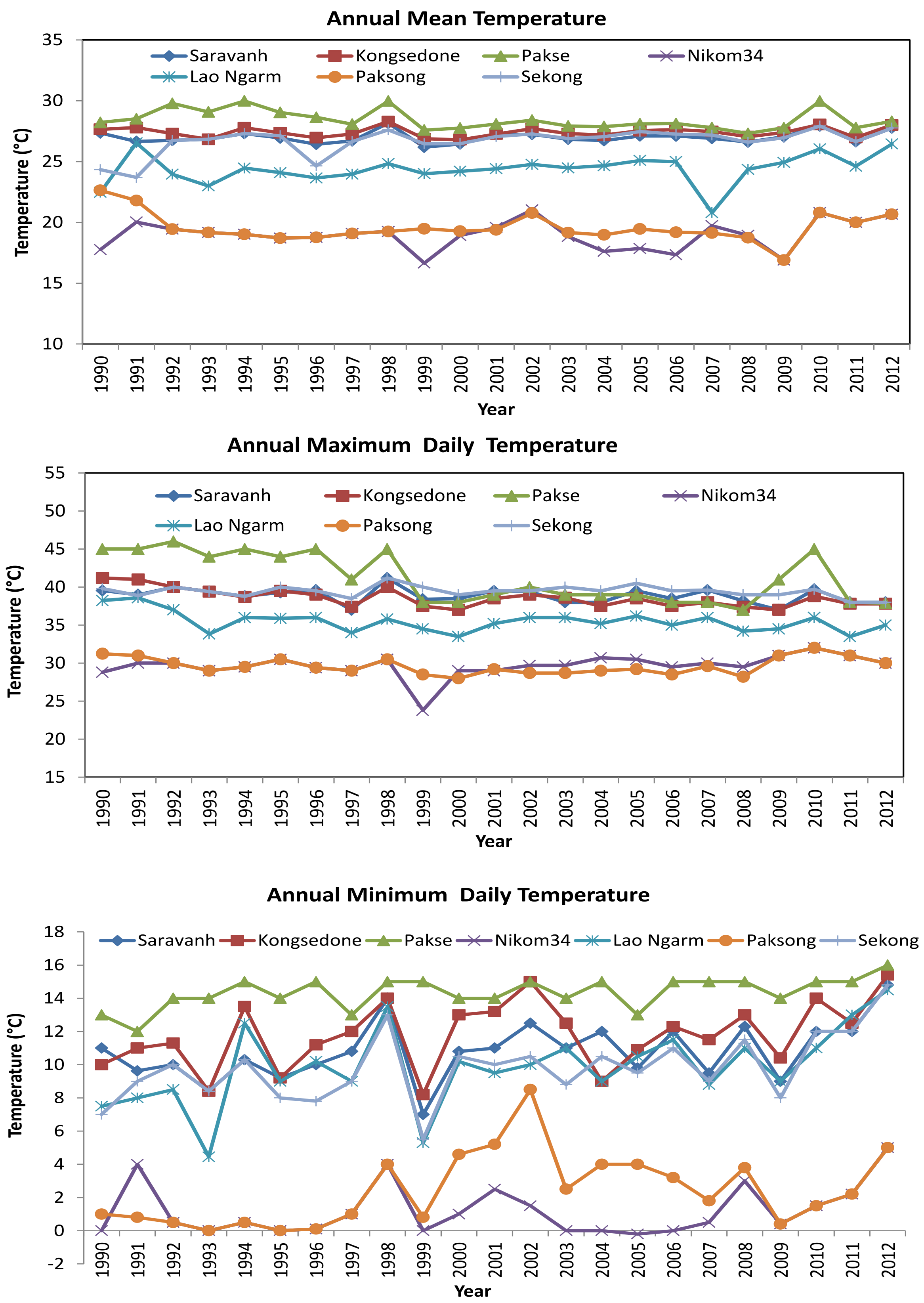

Figure 2.7 Temperature data of the Xedone River Basin for analysis (annual temperature, annual daily maximum temperature and annual daily minimum temperature).

2.3 Methods

The Mann-Kendall test (MKT) was applied in this study in order to calculate the trend values for precipitation and temperature. MKT is a non-parametric statistical procedure used to test for trends in time-series data (Yu et al., 1993; Partal and Kahya, 2006). The null hypothesis of the Mann-Kendall test is that the data are independent and randomly ordered, i.e. there is no trend or serial correlation structure in the time-series (Hamed and Rao, 1998; Xu et al., 2010). For independent and randomly ordered data in a time-series of n data point and x_i and x_j as two subsets of data where x_i $\{x_i, i = 1, 2, . . . , n - 1\}$ and x_j $\{x_j, j = i+1, i+2, . . . , n+1\}$, the null hypothesis H_0 is tested on the observations x_i against the alternative hypothesis H_1, where there are an increasing or decreasing monotonic trend (Yu et al., 1993). According to the condition of $n \geq 10$, the S variance is described according to equation (2.1) as below:

$$Var(S) = \frac{n(n-1)(2n+5) - \sum_{i=1}^{e} t_i(t_i-1)(2t_i+5)}{18} \qquad (2.1)$$

where e is the number of tied groups, and t_i is the number of data values in the i^{th} group. The statistical S test is given as follows:

$$S = \sum_{i=1}^{n-1} \sum_{j=i+1}^{n} sgn(x_j - x_i) \qquad (2.2)$$

where x_j and x_i are the annual values in years j and i, $j > i$, respectively, and

$$sgn(x_j - x_i) = \begin{cases} 1 & if\ x_j - x_i > 0 \\ 0 & if\ x_j - x_i = 0 \\ -1 & if\ x_j - x_i < 0 \end{cases} \qquad (2.3)$$

The normal approximation Z test by using the statistical value S and the variance value $Var\ (S)$ is written in the following form:

$$Z = \begin{cases} \frac{S-1}{\sqrt{Var(S)}} & if\ S > 0 \\ 0 & if\ S = 0 \\ \frac{S+1}{\sqrt{Var(S)}} & if\ S < 0 \end{cases} \quad (2.4)$$

The presence of a statistically significant trend is evaluated using the *Z* value. A positive (negative) value of *Z* indicates an upward (downward) trend. The statistic *Z* has a normal distribution. To test for either an upward or downward monotone trend (a two-tailed test) at α level of significance, H_o is rejected if the absolute value of *Z* is greater than $Z_{1-\alpha/2}$, where $Z_{1-\alpha/2}$ is obtained from the standard normal cumulative distribution **Table 2.2**.

Table 2.2 Standard normal cumulative distribution table.

α	0.0002	0.002	0.01	0.02	0.05	0.1	0.2	0.3	0.5	0.8	1
$1-\alpha/2$	0.9999	0.999	0.995	0.990	0.975	0.95	0.90	0.85	0.75	0.60	0.5
$Z_{1-\alpha/2}$	3.72	3.090	2.576	2.326	1.960	1.645	1.282	1.04	0.67	0.25	0.00

2.4 Results and Discussions

The observed daily data of precipitation from seven stations and temperature from six stations in the Xedone River Basin were used as inputs for the MKT analysis. Results are presented in **Table 2.3** and **2.4** with the long-term MKT trends of the *Z* values of annual and season in the Xedone River Basin. In **Figure 2.8** and **2.9,** the precipitation and temperature values were interpolated by Inverse Distance Weighting (IDW) interpolation method. The trend values all of the stations have been plotted on the spatial map with red color indicating increasing trend and blue color indicating a decreasing trend. The trend values have been classified into 3 levels: small (α > 0.05), middle (0.01 < α ≤ 0.05) and large (α ≤ 0.01) level of significance of trend respectively. The detailed results are summarized in the **Appendix:** page 85.

2.4.1 Precipitation Trend

Figure 2.8 (a) shows the distribution map of historical total annual precipitation and the spatial map of long-term MKT trend of total annual precipitation in the Xedone River Basin. From this figure was clearly the trend of total annual precipitation of each station in the basin. The stations with a decreasing trend concentration in the basin four stations (Saravan, LaoNgam, Batieng and Pakse). With increasing trends concentrate in three stations (Kongxedone, Selabam and Nikhom34). In the southern part of the basin one station as Nikhom34 has similar precipitation trend. This is considered preliminary as the climatic homogeneity of each part in the Xedone River Basin.

Figure 2.8 (b) shows the distribution map of annual maximum daily precipitation and the spatial map of long-term MKT trend of annual maximum daily precipitation in the Xedone River Basin. The MKT trend of annual maximum daily precipitation has been found at three stations with decreasing trend and four stations with increasing trend distribution in the whole basin. Another finding of this figure is that stations with increasing trend in the northern part to southeast part. As increased annual maximum daily precipitation is considered as an increased extreme flood events the situation of flooding environment is speculated to have become worse in most of the areas of the Xedone River Basin. Usually, flooding hazard is found in the river mouth of the basin every year.

Figure 2.8 (c) shows the distribution map of historical total precipitation in rainy season and the spatial map of long-term MKT trend of total precipitation in rainy season in the Xedone River Basin. The total precipitation in rainy season in northern and southern parts of the basin is similar to other parts with the total annual precipitation, the increasing trend of precipitation in the rainy season has been found one station concentrated in the north of the basin as Saravan station.

Figure 2.8 (d) shows the distribution map of total precipitation in the dry season and the spatial map of long-term MKT trend of total precipitation in the dry season in the Xedone River Basin. The total precipitation in the dry season has been found concentrated in the three stations with a decreasing trend and four stations with increasing trend distribution in the whole basin. Another finding of this figure is found station with increasing trend in southern part of basin three stations, one station of Nikhom34 was similar increasing trend as shown in **Figure 2.8 (a), (b)** and **(c)**., and LaoNgam station was a similar decreasing trend in the middle part of the basin. This part is shortage of water in dry season

The calculation of the trend statistics is started by MKT trend, the calculate trend statistics are used the daily data of precipitation. The results are summarized in **Table 2.3** and the detailed results are summarized in the **Appendix**: A1, A2, A3, A4 and A5.

Table 2.3 Results of the Mann-Kendall test Z values for precipitation data.

Station	Total annual precipitation	Annual maximum daily precipitation	Total precipitation in rainy season	Total precipitation in dry season
KongXedone	1.000	-1.515	0.671	0.224
LaoNgam	-4.581	0.246	-3.223	-4.864
Pakse	-0.992	0.007	-1.052	0.418
Saravan	-0.719	-0.075	0.694	-3.931
Selabam	0.195	-2.395	0.228	-0.856
Nikom34	0.563	0.846	0.178	0.059
Batieng	-1.141	-1.092	-1.191	0.868

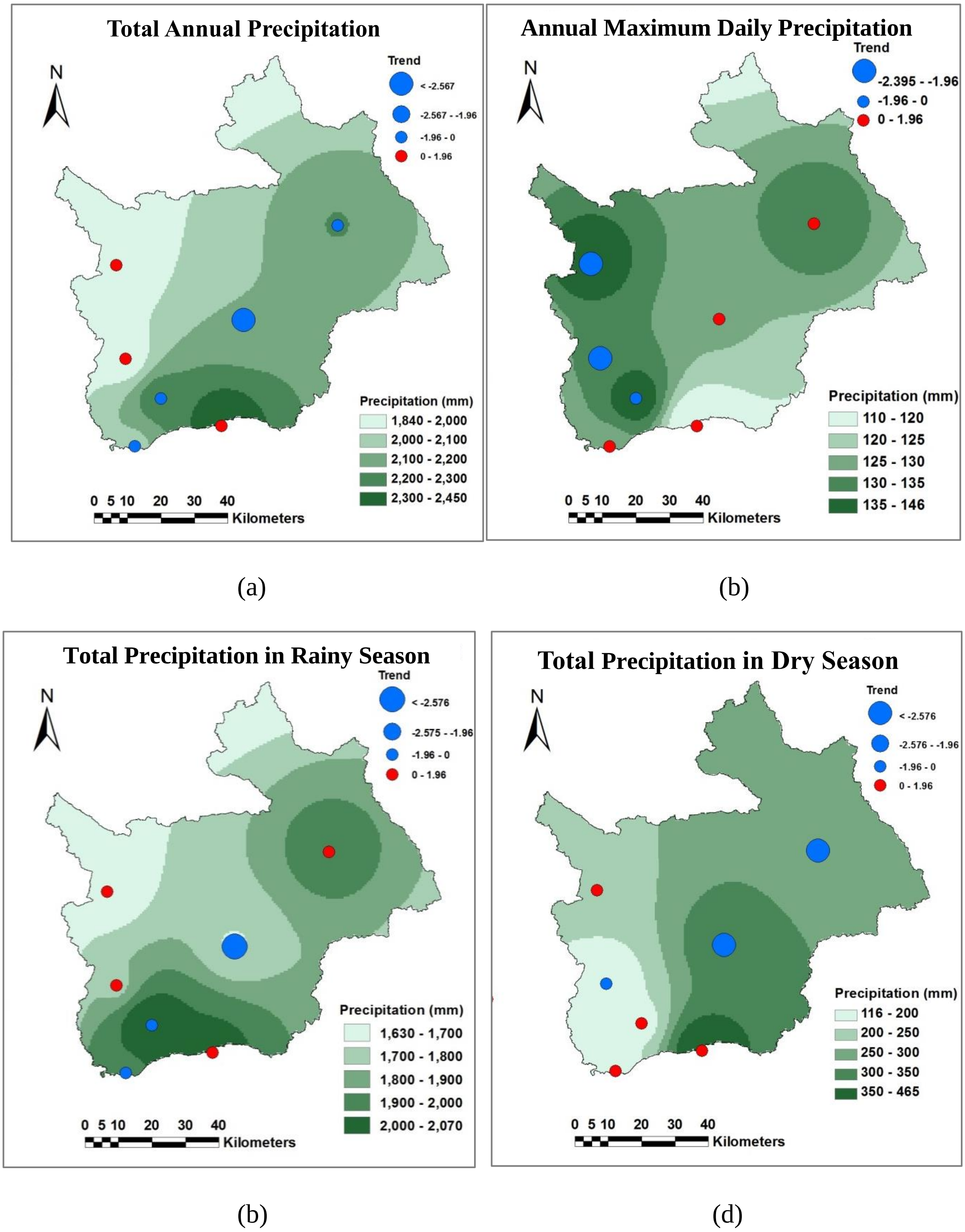

Figure 2.8 Distribution map of precipitation and spatial map of long-term MKT trend of (a) total annual (b) annual maximum daily (c) total precipitation in rainy season and (d) total precipitation in dry season.

2.4.2 Temperature Trend

Figure 2.9 (a) shows the distribution map of historical average temperature and the spatial map of long-term MKT trend of annual meantemperature in the Xedone River Basin. The two stations show while for station decreasing trends (Pakse and Paksong), show increasing trends in four stations (Kongxedone, Saravan, LaoNgam and Nikhom34). In the central part of the basin, LaoNgam station shows statistically significant of (MKT Z= 2.75) and increasing trend Nikhom34 is also similar trend, with comparing annual maximum daily temperature and annual minimum daily temperature, this is considered preliminary as the climatic homogeneity of each part in the Xedone River Basin.

Figure 2.9 (b) shows the distribution map of historical annual maximum daily temperature and the spatial map of long-term MKT trend of annual maximum daily temperature in the Xedone River Basin. The stations with a decreasing trend concentration in the basin one station Nikhom34. With increasing trends concentrate in five stations with Saravan, Kongxedone, LaoNgam, Pakse and Paksong. In the southeast part of the basin had one station, as Nikhom34 is a similar trend of annual mean temperature and annual minimum daily temperature.

Figure 2.9 (c) shows the distribution map of historical annual minimum daily temperature and the spatial map of long-term MKT trend of annual minimum daily temperature in the Xedone River Basin. All of the stations in this figure are increasing trend. There are three stations with high increasing trend of Z value such as Saravan, LaoNgam and Pakse stations. According to the comparison with annual maximum daily temperature, Nikom34 station shows similar increase trend. For flooding disasters, the impact by temperature increase is not as obvious as precipitation, however, the global warming is said to have an indirect effect on it as it accelerates the water cycle process thus increases the intensity and the probability of extreme precipitation event.

The calculation of the trend statistics is started by MKT trend, the calculate trend statistics are used the daily data of temperature. The results are summarized in **Table 2.4** and the detailed results are summarized in the **Appendix**. A5, A6 and A7.

Table 2.4 Results of Mann-Kendall test Z values for temperature data.

Station	Annual mean temperature	Annual maximum daily temperature	Annual minimum daily temperature
Saravan	0.53	-1.67	2.04
KongXedone	0.21	-3.21	1.82
Pakse	-2.09	-3.48	2.6
Nikom34	0.37	2.35	1.1
LaoNgarm	2.75	-1.84	2.81
Paksong	-0.21	-0.5	1.93

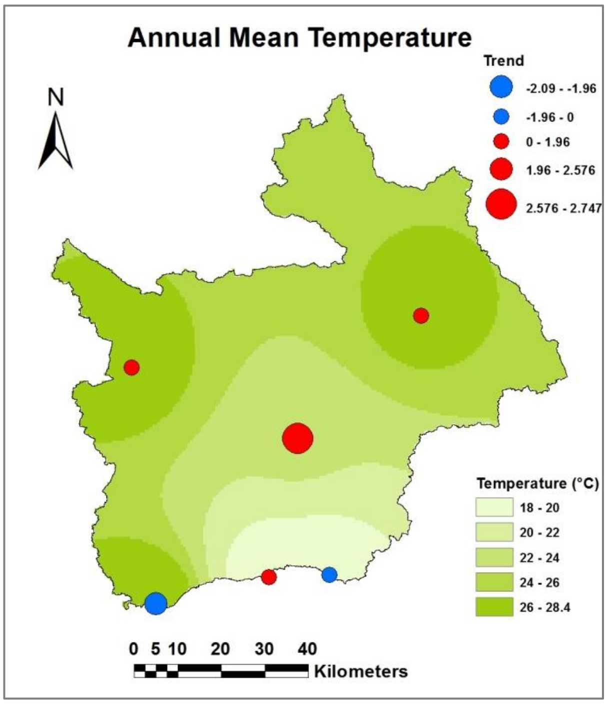

(a)

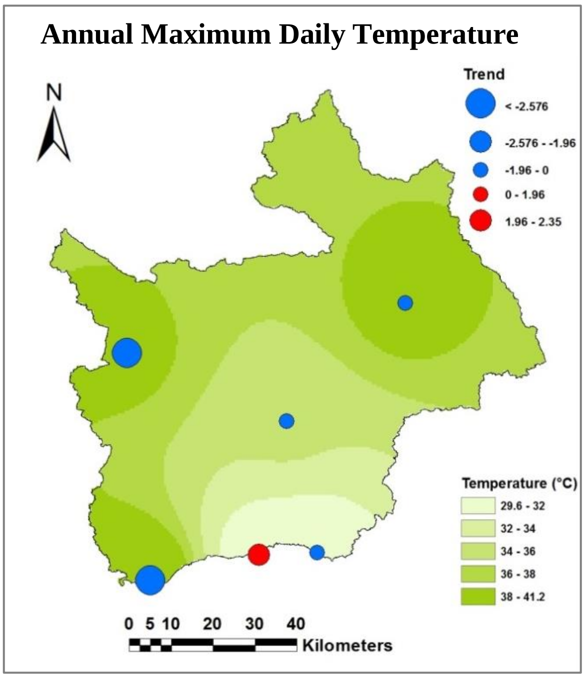

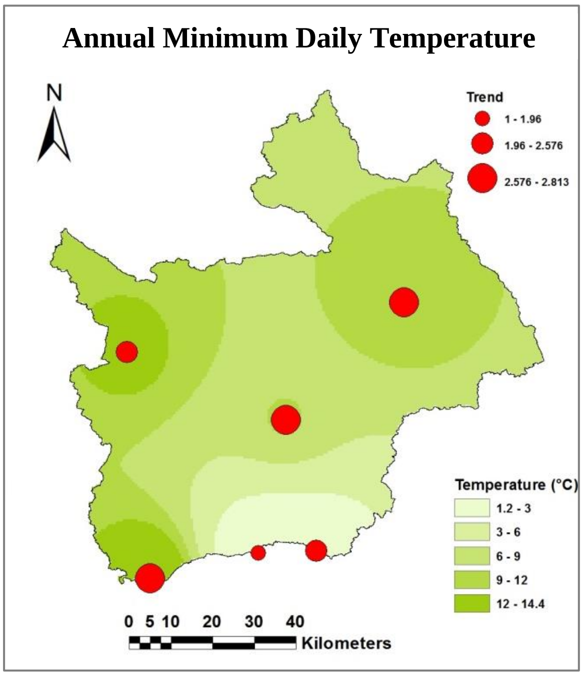

(b) (c)

Figure 2.9 Distribution map of temperature and spatial map of long-term MKT trend of temperature (a) annual mean (b) annual maximum daily and (c) annual minimum daily period 1990 to 2012.

2.4.3 Discussions

The climate in the area is characterized by two distinct seasons: a rainy season (May to October) and a dry season: (November to April). The area is influenced by the tropical monsoons the south-west monsoon reverses its maximum activity, especially on the windward side. As well temperature at Khongxedon station within Area (1991-2005) ranges from 29.8 to 34.8^{o}c and 18 to 25.6^{o}c maximum and minimum respectively except Bolaven plateau at the Nikhom34 station (1991-2005) ranges from 23.5 to 26.2 and 6.6 to 16.4^{o}c maximum and minimum respectively.

The Xedone River Basin is occasionally inundated because of typhoon during rainy season. Extremely heavy rainfall has frequently been observed in the area and it the cause of the flood is in the lower part of the Xedone River Basin. As shown in **Figure 2.8** and the precipitation is increased trend at Nikhom34 station. Further, the rainfall is erratic in every year but the intensity of rainfall is high. This is very common in area and southern part of Laos.

The precipitation increased trend of (annual daily maximum etc.) scale was found in the southeastern part of the Xedone River Basin at Nikhom34 station. The annual decreased trend precipitation of associated to drought risk was also found in the middle part of the Xedone River Basin at the LaoNgam station. This part is shortage of water in dry season.

2.5 Summary

In this chapter, trend analysis of precipitation and temperature data in the Xedone River Basin, Lao PDR is conducted by Mann-Kendall test to find the effect of climate change and attempt to relate these changes to recently increased natural disaster.

The analysis used precipitation data from seven stations and temperature from six stations, focused on total annual precipitation, annual maximum daily precipitation, total precipitation in rainy season, total precipitation in dry season, annual mean temperature, annual maximum daily temperature and annual minimum daily temperature.

The results of trend analysis of precipitation data period 1960 to 2013. The total annual precipitation is increased at three stations, annual maximum daily precipitation increased at four stations, total precipitation in rainy season is increased at two stations, and total minimum daily precipitation is increased at four stations.

The results of trend analysis of temperature data period 1990 to 2012. The mean annual temperature is increased at four stations. Annual maximum daily is increased at two stations and annual minimum daily temperature is increased at six stations.

The results also suggest further investigations, to examine other meteorological series available in the Xedone River Basin, which could be useful in knowing the effect of the climate change in the study area.

References

Burn DH and Hag Elnur MA., 2002. Detection of hydrological trends and variability. Journal of Hydrology, 255: 107–122.

Delgado, J.M., Apel, H., & Merz, B., 2010. Flood trends and variability in the Mekong river. Hydrology and Earth System Sciences, 14, 407–418, 2010.

Duan, W., Takara, K., He, B., Luo, P., Hu, M., and Alias, N.E., Ishihara, M., and Yamashiki, Y., 2014. Changes of precipitation amounts and precipitation extremes in Japan, 1901-2012, Climate Dynamics, submitted, 2014.

Hamed, K.H., 2008. Trend detection in hydrologic data: The Mann–Kendall trend test under the scaling hypothesis. Journal of Hydrology, 349(3-4), 350-363. doi: 10.1016/j.jhydrol.2007.11.009.

Hamed, KH., Rao, A.R., 1998. A modified Mann-Kendall trend test for autocorrelated data. Journal of Hydrology 204, pp. 182-196.

Hirsch, RM., Slack, J.R., Smith RA., 1982. Techniques of trend analysing for monthly water quality data. Water Resources Research 18: 107–121.

Juahir, H., Zain, S.M., Aris, A.Z., Yusof, M.K., Samah, M.A.A., & Mokhtar, M.B., 2010. Hydrological Trend Analysis Due to Land Use Changes at Langat River Basin. EnvironmentAsia is the international journal published biannually by the Thai Society of Higher Education Institutes on Environment, (2010) 20-31.

Kahya, E., & Kalaycı, S., 2004. Trend analysis of streamflow in Turkey. Journal of Hydrology, 289(1-4), 128-144. doi: 10.1016/j.jhydrol.2003.11.006.

Longobardi, A., & Villani, P., 2009. Trend analysis of annual and seasonal rainfall time series in the Mediterranean area. International Journal of Climatology, n/a-n/a. doi: 10.1002/joc.2001.

Luo, P., He, B., Takara, K., Razafindrabe, B. H., Nover, D., & Yamashiki, Y., 2011. Spatiotemporal trend analysis of recent river water quality conditions in Japan. J Environ Monit, 13(10), 2819-2829. doi: 10.1039/c1em10339c.

Milliman, J. D., Farnsworth, K. L., Jones, P. D., Xu, K. H., & Smith, L. C., 2008. Climatic and anthropogenic factors affecting river discharge to the global ocean, 1951–2000. Global and Planetary Change, 62 (3-4), 187-194. doi: 10.1016/j. gloplacha. 2008.03.00.

Mu, X., Zhang, L., McVicar, T. R., Chille, B., & Gau, P., 2007. Analysis of the impact of conservation measures on stream flow regime in catchments of the Loess Plateau, China. Hydrological Processes, 21 (16), 2124-2134. doi: 10.1002/hyp.6391.

Partal, T., & Kahya, E., 2006. Trend analysis in Turkish precipitation data. Hydrological Processes, 20 (9), 2011-2026. doi: 10.1002/hyp. 5993

Qin, N., Chen, X., Fu, G., Zhai, J., & Xue, X., 2010. Precipitation and temperature trends for the Southwest China: 1960-2007. Hydrological Processes, 24(25), 3733-3744. doi: 10.1002/hyp.7792.

Su, B. D., Jiang, T., & Jin, W.B., 2005. Recent trends in observed temperature and precipitation extremes in the Yangtze River basin, China. Theoretical and Applied Climatology, 83(1-4), 139-151. doi: 10.1007/s00704-005-0139-y.

Tao, H., Gemmer, M., Bai, Y., Su, B., & Mao, W., 2011. Trends of streamflow in the

Tarim River Basin during the past 50years: Human impact or climate change. Journal of Hydrology, 400(1-2), 1-9. doi: 10.1016/j.jhydrol.2011.01.016.

Wang, S., & Zhang, X., 2012. Long-term trend analysis for temperature in the Jinsha River Basin in China. Theoretical and Applied Climatology, 109(3-4), 591-603. doi: 10.1007/s00704-012-0603-4.

Wu, F., Wang, X., Cai, Y., & Li, C., 2013. Spatiotemporal analysis of precipitation trends under climate change in the upper reach of Mekong River Basin. Quaternary International. doi: 10.1016/j.quaint.2013.05.049.

Xu, K.H., Milliman, J.D., Xu, H., 2010. Temporal trend of precipitation and runoff in major Chinese River since 1991. Global and Planetary Change, 219-232, doi: 10.10.1016/j. gloplacha. 2010.07.002.

Yu, Y.S., Zou, S., Whittenmore, D., 1993. Non-Parametric trend analysis of water quality data of rivers in Kansas. Journal of Hydrology, 15, pp. 61-80.

Chapter 3 Calibration and Validation of SWAT Model in the Xedone River Bsasin for Water Resources Assessment

3.1 Introduction

Water is a key resource for sustainable economic and social development. Due to the human activities (e.g., increasing global population Pangare, 2006), land use change (Vörösmarty, 2010), water pollution (Duan et al., 2013) and climate change, water shortages have become the major crises of sustainable development of communities all over the world. Therefore, to improve water resources, management is momentous for sustainable development of human society.

The Xedone River Basin is a sub-basin of the Mekong River Basin (MRB). The existing land and water resources system of the area are adversely affected by the rapid growth of population, construction, development, deforestation, surface erosion and sediment transport. There is a need for hydrological research in the Xedone River Basin that can support the improved catchment management programs and that can safeguard the alarming degradation of soil and water resources in Lao PDR highlands better. The analysis of water resources and flood disaster in the MRB have been carried out by my hydrological simulation studies for environmental impact assessment (Hydrological-solutions et at., 2001; Rossi et al., 2009). The Mekong River Commission has played the important role in addressing water resource problems by considering the population growth, environmental pollution, and urban development (Jacobs, 2002). The future hydro-climatology of the MRB has been studied by using the high-resolution Japan Meteorological Agency (JMA) AGCM (Kiem et al., 2008). An increase in the number of wet days in the 'future' has been found in the MRB. There is one report, which describes a brief introduction of the flood hazard map in the Xedone River Basin (Tanaka and Kuribayashi, 2010). However, we cannot find a detail study of the hydrological simulation in the Xedone River Basin. The hydrological modelling is quite important to predict the flood events in the future.

The Soil and Water Assessment Tool (SWAT) (Arnold et al., 1998) is a physically-based, long-term, distributed hydrological model, and it has been applied worldwide as an assessment model for hydrological modelling and water resource management. This model is applied to runoff and soil loss prediction (Morgan R.P.C, 2001; Grønsten and Lundekvam, 2006; Somzay and Ashish, 2013), water quality modelling (Debele et al, 2006; Zhang et al., 2011), land use change effect assessment (Sheng et al., 2003; Wu et al, 2007) and climate change affects water quality modelling (Abbaspour et al., 2007), land use change effect assessment (Wang et al., 2012) and climate change impact assessment (Andersson et al., 2006; Shrestha et al., 2013). A comprehensive review of SWAT model applications is given by Gassman et al. (2007). Several studies proposed calibration and uncertainty analysis using the SWAT model (Abbaspour et al., 2004; Yang et al., 2007).

In this study, SWAT model application and the uncertainty analysis will be carried out in the Xedone River Basin of Lao PDR. We focused on calibration, evaluation and application of SWAT2009 model for simulation of the hydrology of the Xedone River Basin. The main objective of this study is to test the performance and feasibility of the SWAT2009 model for prediction of stream flow in the Xedone River Basin, which will contribute to the water resources management in the Xedone River Basin and thereby is useful for the sustainable development of the country.

3.2 Data Collection

In this study, we collected geographical data and hydro-climate data for the SWAT model, including digital elevation model (DEM), soil data, land use and stream network layers. The weather and river discharge are also used for prediction of stream flow, model parameter calibration and validation in this study. The procedure is shown in **Figure 3.1**

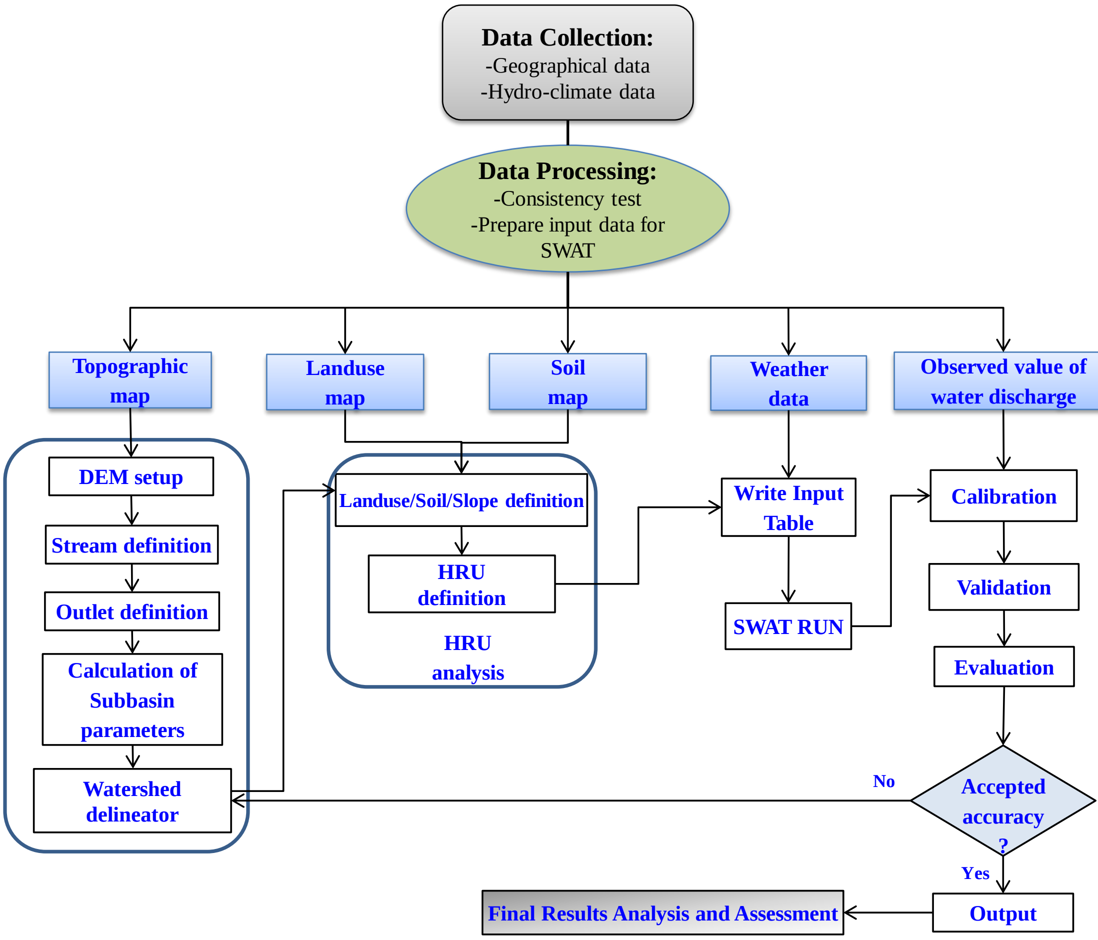

Figure 3.1 Flow chart for SWAT model application.

3.2.1 Geographical Data

(1) Digital Elevation Model (DEM)

Topography is defined by a DEM that describes the elevation of any point in a given area at a specific spatial resolution. A30 x 30 m resolution DEM was taken from the NASA citation link (http://www.yale.edu/ceo/Documentation/dem.html) as shown in **Figure 3.2**. The DEM is used to delineate the basin and to analyze the drainage patterns of the land surface terrain. Sub-basin parameters such as slope gradient, slope length of the terrain and the stream network characteristics such as channel slope, length and width were derived from DEM.

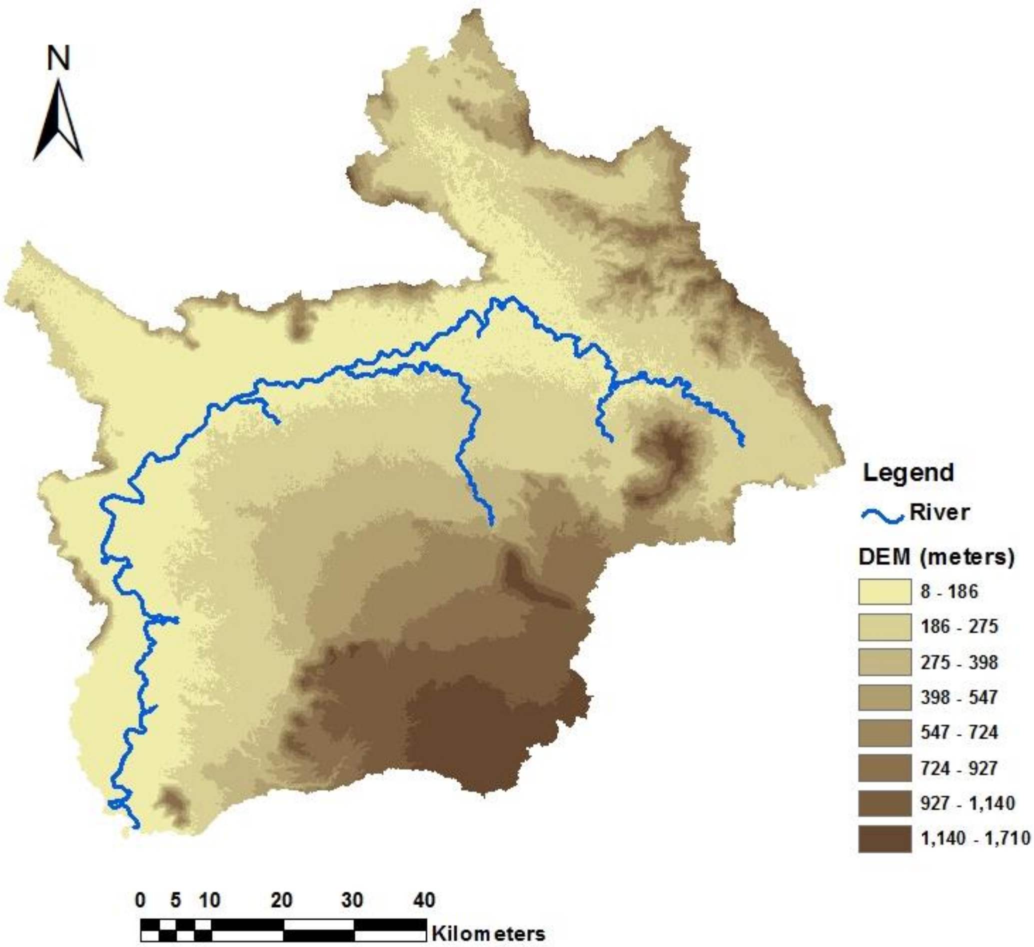

Figure 3.2 Digital Elevation Model (DEM) of the Xedone River Basin.

(2) Land Use

Land use is one of the most important factors that affect surface erosion, runoff, and evapotranspiration in the basin. The land use map of this study area is 50 m in the year 2002, obtained from Department of Meteorology and Hydrology, Ministry of Natural Resource and Environment, Lao PDR, We have reclassified the land use map of the area based on the available topographic map (1:50,000) scale field, aerial photographs and satellite images. The reclassification of the land use map is done to represent the land use according to the specific land cover types such as the type of crop, pasture and forest as shown in **Figure 3.3** and **Table 3.1**.

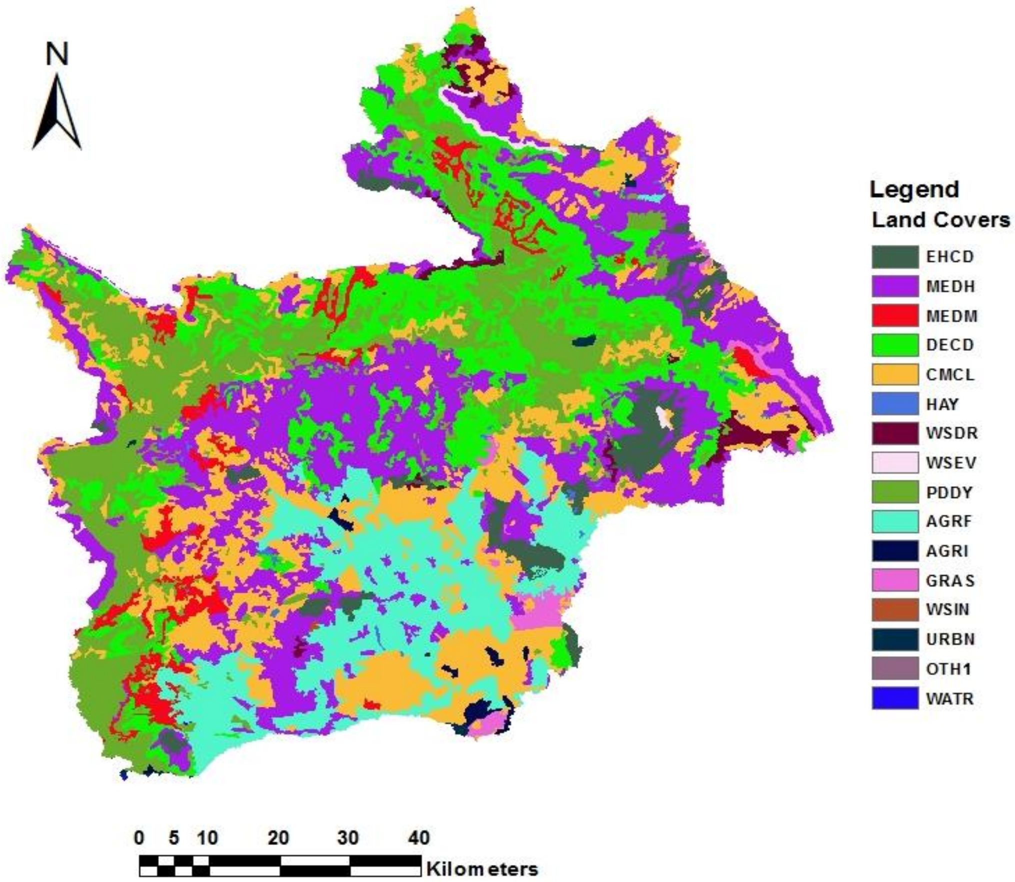

Figure 3.3 Land cover map of the Xedone River Basin.

Table 3.1 Land use class of the Xedone River Basin before threshold application.

No	Land use	SWAT code	Area (km^2)	Area %
1	Evergreen, high cover density	EHCD	253.64	3.51
2	Mixed (evg&dec) high cover density	MEDH	1758.18	24.34
3	Mixed (evg&dec) med-low cover density	MEDM	266.62	3.69
4	Deciduous	DECD	1189.72	16.47
5	Crop mosaic, cropping area>30	CMCL	1355.60	18.76
6	Hay	HAY	20.04	0.28
7	Wood and Shrub land dry	WSDR	93.76	1.30
8	Wood- and shrub land, evergreen	WSEV	33.00	0.46
9	LMB Paddy field	PDDY	1259.71	17.44
10	Agricultural land - transition	AGRF	863.03	11.95
11	Agricultural land - intensive	AGRI	30.45	0.42
12	Grassland	GRAS	84.13	1.16
13	Wood- and shrub land, inundated	WSIN	1.52	0.02
14	Urban or built over area	URBN	13.31	0.18
15	Other	OTH1	1.05	0.01
16	Water	WATR	0.84	0.01
	Total		7224.62	100

(3) Soil Data

The SWAT model requires different soil textural and physicochemical properties such as soil texture, available water content, hydraulic conductivity, bulk density and organic carbon content. For different layer of each soil type is shown in **Figure 3.4** and **Table 3.2**. These data are obtained from the Forest Inventory and Planning Division (FIPD) and the Ministry of Agriculture and Forestry, Lao PDR. For this study area was generated by field survey and interpolated from old map 1:250,000. The scale soil type maps in the year 1998. Major soil types in the Xedone River Basin are Acrisols, Cambisols and Luvisols (sandy, loamy, clay and gravity).

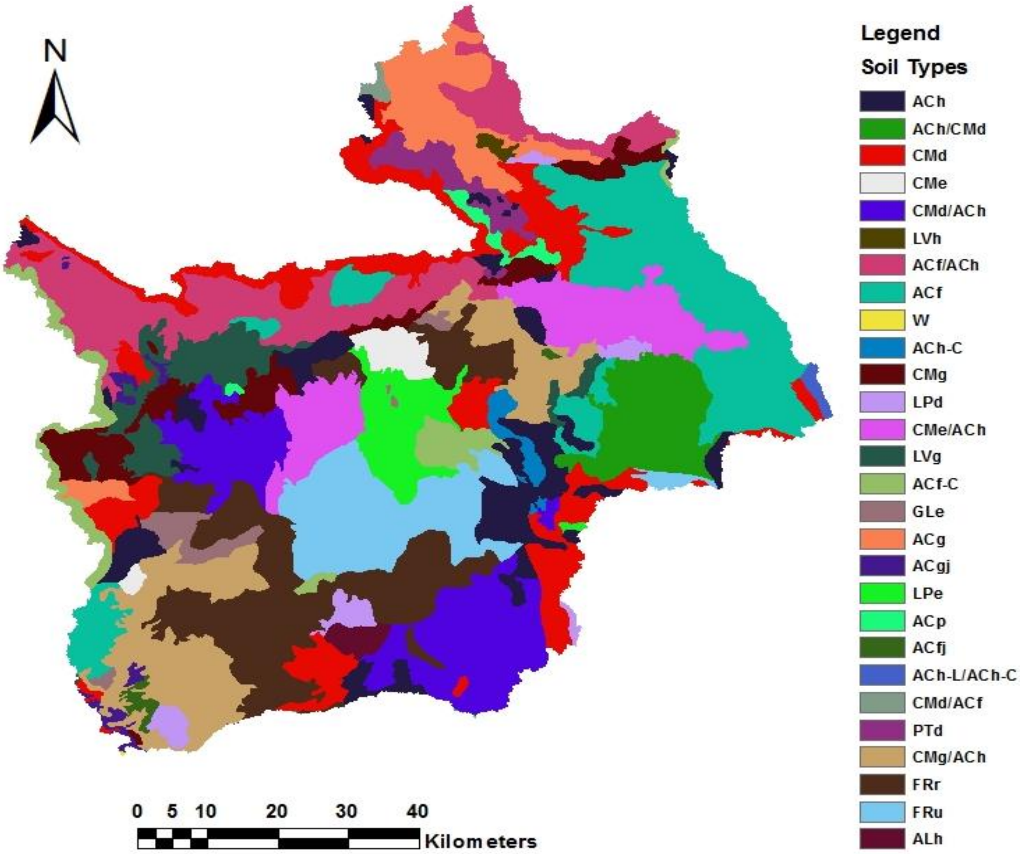

Figure 3.4 Soil type map of the Xedone River Basin.

Table 3.2 Soil class of the Xedone River Basin before threshold application.

No	Soil Details	SWAT code	Area (km^2)	Area (%)
1	HaplicAcrisols (clay)	ACh	450.02	5.61
2	Acrisols (clay)	ACh/CMd	314.36	3.92
3	Cambisols (loamy)	CMd	768.31	9.57
4	Cambisols (loamy)	CMe	83.58	1.04
5	Cambisols (loamy, clay)	CMd/ACh	616.89	7.69
6	Luvisols (clay)	LVh	14.74	0.18
7	Acrisols (loamy)	ACf/ACh	696.12	8.67
8	Ferric Acrisols (loamy)	ACf	894.69	11.15
9	Acrisols (loamy)	ACh-C	47.91	0.60
10	Cambisols (loamy)	CMg	287.72	3.59
11	Leptosols (loamy)	LPd	102.22	1.27
12	Cambisols (loamy, clay)	CMe/ACh	451.59	5.63
13	Luvisols (clay)	LVg	261.18	3.25
14	Acrisols (loamy	ACf-C	197.00	2.45
15	Glaysols (clay)	GLe	91.58	1.14
16	GleyicAcrisols (clay)	ACg	322.64	4.02
17	Acrisols (clay)	ACgj	44.50	0.55
18	Leptosols (loamy)	LPe	215.15	2.68
19	Plinthic Acrisols (clay)	ACp	42.20	0.53
20	Acrisols (loamy)	ACfj	24.48	0.31
21	Acrisols (loamy)	ACh-L/ACh-C	17.14	0.21
22	Cambisols (loamy, clay)	CMd/ACf	14.48	0.18
23	Leptosols (loamy)	PTd	111.35	1.39
24	Cambisols (loamy, clay)	CMg/ACh	602.24	7.50
25	Ferransols (clay)	FRr	828.28	10.32
26	Ferransols (loamy)	FRu	485.70	6.05
27	Haplic Alisols (loamy)	ALh	40.72	0.51
	Total		7224.62	100

3.2.2 Hydro-Climate Data

(1) Rainfall

Observed daily rainfall data for 20 years (1990-2009) from seven stations are used to import the model. All of rainfall stations are namely Batieng, Khongxedone, LaoNgam, Nikhom34, Pakse, Paksong, Saravan and Selabam. These data are aggregated to sub-basins by using a MQUAD program (Shrestha et al., 2013) in the MRC toolbox of the Mekong River Commission (MRC). MQUAD is based on multiquadric analysis developed by Hardy. (1971). In MQUAD generates estimations of areal rainfall (catchment averaged rainfall) by calculating a multi-quadratic surface from available point rain gauge data, such as the surface passes through all gauge points. The surface is defined for a user specified area, consisting of one or more catchments, and is made up from a grid of estimated point rainfall values calculated by the software. The values at each grid are then aggregated to produce a mean rainfall depth for each catchment. This process is repeated for each time step of the input point rainfall datasets.

(2) Climate Data

SWAT requires daily climate data that can be read either from a measured data set or be generated by a weather generator model. The weather variables used in this study for driving the hydrological model consist of daily maximum and daily minimum temperature, wind speed, solar radiation, and relative humidity. The daily rainfall is described above and temperature, wind velocity, solar radiation, and humidity record of 20 year (1990-2009) are used to develop the climate input files required for the model. All of the data are obtained from the Meteorology and Hydrology Department., Ministry of Natural Resource and Environment in Lao PDR. Stations name of the data include with the Khongxedone, LaoNgam, Nikhom34, Pakse, Paksong and Saravan are used for the model, except solar radiation only four gauges are used as Nikhom34, Pakse, Paksong and Saravane, all of meteorology data stations are shown in **Figure 3.5**.

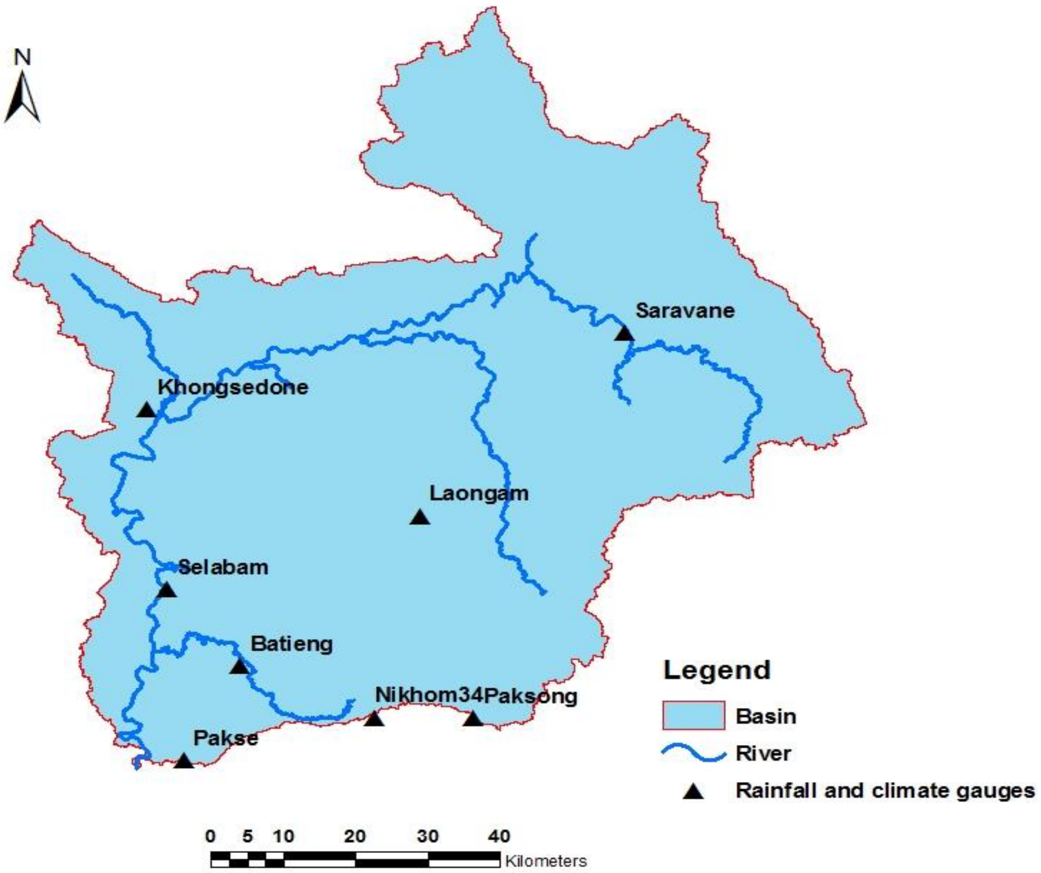

Figure 3.5 Rainfall and climate gauges of the Xedone River Basin.

(3) Discharge Data

Observed daily discharge data during in the year 1990-2008 at Souvannakhili station were obtained from Department of Meteorology and Hydrology, Ministry of Natural Resource and Environment. Annual average discharge at Souvannakhili is 179.43 m^3/s, the discharges from this station are used for calibration and validation of the ArcSWAT hydrological model, the station of discharge is shown in the **Figure 3.6**.

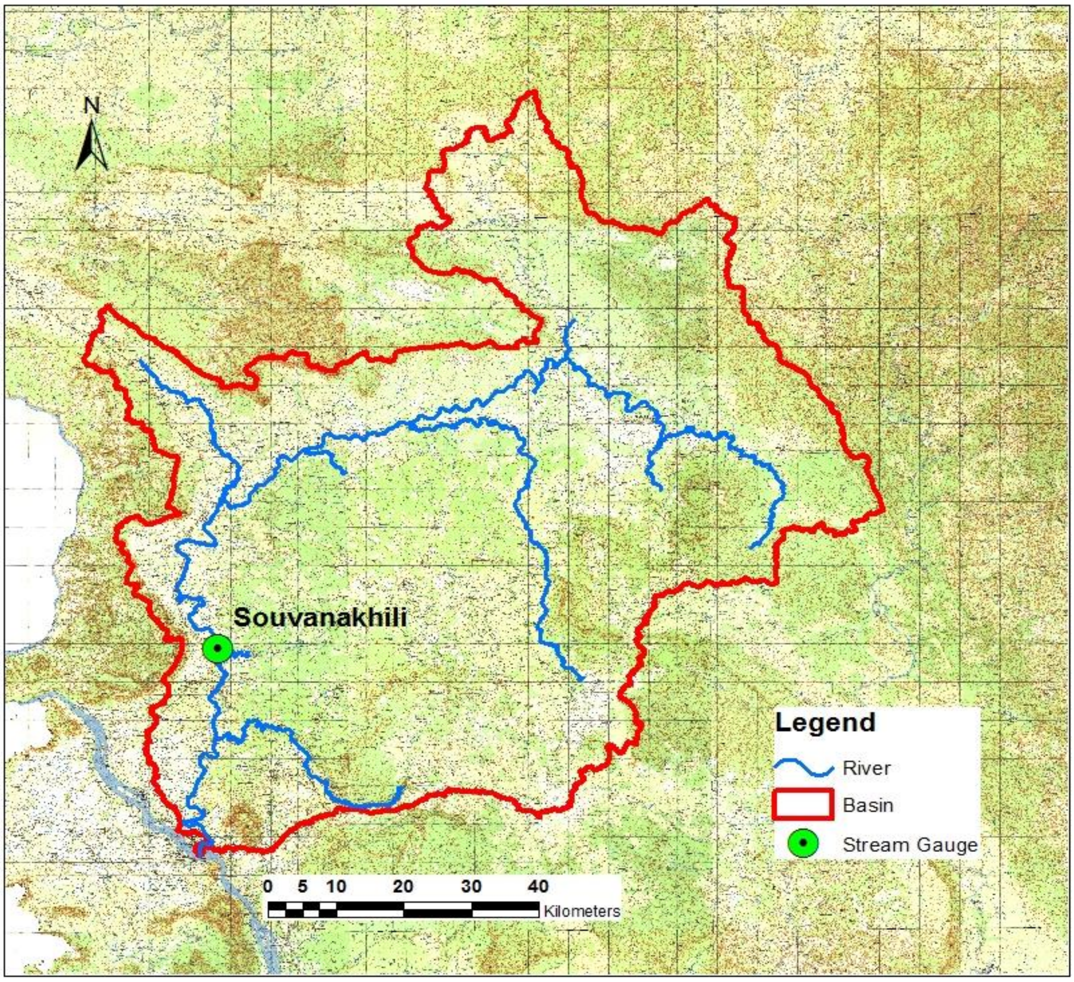

Figure 3.6 Stream gauge of the Xedone River Basin.

3.3 Methods

3.3.1 SWAT Model

The SWAT model is a physically-based continuous time, spatially distributed model designed to simulate water, sediment, nutrient and pesticide transport at a catchment scale on a daily time step. It uses hydrological response units (HRUs) that consist of specific land use, soil and slope characteristics. The HRUs are used to describe the spatial heterogeneity in terms of land cover, soil type and slope class within a watershed. The model estimates relevant hydrological components such as evapotranspiration, surface runoff and peak rate of runoff, groundwater flow and sediment yield for each HRU. ArcSWAT ArcGIS extension is a graphical user interface for the SWAT model. The SWAT model is developed and refined by the U.S. Department of Agricultural Research Service (ARS) and scientists at universities and research agencies around the world. The water balance equation is the base of the hydrologic cycle simulation in SWAT:

$$SW_t = SW_0 + \sum_{i=1}^{t} (R_{day} + Q_{surf} - E_a - w_{seep} - Q_{gw}) \qquad (3.1)$$

in which SW_t is the final soil water content (mm), SW_0 is initial soil water content on day i (mm), t is the time (days), R_{day} is the amount of precipitation on day i (mm), Q_{surf} is the amount of surface runoff on day i (mm), E_a is the amount of evapotranspiration on day i (mm), w_{seep} is the amount of water entering the vadose zone from the soil profile on day i (mm), and Q_{gw} is the amount of return flow on day i (mm).

In this study, the SCS runoff equation is an empirical model that came into common use in the 1950s. It was the product of more than 20 years of studies involving rainfall-runoff relationships from small rural watersheds across the U.S. The model was developed to provide a consistent basis for estimating the amounts of runoff under varying land use and soil types (Rallison and Miller, 1981). The SCS curve number equations (3.2) is described by (SCS, 1972).

$$Q_{surf} = \frac{(R_{day} - 0.2S)^2}{(R_{day} + 0.8S)} \qquad (3.2)$$

in which, S is the retention parameter (mm), which is defined by equation (3.3).

$$S = 25.4\left(\frac{100}{CN} - 10\right) \qquad (3.3)$$

The SCS curve number is function of the soil's permeability, land use and antecedent soil water condition and CN is the curve number for the day and is a function of soil's permeability, land use and antecedent moisture condition.
The steady-state response of groundwater flow to recharge is (Hooghoudt, 1940):

$$Q_{gw} = \frac{8000 \cdot K_{sat}}{L_{gw}^{2}} \cdot h_{wtbl} \qquad (3.4)$$

in which K_{sat} is the hydraulic conductivity of the aquifer (mm/day), L_{gw} is the distance from the ridge or sub-basin divide for the groundwater system to the main channel (m), and h_{wtbl} is the water table height (m).

3.3.2 SWAT-CUP

The SWAT-CUP is a computer program for the calibration of SWAT models. SWAT-CUP is a public domain program. The program is linked to five different algorithms such as Sequential Uncertainty Fitting SUFI-2 (Abbaspour et al., 2004; Abbaspour et al., 2007) Particle Swarm Optimization, (POS), Generalized Likelihood Uncertainty Estimation (GLUE) (Beven and Binley, 1992), Parameter Solution (ParaSol) (Alamirew, 2006), and Markov chain Monte Carlo (MCMC) (Kassa and Foerch, 2007) procedures to SWAT. It enables sensitivity analysis, calibration, validation, and uncertainty analysis of SWAT models. Therefore, the SUFI-2 methods are applied in this study. The brief descriptions and procedures of SUFI-2 are given below.

SUFI-2

The parameter uncertainty is calculated from all the input and output source uncertainties such as the uncertainty in the input rainfall data, the land use and soil type, parameters, and observed data, in SUFI-2. The simulation uncertainty is quantified by the 95% prediction uncertainty (95PPU) which is referred to as the p-factor. The 95PPU is calculated at the 2.5% and 97.5% levels of the cumulative distribution of an output variable obtained through Latin hypercube sampling (Abbaspour et al., 2007). Another measure quantifying the strength of a calibration or uncertainty analysis is the r-factor which is the average thickness of the 95PPU band divided by the standard deviation of the measured data.

The goodness of calibration and prediction uncertainty is judged based on the closeness of the p-factor to 100% (i.e., all observations bracketed by the prediction uncertainty) and the r-factor to 1 (i.e., achievement of a rather small uncertainty band) (Hornberger et al., 2009; Talebizadeh et al., 2009). If the two factors are in satisfactory values, a uniform distribution in the parameter hypercube is explained as the following parameter distribution. The goodness of fit in SUFI-2 is quantified by the R^2 and Nash-Sutcliffe (NS) coefficient between the observed data and the best simulation. The average thickness of the 95PPU band ($\bar{r}$) and the r-factor are calculated by equations (3.5) and (3.6). (Luo et al., 2014).

$$\bar{r} = \frac{1}{n}\sum_{t_i}^{n}\left(y^M_{t_i,97.5\%} - y^M_{t_i,2.5\%}\right) \tag{3.5}$$

$$r - factor = \frac{p - factor}{\sigma_{obs}} \tag{3.6}$$

in which $y^M_{t_i,97.5\%}$ and $y^M_{t_i,2.5\%}$ represent the upper and lower boundaries of the 95PPU, and σ_{obs} is the standard deviation of the measured data.

The other factor is the goodness of fit that can be quantified by the coefficient of determination (R^2) and Nash-Sutcliff efficiency (NSE) (Setegn et al., 2008) between the observations and the final best simulations. Coefficient of determination (R^2) and Nash-Sutcliffe coefficient (NSE) are calculated by equation (3.7) and (3.8).

$$R^2 = \frac{\left[\sum_i (Q_{m,i} - \bar{Q}_m)(Q_{s,i} - \bar{Q}_s)\right]^2}{\sum_i (Q_{m,i} - \bar{Q}_s)^2 \sum_i (Q_{s,i} - \bar{Q}_s)^2} \tag{3.7}$$

$$NSE = 1 - \frac{\sum_i (Q_m - Q_{s,i})^2}{\sum_i (Q_{m,i} - \bar{Q}_m)^2} \tag{3.8}$$

in which Q_m is the measured discharge (m^3/s), Q_s is the simulated discharge (m^3/s), $\bar{Q}_m$ is the average measured discharge (m^3/s) and $\bar{Q}_s$ is the average simulated discharge (m^3/s).

3.3.3 Model Setup

(1) Data Preparation

The spatially distributed data (GIS input) needed for the ArcSWAT interface include the Digital Elevation Model (DEM), soil data, land use and stream network layers. The non-spatial data on weather and river discharge are also used for prediction of river discharge and calibration purposes as described above.

(2) Basin Delineation

Basin delineation depends on the DEM to delineate the watershed and to analyze the drainage patterns of the land surface terrain. The ArcSWAT interface uses the mask area for stream delineation, and the stream networks are delineated from the DEM by using an automatic delineation to the SWAT model. The model fills all of the non-draining zones to create a flow direction, and superimposes the digitized stream network into the DEM to define the location of stream networks.

The ArcSWAT proposes the minimum, maximum and suggested size of the sub-basin area in hectare to define the minimum drainage area. Generally, the smaller the threshold area, the more detailed the drainage networks and the number of sub-basins and HRUs. In addition, more processing times and spaces are needed. In this study, the smaller area (50 km^2) is provided to get all sub-basin of the Xedone River Basin and outlet is defined, in which it is later taken as a point of calibration of the simulated flows. As a result, there are 17 sub-basins of the Xedone River Basin as shown in **Figure 3.7**.

Successful execution of terrain processing module of ArcSWAT interface resulted in generation of appropriate databases for the sub-basin parameters and detailed topographic report of the basin, area elevation statistics of each sub-basin is shown in **Table 3.3**.

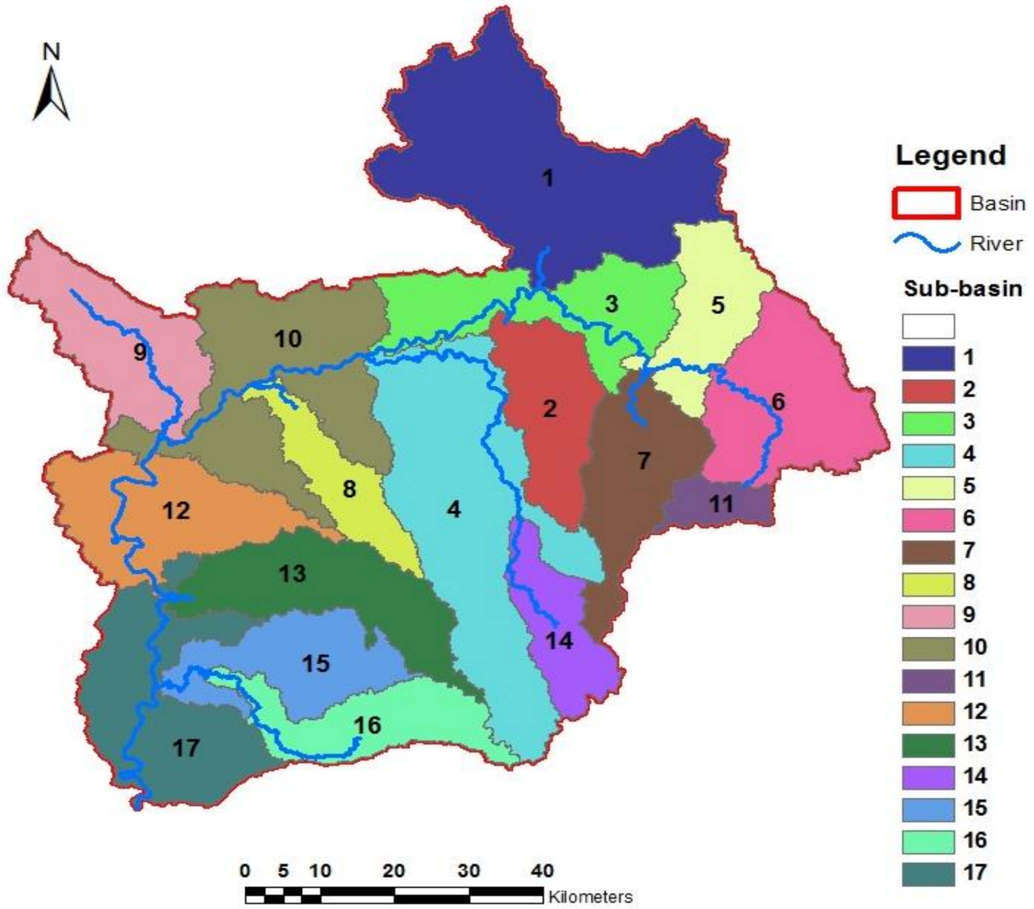

Figure 3.7 Sub-basin delineation and discharge network of the Xedone River Basin.

Table 3.3 Topographic statistics of sub-basin in the Xedone River Basin.

Sub basin	**Minimum** elevation (m)	**Maximum** elevation (m)	**Mean** elevation (m)	**Area** (km^2)	**Area** (%)
1	116	1346	309.19	962.72	13.33
2	142	798	276.74	302.24	4.18
3	89	1076	226.23	418.88	5.80
4	123	1600	590.89	891.22	12.34
5	135	1362	400.53	274.28	3.80
6	133	1602	374.33	454.58	6.30
7	148	1603	551.55	350.56	4.85
8	119	662	323.99	204.70	2.83
9	98	609	173.97	381.69	5.28
10	80	873	210.77	666.71	9.23
11	217	1364	513.63	86.86	1.20
12	75	708	184.49	441.43	6.11
13	109	1282	496.59	420.35	5.82
14	492	1706	1042.5	220.93	3.06
15	70	1219	485.05	327.53	4.53
16	130	1427	827.52	300.94	4.17
17	8	922	173.35	518.99	7.18
		Total		7224.62	100

(3) Hydrologic Response Unit (HRU) Definition

The analysis of HRU definition indicates that dominant type of HRU definition results in a single HRU for each sub-basin where the dominant land use, soil and slope within the basin are considered to be the land use, soil and slope of each sub-basin. This single HRU within each sub-basin is not able to properly represent the characteristics of the sub-basins. Accordingly, the simulated river discharge shows the unsatisfactory result as compared to the measured discharge flows in the observed stations of the Xedone River Basin. The multiple scenarios that account for 15% land use, 15% soil and 15% slope threshold combination give a better estimation of discharge flow. The Xedone River Basin results in 230 HRUs in the whole basin. This scenario results in the detailed land use, slope and soil database, containing many HRUs, which in turn represent the heterogeneity of the study area. The comparison between the default model predictions and measured discharge produces the highest Nash-Sutcliffe efficiency (NSE). The distribution of land use, soil and slope characteristics within each HRU have the greatest impact on the predicted river discharge. As the percentage of land use, slope and soil threshold increases, the actual evapotranspiration decreases due to eliminated land use classes. Hence, the characteristics of HRUs are the key factors affecting the stream flow. The final area under each land use, soil and slope class after threshold criteria, the application is given in **Tables 3.4**, **Tables 3.5**, and **Tables 3.6**.

Table 3.4 Land use class of the Xedone River Basin after threshold application.

No	**Land use**	**SWAT** code	**Area** (km^2)	**Area** %
1	Mixed(evg&dec), high cover density	MEDH	2143.77	29.67
2	Deciduous	DECD	1176.47	16.28
3	Crop mosaic-cropping area >30	CMCL	1339.71	18.54
4	LMB Paddy field	PDDY	1233.82	17.08
5	Agricultural land - transition	AGRF	1025.60	14.20
6	Evergreen, high cover density	EHCD	192.69	2.67
7	Mixed (evg&dec) med-low cover de	MEDM	112.57	1.56
	Total		7224.62	100

Table 3.5 Soil class of the Xedone River Basin after threshold application.

No	Soil Details	SWAT code	Area (km^2)	Area (%)
1	Ferric Acrisols (loamy)	ACf	946.45	13.10
2	Acrisols (loamy)	ACf/ACh	800.02	11.07
3	Cambisols (loamy)	CMd	640.28	8.86
4	GleyicAcrisols (clay)	ACg	283.71	3.93
5	Cambisols (loamy, clay)	CMg/ACh	659.70	9.13
6	Ferransols (clay)	FRr	844.49	11.69
7	HaplicAcrisols (clay)	ACh	269.09	3.72
8	Cambisols (loamy, clay)	CMe/ACh	475.93	6.59
9	Cambisols (loamy)	CMe	79.58	1.10
10	Leptosols (loamy)	LPe	182.98	2.53
11	Cambisols (loamy, clay)	CMd/ACh	739.01	10.23
12	Ferransols (loamy)	FRu	509.19	7.05
13	Acrisols (clay)	ACh/CMd	291.35	4.03
14	Cambisols (loamy)	CMg	132.68	1.84
15	Acrisols (loamy	ACf-C	91.35	1.26
16	Luvisols (clay)	LVg	185.60	2.57
17	Glaysols (clay)	GLe	28.57	0.41
18	Leptosols (loamy)	LPd	41.16	0.57
19	Haplic Alisols (loamy)	ALh	23.46	0.32
	Total		7224.62	100

Table 3.6 Slope class of the Xedone River Basin after threshold application.

No	Slope ranges (%)	Area (km^2)	Area (%)
1	0-2	197.92	2.74
2	2-10	3812.57	52.77
3	10-45	2903.61	40.19
4	>45	310.52	4.30
	Total	7224.62	100

(4) Weather Data Input

Weather data to be used in a basin simulation is imported once the HRU distribution has been defined. The weather data are formulated in dbf file conforming to the ArcSWAT format.

Location for the outlet of the basin, weather gauge, temperature gauge, relative humidity gauge, solar radiation gauge and wind gauge namely as shown in **Figure 3.5**, are prepared in dBase format as per Data Transfer Tool (DTT) embedded in the MRC Toolbox. Coordinates have been provided in term of X and Y projected coordinates for all gauging stations and watershed outlet, accepted the precipitation station namely Batieng, Khongxedone, LaoNgam, Pakse, Paksong, Saravan and Selabam stations. In a period of 1990-2008 is prepared according to ArcSWAT format by DTT and MQUAD embedded in MRC Toolbox as described in (3.2.2 Rainfall) and integrated into the model using the weather data input wizard.

(5) Calibration and Validation Model

The calibration is the modification or adjustment of model parameters, within the recommended ranges, to optimize the model output so that it matches with the observed set of data. The calibration provides several different parameters for adjustment through user intervention. These parameters can be adjusted manually or automatically until the model output best matches with the observed data. This study is done by applying SWAT-CUP for calibrating outlet stream flow. The validation is the process of determining the degree in which a model or simulation is an accurate representation of the observed set of data from the perspective of the intended uses of the model. The discharge data were recorded during the years 1990-2008 at Souvannakhili station, and the daily discharges from the years 1990-1992 it was skipped for model warm-up.

The model calibration of this study is done by Calibration and Uncertainty Programs for SWAT called **SWAT-CUP** and this study is calibrated and validated as described below, the model performance can be evaluated using established indices mainly like coefficient of determination R^2, Nash-Sutcliffe efficiency NSE and others embedded in SWAT-CUP. The sensitive parameters are considered the model calibration in SWAT-CUP model. The models are calibration period 1993-2000 and validation period 2001-2008.

(6) Sensitive Analysis

SWAT model is a comprehensive conceptual model and use several parameters varying widely in space and time while transforming inputs into output. To obtain the useful results, each parameter entered in the form of database tables needs to be assigned a value representative to the condition of the study basin. To arrive at appropriate value for a parameter, it is necessary to understand the relative sensitivity of a parameter in terms of model computed outputs.

A sensitivity analysis also identifies the most sensitive parameters, which ultimately dictates the set of parameters to be used in the subsequent calibration process. A sensitivity analysis was performed for parameters governing surface, subsurface and basin response. Parameters related to snowmelt, nutrient and pesticide transport were excluded from sensitivity analysis as the basin under study does not have snow melt contribution and nutrient and pesticide transport is not being studied in the current application. Result of sensitivity analysis in terms of order of sensitivity of parameters, starting from the most sensitive to least sensitive parameter is shown in **Table 3.7.**

3.4 Results and Discussions

3.4.1 Parameter Sensitivity Analysis

In this study, we have evaluated the relative sensitivity values of the parameters during model calibration by SWAT-CUP. Among twelve parameters, the following parameters are found to be sensitive with the relative sensitivity values. The sensitive parameters include initial SCS runoff curve number to moisture condition II (CN2), base flow alpha factor (ALPHA_BF), groundwater delay time (GW_DELAY), threshold depth of water in the shallow aquifer for return flow to occur (GWQMN), groundwater "revap" coefficient (GW_REVAP), soil evaporation compensation factor (ESCO), Manning's "n" value for the main channel (CH_N2), effective hydraulic conductivity in main channel alluvium (CH_K2), base-flow alpha factor for bank storage (ALPHA_BNK), available water capacity of the soil layer (SOL_AWC), saturated hydraulic conductivity (SOL_K), and moist bulk density (SOL_BD) based on the sensitivity analysis.

The most sensitive parameters for the calibration of the discharge are the ones governing the surface runoff response, the subsurface response, and the basin response. All of them parameters were calibrated by SUFI-2, shown in **Table 3.8**.

Table 3.7 Sensitive parameters and fitted values after calibration using SUFI-2.

Parameter name	Rank	Fitted value	Min value	Max value
r__CN2.mgt	1	0.684	0.583	0.691
v__ALPHA_BF.gw	2	-0.047	-0.051	-0.037
v__GW_DELAY.gw	3	205.951	196.110	208.316
a__GWQMN.gw	4	2.546	2.499	2.619
v__GW_REVAP.gw	5	0.154	0.147	0.156
v__ESCO.hru	6	0.943	0.921	0.959
v__CH_N2.rte	7	0.634	0.598	0.672
v__CH_K2.rte	8	126.312	125.130	127.025
v__ALPHA_BNK.rte	9	0.684	0.676	0.727
r__SOL_AWC .sol	10	0.163	0.155	0.170
r__SOL_K .sol	11	0.726	0.676	0.747
r__SOL_BD .sol	12	0.166	-0.069	0.396

3.4.2 Daily Calibration and Validation

The comparison between simulated daily stream flow and observed data is a good result for the calibration and validation, periods respectively. The flow calibration and validation were performed for eight years from 1993 to 2000 for calibration and from 2001 to 2008 for validation. However, the flow had been simulated for sixteen years, including one year of the warm-up period. The simulated daily flow matches the observed values for the calibration and validation periods with R^2 = 0.821, 0.732 and NSE = 0.819, 0.707 respectively. The coefficients of the simulation are shown in **Figure 3.8, Figure 3.9** and **Table 3.6**, in which there is a good agreement between simulated and gauged flows. From the hydrograph of the daily observed and simulated flows shown in that we can see that the simulated flows closely match the observed flows, except on 18/09/1996 when the peak of the simulation is high, because heavy rainfall during this month of year in Laos. The results show that SWAT is able to simulate the hydrological characteristics of the Xedone River Basin very well. Hence, the model can be used for further hydrological studies in the basin.

Table 3.8 Statistical analysis of simulated and observed daily discharges at Souvannakhili station.

Time period	**Observed 1993-2008**	**Simulated 1993-2008**
Mean (m^3/s)	179.43	159.21
Standard deviation (m^3/s)	370.18	293.47
Maximum (m^3/s)	3793.79	3851
Time period	**Calibrated 1993-2000**	**Validated 2001-2008**
Coefficient of determination R^2	0.821	0.732
Nash-Sutcliffe efficiency NSE	0.819	0.707

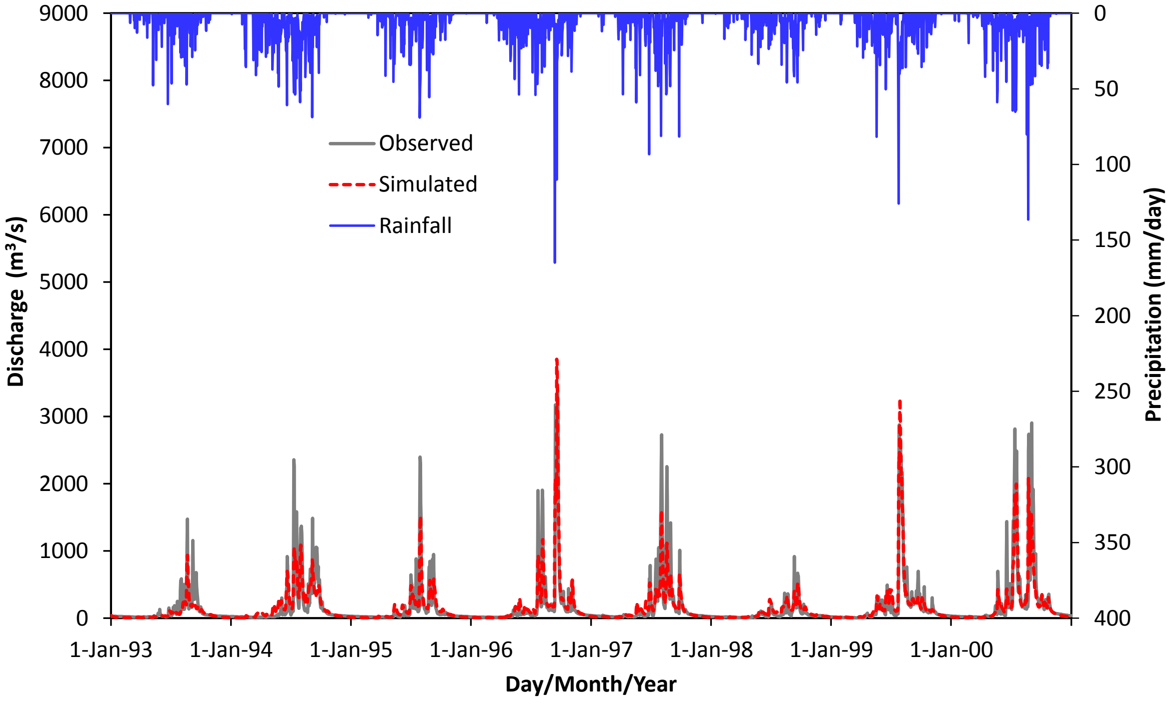

Figure 3.8 Simulated and observed daily river discharges for the calibration (1993-2000)

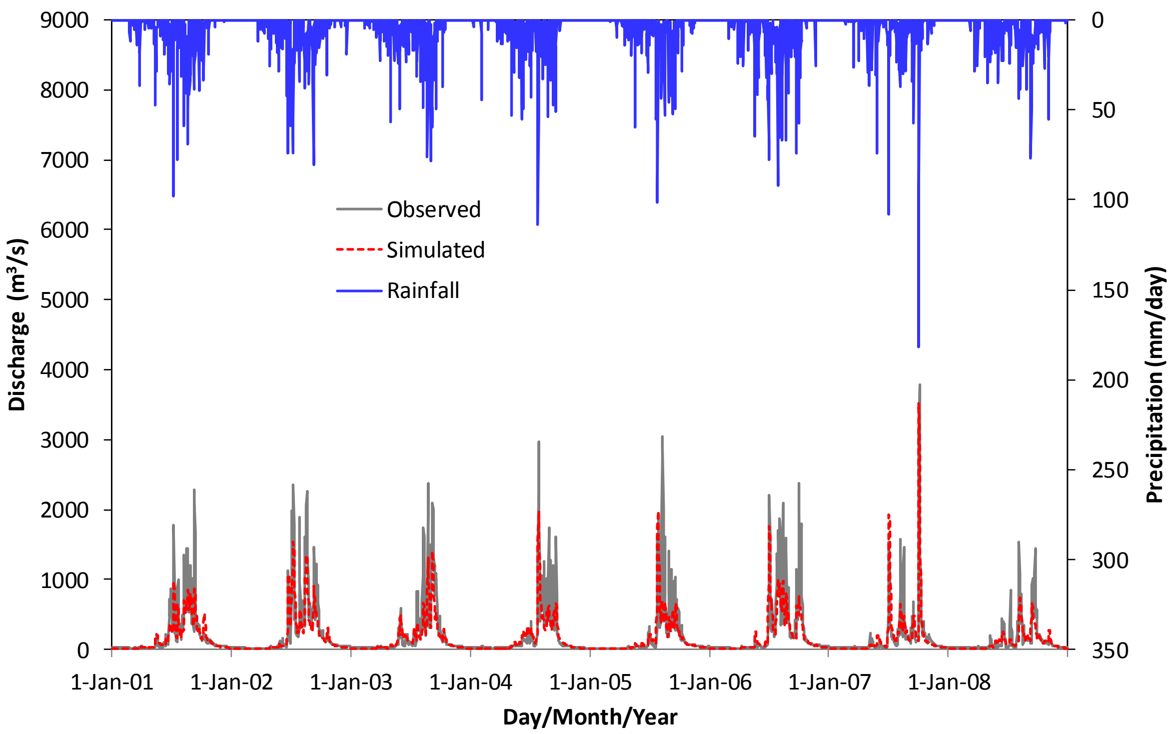

Figure 3.9 Simulated and observed daily river discharges for the validation (2001-2008)

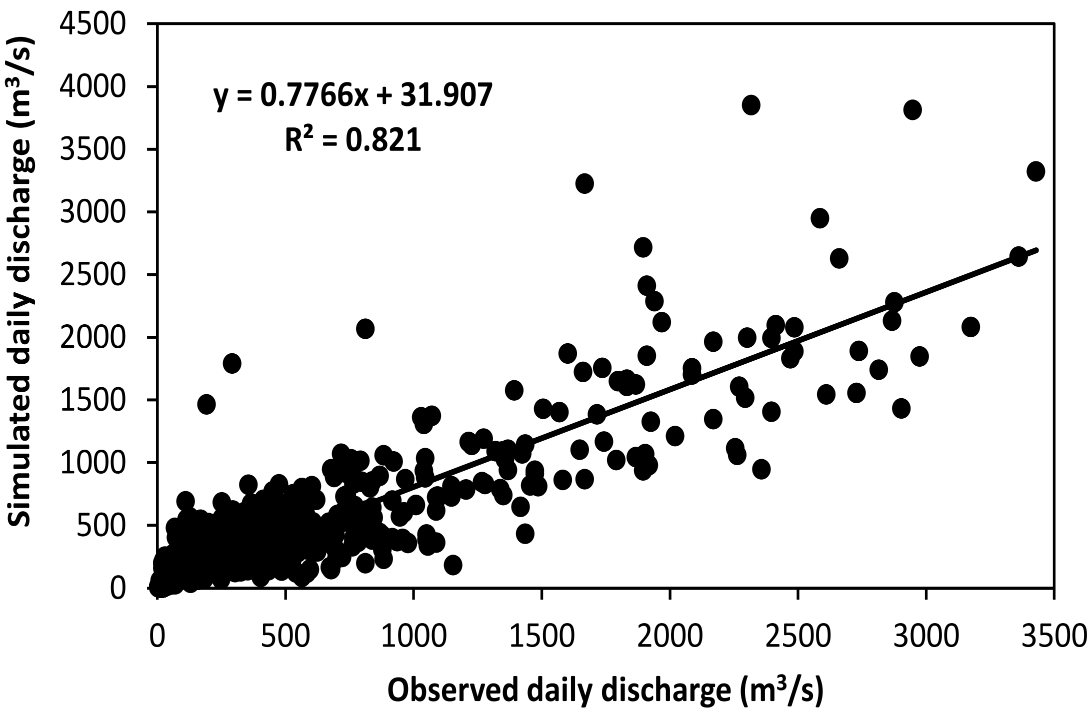

Figure 3.10 Scatter plot of the daily discharges for the calibration period (1993-2000)

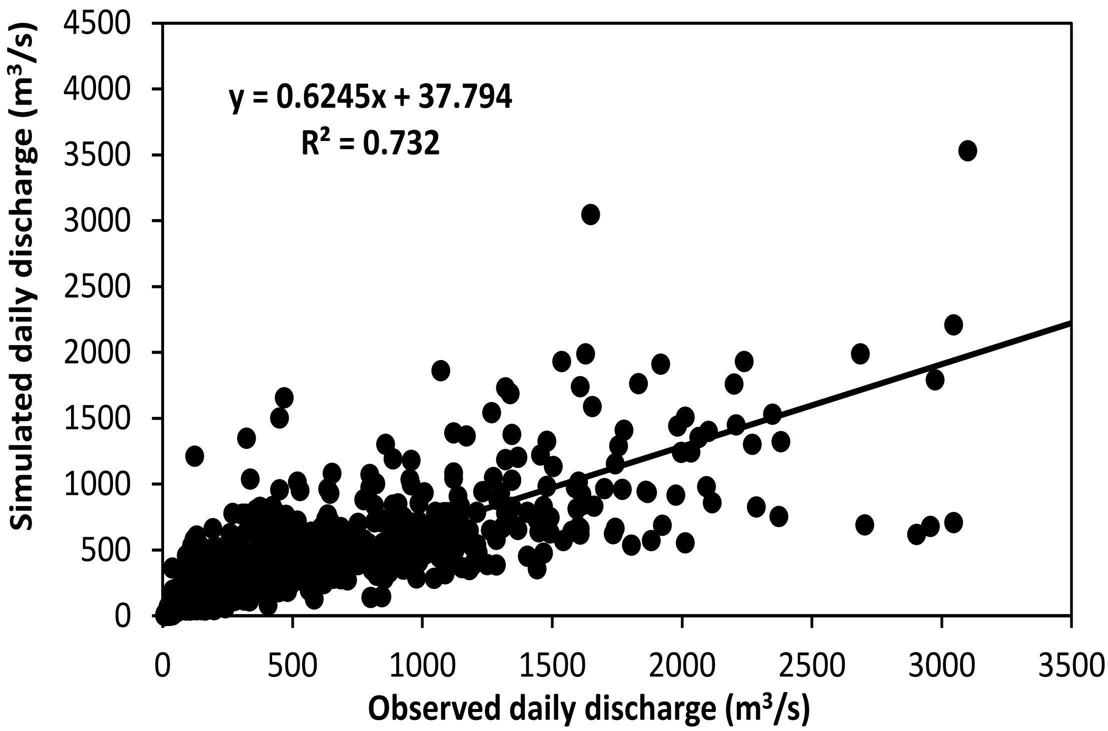

Figure 3.11 Scatter plot of the daily discharges for the validation period (2001-2008)

3.4.3 Simulated Monthly Discharge

The comparison of the observed and simulated monthly discharges for the Souvanakhili station during the calibration period (1993-2000) is presented in **Figure 12.** Comparing of the monthly hydrographs between simulated and observed of the discharge at Souvannakhili station during validation period (2001-2008), we can see that the SWAT model under-predicts the high peak values as shown in **Figure 3.13**. The poor prediction of the peak flows of the SWAT model has been reported by some researchers. The performance of the SWAT model for the study area is very good during the validation period also with R^2> 0.80 and NSE> 0.80 for the gauging sites. Therefore, the SWAT model can be adopted for the hydrological evaluation of the MRB or all of the basin in Lao PDR. From these hydrographs observed and simulated flows were shown at the peak of stream flow during in September, 1996. This year, is heavy rainfall in China, Laos, Vietnam and Cambodia. Many areas were inundated by affecting from the Mekong River Basin (http://www.adrc.asia/countryreport/KHM/KHMeng02 /Cambodia 3.htm). However, the same thing is not reflected in the observed runoff data in **Figure 3.8.** It is assumed that there may be some uncertainty in the data. Scatter plots of the simulated and observed monthly discharges of the Souvanakhili station during the calibration and validation periods are presented in **Figure 3.14** and **Figure 3.15**. Both plots show relatively good R^2values: 0.927 and 0.910, respectively.

From **Table 3.7**, the Nash-Sutcliffe efficiency (NSE), it generally ranges from 0 to 1. Value of (NSE) is greater than 0.65 indicates better model prediction, whereas lower (NSE) indicates a poor model prediction; Saleh et al. (2004).

Moriasi et al. (2007) presented general performance ratings of the SWAT model for monthly time step simulations. Based on these recommendations, the performance of SWAT model for the study area is **very good** during the calibration period of NSE > 0.65, and less value of NSE is assumed that there may be some uncertainty in the data.

Based on goodness-of-fit criteria for model evaluation and recommendation the above-indicated are acceptable for baseline. The same is ready to use for Xedone River Basin scenarios.

Table 3.9 Results of the monthly simulated and observed at Souvannakhili station.

	Calibrated	**Validated**
Time period	**1993-2000**	**2001-2008**
Coefficient of determination R^2	0.927	0.910
Nash-Sutcliffe efficiency (NSE)	0.925	0.856

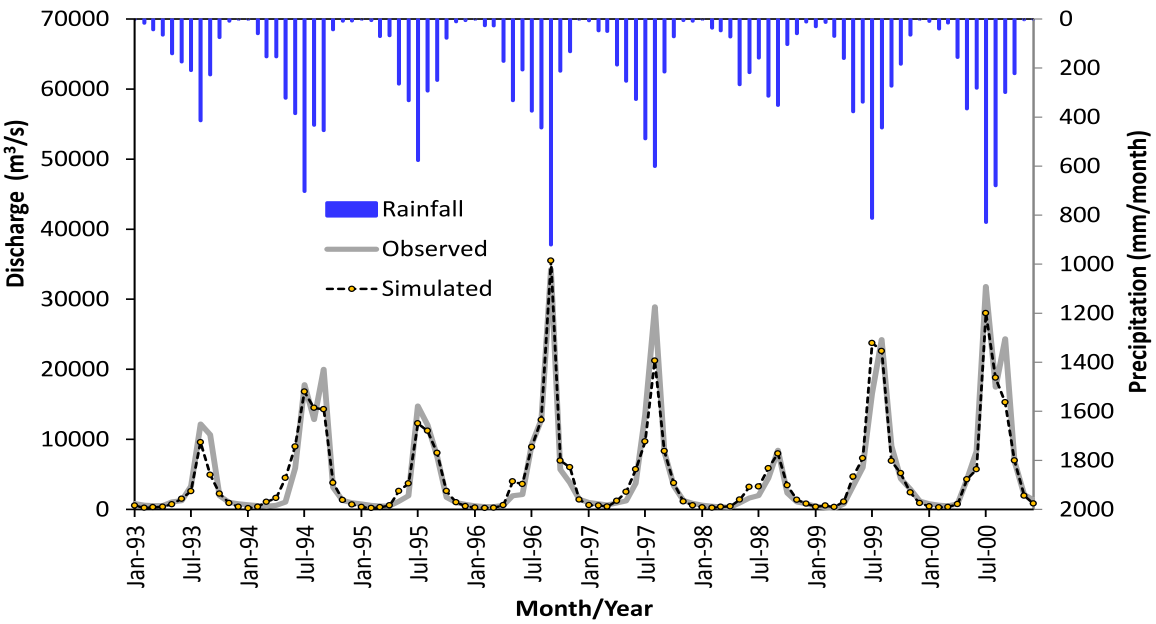

Figure 3.12 Result of the calibration of the monthly discharge period (1993-2000)

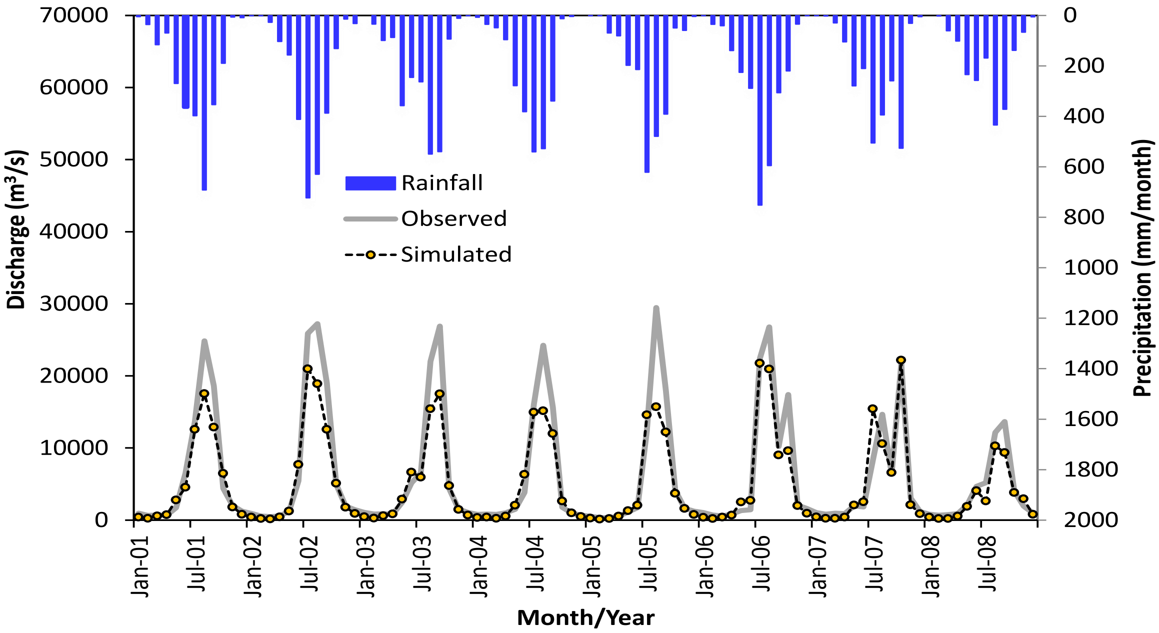

Figure 3.13 Result of the validation of the monthly discharge (2001-2008)

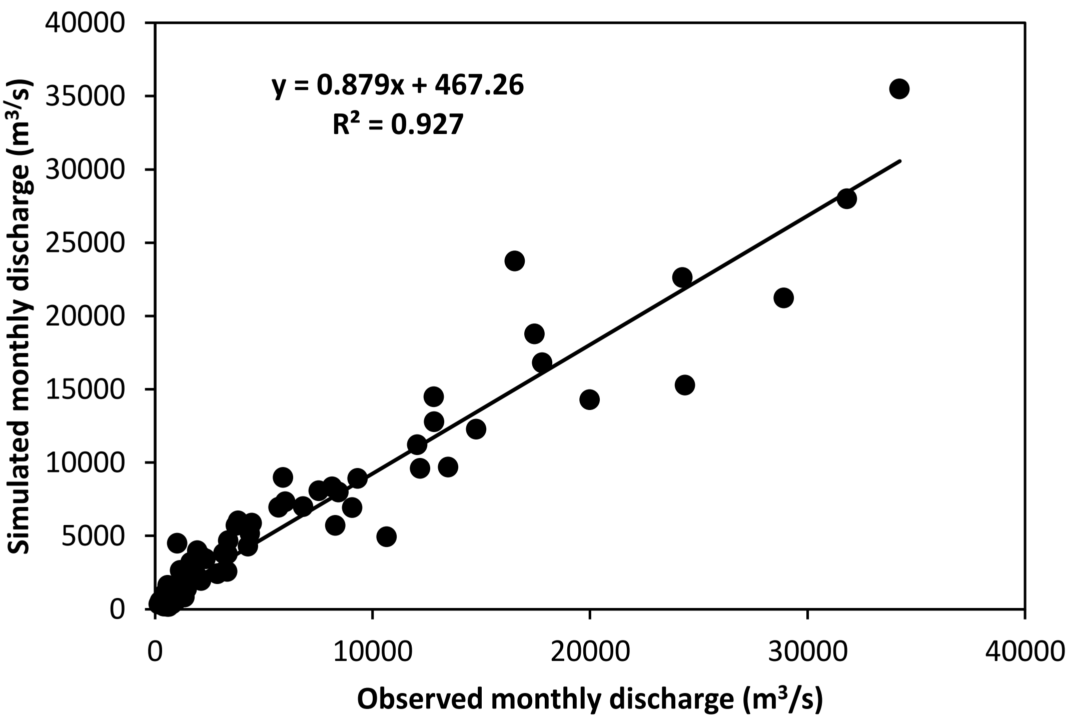

Figure 3.14 Scatter plot of the monthly discharges for the calibration period (1993-2000)

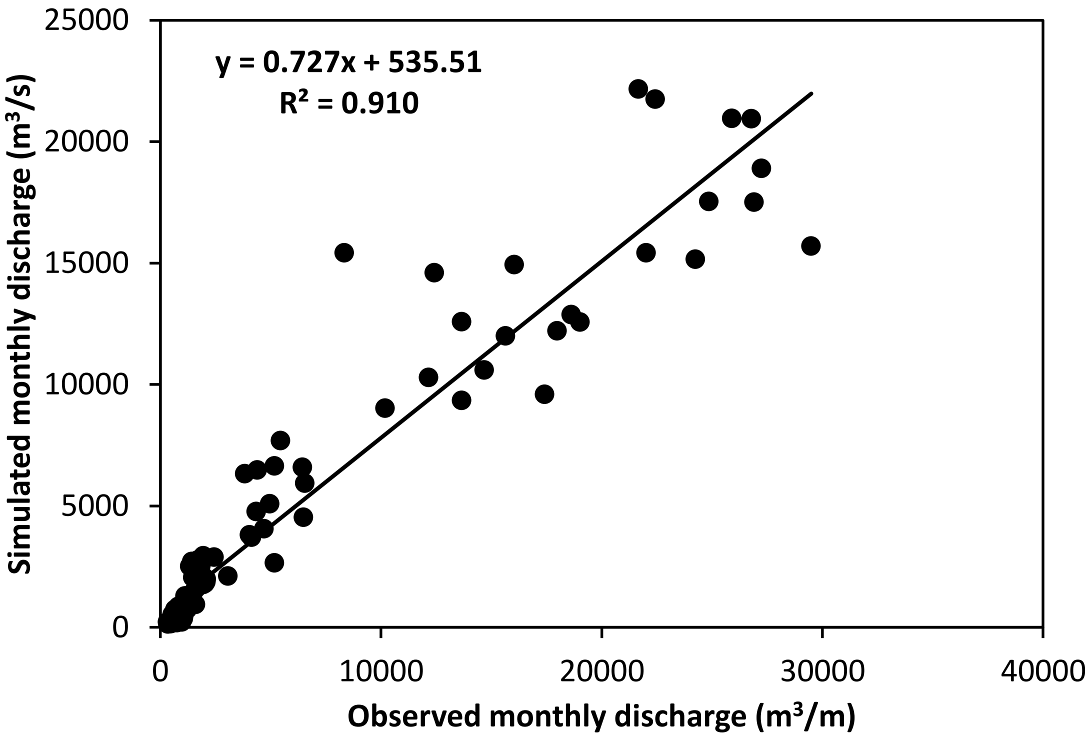

Figure 3.15 Scatter plot of the monthly discharges for the validation period (2001-2008)

3.4.4 Uncertainty Analysis

Sequential Uncertainty Fitting version 2, which appreciates SUFI-2 embedded in SWAT-CUP, is selected to calibrate the Xedone model. SWAT-CUP enables sensitivity analysis, calibration, validation, and uncertainty analysis of SWAT model. SUFI-2 is given several iterations to get the acceptable result. Each of iterations provides the suggested values for the new parameters to be used in the next iteration. Finally, it provides the acceptable result with the values of the Nash-Sutcliffe, Coefficient of Determination and others embedded in SWAT-CUP. Moriasi et al. (2007) presents general performance ratings of the SWAT model for monthly time step simulations. Based on these recommendations, the performance of SWAT model for the study area is very good during the calibration period with NSE > 0.70, and the less value of NSE assumes that there may be some uncertainty in the data. The uncertainty analysis indicates that the parameters of effective hydraulic conductivity in main channel alluvium (CH_K2) and base-flow alpha factor for bank storage (ALPHA_BNK) play important roles in the calibration and validation of SWAT model Luo et al. (2012) report that the parameters of CH_K2 and ALPHA_BNK had the significant impact on the model calibration, and the sampling size may also affect the model sensitivity. In this study, we do not check the uncertainty from the model structure and the input data. Based on this study, it is necessary to do the further study focusing on these topics of the uncertainty analysis.

3.5 Summary

Hydrological modelling of this study is successfully calibrated and validated by using the SWAT model in the Xedone River Basin. The results are shown with the possible measure of the model calibration and validation for two periods: 1993-2000 and 2001-2008. The results of daily simulation values of R^2 and NSE are 0.821and 0.819 during the calibration period, and 0.732 and 0.707 during the validation period. Results of monthly simulation R^2 and NSE are 0.927 and 0.925 during the calibration period, and 0.910 and 0.856 during the validation period. The sensitivity analysis of the model to sub-basin delineation and HRU definition thresholds shows that of the flow is more sensitive to the HRU definition thresholds than sub-basin discretization effect. The results were found 230 HRUs in the whole basin. The 95PPU brackets very well with the observed data for the calibration and validation periods. The p-factor and r- factor computed using SUFI-2 give good results by bracketing value higher than 65% of the observed data. The SUFI-2 algorithm is an effective method, but it requires additional iterations as well as the need for adjustment of the parameter ranges. Despite data uncertainty, the SWAT model produces good simulation results of daily, monthly time steps, which are useful for water resources management in this basin. The results from this study can be utilized to water management and disaster prevention. Also, it can be invoked as the benchmark for future research on water quality analysis and sediment yield analysis. Furthermore, the research can be implemented in the planning of dam construction and flood disaster risk management, which is useful for the sustainable development of the country.

References

Abbaspour, K.C., Johnson, C.A., and van Genuchten, M.T., 2004. Estimating uncertain flow and transport parameters using a sequential uncertainty fitting procedure. Vadose Zone Journal, 3 (4), pp. 1340–1352.

Abbaspour, K.C., Yang, J., Maximov, I., Siber, R., Bogner, K., Mieleitner, J., and

Srinivasan, R., 2007. Modelling hydrology and water quality in the pre-alpine/alpine Thur watershed using SWAT. Journal of Hydrology, 333 (2-4), 413-430. doi: 10.1016/j.jhydrol.

Abbaspour, K.C., Yang, J., Maximov, I., Siber, R., Bogner, K., Mieleitner, J., Zobrist, J., and Srinivasan, R., 2007. Spatiallydis-tributed modelling of hydrology and water quality in the pre-alpine/alpine Thur watershed using SWAT. Journal of Hydrology, 333, pp. 413–430.

Alamirew, C.D., 2006. Modeling of Hydrology and Soil Erosion in Upper Awash River Basin. University of Bonn, Institute für Städtebau, Bodenordnung und Kulturtechnik, pp. 235.

Andersson, L., Wilk, J., and Todd, M.C. et al., 2006. Impact of climate change and development scenarios on flow patterns in the Okavango River. Journal of Hydrology, 331 (1): 43-57.

Arnold, J.G., Srinivasan, R., Muttiah, R.S. and Williams, J.R., 1998. Large area hydrologic modeling and assessment, Part I: model development. Journal of American Water Resources Association, 34 (1), pp. 73–89.

Beven, K., Binley, A., 1992. The future of distributed models – model calibration & uncertainty prediction. Hydrological Processes, 6 (3), pp. 279–298.

Debele, B., Srinivasan, R., and Yves Parlange J., 2006. Coupling upland watershed and downstream water hydrodynamic and water quality models (SWAT and CE-QUAL-W2) for better water resources management in complex river basins. Environ Model Assess., doi: 10.1007/s10666-006-9075 -1.

Duan, W., He, B., Takara, K., Luo, P., Nover, D., Sahu, N., and Yamashiki, Y., 2013. Spatiotemporal evaluation of water quality incidents in Japan between 1996 and 2007. Chemosphere, in press. doi: 10.1016. Journal of chemosphere, 05.060.

Duan, W., Takara, K., He, B., Luo, P., Nover, D., and Yamashiki, Y., 2013. Spatial and temporal trends in estimates of nutrient and suspended sediment loads in the Ishikari River, Japan, 1985 to 2010. Science of the Total Environment., doi: 10.1016.

Dutta, D., Alam, J., Umeda, K., Hayashi, M., and Hironaka, S., 2007.A two-dimensional hydrodynamic model for flood inundation simulation: a case study in the lower Mekong River Basin. Hydrological Processes, 21: 1223–1237. doi: 10.1002/hyp.6682.

Gassman, P.W., Reyes, M.R., Green, C.H., and Arnold, J.G., 2007. The soil and water assessment tool: Historical development, appli-cations, and future research directions. Trains ASABE, 50 (4): 1211-1250.

Grønsten, H.A., and Lundekvam H., 2006. Prediction of surface runoff and soil loss in southeastern Norway using the WEPP Hillslope model. Soil and Tillage Research, 85: 186-199.

Hardy, R.L., 1971. Multiquadric equations of topology and other irregular surface, Journal of Geophys Resources, 76, 1905–1915.

Hornberger, G.M., and Spear, R.C., 1981. An approach to the pre-liminary-analysis of environmental systems. Journal of Environmental Management, 12 (1), pp. 7–18.

Hydrological-Solution, Bry Eithin, Cefn ychan Rd., Pantymwyn, Flintshire, CH7 5EN, UK., 2001. Modelling The Mekong: Hydrological Simulation for Environmental Impact Studies. Journal Hydrology, 253: 1-13.

Jacobs, J. W., 2002. The Mekong River Commission: transboundary water resources planning and regional security. The Geographical Journal, 168: 354–364. doi: 10.1111/j.0016-7398.2002.00061.

Kassa, T., and Foerch, G., 2007. Impacts of Land use/cover dynamics on stream flow: The case of Hare watershed, Ethiopia. In the proceedings of the 4th International SWAT 2005 Conference.

Kiem, A.S., Ishidaira, H., Hapuarachchi, H.P., Zhou, M.C., Hirabayashi, Y., and Takeuchi, K., 2008. Future hydroclimatology of the Mekong River Basin simulated using the high-resolution Japan Meteorological Agency (JMA) AGCM. Hydrological Processes, 22: 1382–1394. doi: 10.1002/hyp.6947.

Luo, P., Takara, K., Apip, He,B. & Nover, D., 2014. Paleo flood simulation in The kamo river basin by using a grid-cell distributed rainfall-runoff model. Journal of Flood Risk Management., Vol. 7, Issue 2, pp. 182-192, doi: 10.1111/jfr3. 12038.

Luo, P., Takara, K., He, B., Cao, W., Yamashiki, Y., and Nover, D., 2012. Calibration and uncertainty analysis of SWAT model in a Japanese river catchment. Journal of Japan Society of Civil Engineers, Ser. B1 (Hydraulic Engineering), 67, doi:10.2208/jscejhe. 67. I_61.

Morgan, R.P.C., 2001. A simple approach to soil loss prediction: a revised Morgan–Morgan–Finney model. Catena, 44: 305-322.

Moriasi, D.N., Arnold, J.G., Van Liew, M.W., Bingner, R.L., Harmel, R.D., & Veith, T.L.,

2007. Model Evaluation Guideline for Systemetic Quantification of Accuracy in Watershed Simulates. Journal of American Society of Agricultural and Biological Engineers ISSN 0001−235, 50 (3): 885−900.

Pangare, G., 2006. The source of the problem. Nature, 441, 28.

Rallison, R.E. and N. Miller., 1981. Past, present and future SCS runoff procedure. p. 353-364. In V.P. Singh (ed.). Rainfall runoff relationship. Water Resources Publication, Littleton, CO.

Rossi, C.G., Srinivasan, R., Jirayoot, K., and Duc, Le. T., 2009. Hydrologic Evaluation the Lower Mekong River Basin with the Soil and Water Assessment Tool Model. International Agricultural Engineering Journal, 18 (1-2): 1-13.

Sheng, X.B., Sun, J.Z., and Liu, Y.X., 2003. Effect of land-use and land-cover change on nutrients in soil in Bashang area, China. Journal of Environmental Sciences, 15 (4): 548-553.

Shrestha, B., Babel, M.S., Maskey, S., van Griensven, A., Uhlenbrook, S., Green, A., and Akkharath, I., 2013. Impact of climate change on sediment yield in the Mekong River Basin: a case study of the Nam Ou basin, Lao PDR. Hydrology and Earth System Sciences, 17 (1), 1-20. doi: 10.5194/hess.

Soil Conservation Service., 1972. Section 4: Hydrology In National Engineering Handbook. SCS.

Somzay, C and Ashish, P., 2013. Hydrological Modelling of Xebangfai River Basin in Lao PDR: A Case study using SWAT Model. Journal of Indian Water Resources Society. Vol 33, No. 2, April, 2013.

Talebizadeh, M., Morid, S., Ayyoubzadeh, S. A., and Ghasemzadeh, M., 2009. Uncertainty Analysis in Sediment Load Modeling Using ANN and SWAT Model. Water Resources Management, 24 (9), 1747-1761. doi: 10.1007/s11269-009 -9522-2.

Tanaka, S., & Kuribayashi, D., 2010. Progress Report on flood hazard mapping in Asian countries, Technical note of PWRI no. 4164 International Centre for Water Hazard and Risk Management (ICHARM); Public Works Research Institute (PWRI); United Nations Educational, Scientific and Cultural Organization (UNESCO).

Vörösmarty, C.J. et al., 2010. Global threats to human water security and river biodiversity. Nature, 467 (7315): 555-561.

Wang, G., Yang, H., Wang, L., Xu, Z., and Xue, B., 2012. Using the SWAT model to assess impacts of land use changes on runoff generation in headwaters.

Hydrological Processes, n/a-n/a. doi: 10.1002/hyp.9645.

Wu, W., Hall, C.A.S., and Scatena, F.N., 2007. Modelling the impact of recent land-cover changes on the stream flows in northeastern Puerto Rico. Hydrological Processes, 21: 2944-2956.

Yang, J., Reichert, P., Abbaspour, K.C., and Yang, H., 2007. Hydrological modeling of the chaohe basin in China: Statistical model formulation and bayesian inference. Journal of Hydrology, 340: 167-182.

Zhang, Y., Xia, J., Shao, Q., and Zhai, X., 2011. Water quantity and quality simulation by improved SWAT in highly regulated Huai River Basin of China. Stochastic Environmental Research and Risk Assessment, 27 (1), 11-27. doi: 10.1007/s00477-011-0546-9.

Chapter 4 Projection of River Discharge at the Xedone River Basin under Climate Change Scenarios

4.1 Xedone River Basin Climatic Characteristics

The climate of the Xedone River Basin is primarily influenced by the seasonal southwest and the northeast monsoons and the shift of the Inter-tropical Convergence Zone (ITCZ) and tropical cyclone disturbances (http://reliefweb.int/country/) such as tropical storms and tropical depressions.

The southwest monsoon (wet season) normally affects the basin from mid of May to early October and is predominant when atmospheric pressure is low over Asia (Jasparro & Taylor, 2008., Keskinen et al., 2010; Giang et al., 2010; Räsänen & Kummu., 2013; Thompson et al., 2014). This is a period of frequent and heavy rainfalls. However, rainfall during the rainy season usually has a bimodal distribution, with a short dry period of one to two weeks, usually between June and July. After this period, rainfall becomes more frequent, including heavy storms that result from tropical cyclones entering the region from the South China Sea (http://reliefweb.int/disasters), mostly during September and November. Flooding frequently occurs when two, more of these storms occur in succession, or when the ITCZ passes into one of its more active stages, with tropical cyclones following shortly thereafter.

A transition period, from mid-October to early November, is followed by the dry northeast monsoon (cold season) which normally lasts from October to February. This season is characterized by sparse, relatively light rainfall, lower temperatures and lower humidity. The northeast monsoon is followed by another transition period to the hot season from March to early May and is characterized by increasing temperatures, rainfall and humidity. This transition is slower than the transition from the rainy season to the cold season (Virana, S., 2007).

As presented in the data collection and analysis of the **Chapter 2**, the long-term precipitation record is available in the Xedone River Basin and other nearby locations, which is located near the Xedone River mouth side and the long-term precipitation record available in southern basin areas such as Laongam, Paksong and Nikhom34 station.

4.2 Sources of Climate Change Factor Data

The Mekong River Commission (MRC) requires a set of exploratory climate change factors (MRC, 2014) to use as input for Soil Water Assessment Tool (SWAT). This will be used to get a final conclusion about the suitable range to adopt for Flood Management and Mitigation Programme (FMMP) stress test scenarios.

The stress test scenarios concept is to develop a robust approach that takes account of uncertainty in climate change projections in the FMMP, as discussed in the MRC and Deutsche Gesellschaft für Internationale Zusammenarbeit (GIZ) initial assessment report of climate sensitive flood management in 2012. The stress test involves using the MRC's basin hydrological models (based on SWAT, within several different configurations) to assess how basin hydrology is predicted to respond for giving changes in climatic forcing variables. As discussed and agreed with the MRC's FMMP and CCAI teams during visits to the MRC in 2013, the change factor data produced in this work were derived in a manner that is compatible with the definition of change factors applicable for MRC SWAT models (MRC, 2014). SWAT requires that change factors are provided as monthly resolution in tabular form. Therefore, the present work values for each SWAT model, sub-basin has been provided as a final processing stage. The SWAT sub-basins were defined by the MRC in the form of GIS shape files.

The Xedone River Basin is embedded in the Lower Mekong Basin as shown in the Lao PDR part presented in the **Figure 4.2**. The configuration of the Xedone Sub-basin is similarly from MRC SWAT sub-basin, so that the climate change factors from the regional model can be applied for the SWAT model scenarios of the Xedone River Basin. Factor change, which is applied for the Xedone River Basin scenarios, as presented in **Table 4.1**, **4.2** and **4.3**. All of the factors in tables are obtained from the MRC. It uses to calculate climate change factors in each sub-basin in the Xedone River Basin. More detail will be presented in the simulation of climate change scenarios as detailed below.

Table 4.1 Definitions of the change factors required by SWAT model.

Variable Name	Definition	Units
RFINC (mon)	Monthly precipitation in percent change (+10 corresponds to 110% of present, i.e. a 10% increase10 corresponds to a 90% change, i.e. a 10% decrease).	%
TMPINC (mon)	Absolute increase or decrease in monthly temperature.	°C
RADINC (mon)	Absolute increase or decrease in monthly solar radiation reaching earth's surface.	MJ m-2
HUMINC (mon)	Absolute increase or decrease in monthly relative humidity.	Fraction

Table 4.2 The change factors RFINC of Geophysical Fluid Dynamics Laboratory (GFDL-cm3)

MRC SWAT Sub-basin	Jan	Feb	Mar	Apr	May	Jun	Jul	Aug	Sep	Oct	Nov	Dec
05A031	1.03	4.37	20.04	-6.33	5.26	1.67	-3.63	4.62	11.93	1.69	12.79	5.6
05A032	0.95	4.62	20.3	-6.54	5.04	1.81	-3.69	4.47	11.69	1.7	12.48	5.57
05A033	1.39	4.47	21.29	-6.58	4.89	1.89	-3.64	4.53	11.75	1.73	12.92	5.62
05A038	1.67	4.46	20.86	-6.7	4.77	1.9	-3.52	4.36	11.34	1.83	12.83	5.56
05A042	1.81	4.22	22.76	-6.32	4.88	1.94	-3.77	4.74	12.29	1.7	13.54	5.81
05A051	2.74	4.05	22.66	-6.52	4.58	2.05	-3.5	4.52	11.64	1.9	13.77	5.84
05A065	2.67	4.14	21.89	-6.68	4.53	2.03	-3.39	4.36	11.24	1.96	13.49	5.71
05A066	2.14	4.37	20.75	-6.79	4.6	1.94	-3.39	4.22	10.97	1.95	12.92	5.53

Table 4.3 The change factors RFINC of NASA Goddard Institute for Space Studies (GISS -e2-r-cc)

MRC SWAT Sub-basin	Jan	Feb	Mar	Apr	May	Jun	Jul	Aug	Sep	Oct	Nov	Dec
05A031	-11.65	-2.93	-6.58	0.01	-1.03	2.47	0.37	5.35	2.57	-11.22	0.86	-4.61
05A032	-10.72	-2.95	-5.09	-1.52	-1.73	2.27	2.50	6.14	2.85	-10.50	-0.11	-4.50
05A033	-10.78	-3.84	-7.02	-3.16	-3.38	2.42	-0.14	4.99	2.36	-9.87	0.25	-4.67
05A035	-10.54	-2.67	-4.83	-1.43	-1.61	1.66	3.51	6.28	3.07	-10.04	0.20	-4.44
05A038	-10.56	-3.75	-7.07	-3.33	-3.49	1.95	0.54	5.01	2.51	-9.29	0.50	-4.61
05A042	-11.32	-4.79	-9.00	-4.39	-4.91	2.89	-3.60	3.74	1.64	-10.11	0.79	-4.95
05A051	-10.99	-5.40	-10.61	-5.49	-6.00	2.34	-3.92	3.14	1.52	-8.80	1.62	-4.89
05A065	-10.72	-4.97	-9.92	-5.13	-5.50	1.91	-2.43	3.56	1.86	-8.41	1.54	-4.78
05A066	-10.44	-3.95	-7.87	-3.92	-4.09	1.52	0.27	4.62	2.47	-8.57	1.00	-4.62

Table 4.4 The change factors RFINC of Institute Pierre-Simon Laplace (IPSL-cm5a-mr)

MRC SWAT Sub-basin	Jan	Feb	Mar	Apr	May	Jun	Jul	Aug	Sep	Oct	Nov	Dec
05A031	5.87	-9.98	-19.01	-17.54	-1.87	4.34	0.75	3.85	6.54	29.16	5.24	26.62
05A032	6.61	-11.44	-19.75	-17.41	-1.57	4.45	0.08	4.09	6.17	28.04	5.99	28.15
05A033	6.09	-12.06	-20.45	-17.20	-1.53	4.62	-1.20	3.52	5.87	28.82	5.64	30.61
05A035	1.22	4.62	19.71	-6.61	4.93	1.80	-3.60	4.28	11.26	1.80	12.34	5.51
05A038	5.44	-12.28	-20.80	-17.03	-1.56	4.51	-1.47	3.37	5.51	27.37	5.86	29.72
05A042	6.03	-12.47	-20.59	-17.19	-1.49	4.73	-2.16	3.08	6.05	31.36	5.11	33.95
05A051	4.52	-13.08	-21.57	-16.87	-1.54	4.56	-3.39	2.40	4.96	29.23	5.31	34.18
05A065	4.20	-13.01	-21.70	-16.77	-1.58	4.49	-3.17	2.48	4.78	27.63	5.57	32.40
05A066	4.53	-12.62	-21.32	-16.80	-1.60	4.42	-2.11	3.01	5.06	26.25	5.93	29.55

4.3 Methods

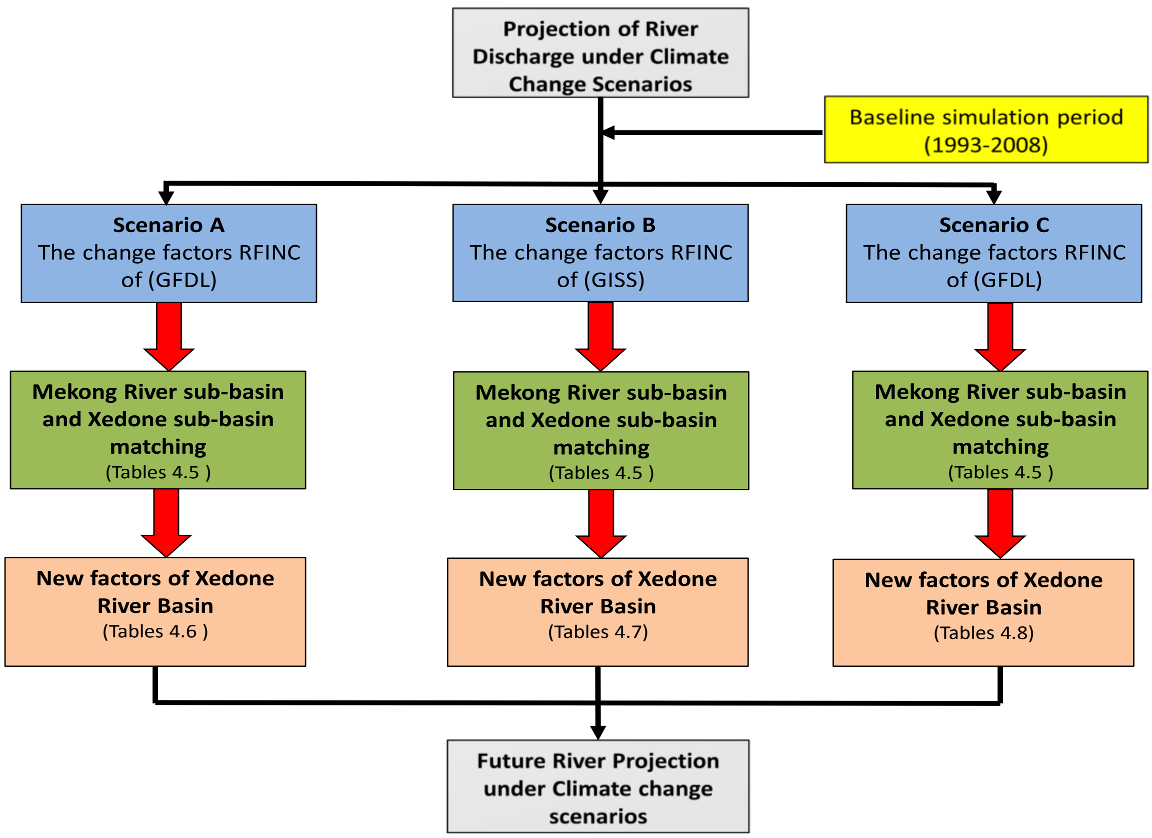

Figure 4.1 Flow chart for climate change scenarios

4.4 Baseline Simulation Prepared for Scenario Simulation

In the baseline simulation period (1993-2008) the daily, monthly of simulated and observed discharge data for the Souvannakhili station has been plotted in the hydrograph for calibration period (1993-2000) and validation period (2001-2008) separately, and the same hydrograph have been presented in **Chapter 3** of **Figures 3.8, 3.9 , 3.12** and **3.13**. Statistical analysis of daily and monthly-simulated discharge at the Souvannakhili station during the calibration period (1993-2000) is shown in **Tables 3.6** and **3.7**. The high value of R^2 and Nash-Sutcliffe efficiency (NSE) indicates satisfactory model performance for the simulation of runoff during the calibration period (daily and monthly) for the Souvannakhili station.

From the hydrograph of daily observed and simulated flows at Souvannakhili in **Figure 3.8,** it is shown the simulated flows closely match observed flows, except in the validation period where the peak of simulation was low shown in **Figure 3.9**. Due to the observed flow was missing and the Department of Meteorology and Hydrology fill data for input of validation period, it is assumed that there may be some uncertainty in the observed flow-recorded data during the month of August-September; according to field survey.

4.5 River Discharge Projections under Climate Change Scenarios

Sub-basin spatial data corrections

More number of issues were identified with the SWAT model, sub-basin definitions supplied by the MRC for this study. These relate to the spatial description of SWAT sub-basins, in the form of ESRI shape files as shown in **Figure 4.2**.

These issues were corrected using standard ArcGIS processing routines. In most cases, this resulted in slight changes in the sub-basin area a little bit not appropriate for analysis. **Figure 4.3** shows that number of MRC SWAT sub-basins are bigger than Xedone sub-basins. An example of sub-basin number 05A035 of MRC SWAT sub-basins are included 4 sub-basins of Xedone sub-basins; No 5,6,7 and 11, the same location. It indicates that sub-basin of Xedone can use the same monthly factors change values of MRC SWAT sub-basin.

Climate change scenarios were simulated by applying climate change factors obtained from the modeling team of FMMP/MRC to the input time series of the SWAT model scenarios. The climate change factors were generated from three global data sources such as (1) GFDL-cm3-2030, (2) GISS-e2-r-cc2030 and (3) IPSL-cm5a-mr2030.

Precipitation is the only time series parameter, that is subject to climate change factors. Climate change scenario is available for the input of the SWAT model such as rainfall as factor change which is presented in **Tables 4.2, 4.3** and **4.4**. Climate change factors were super-imposed from sub-basins of the regional SWAT Mekong model area 5 (Mukdahan-Pakse) to the sub-basins of the new updated model for the Xedone River Basin.

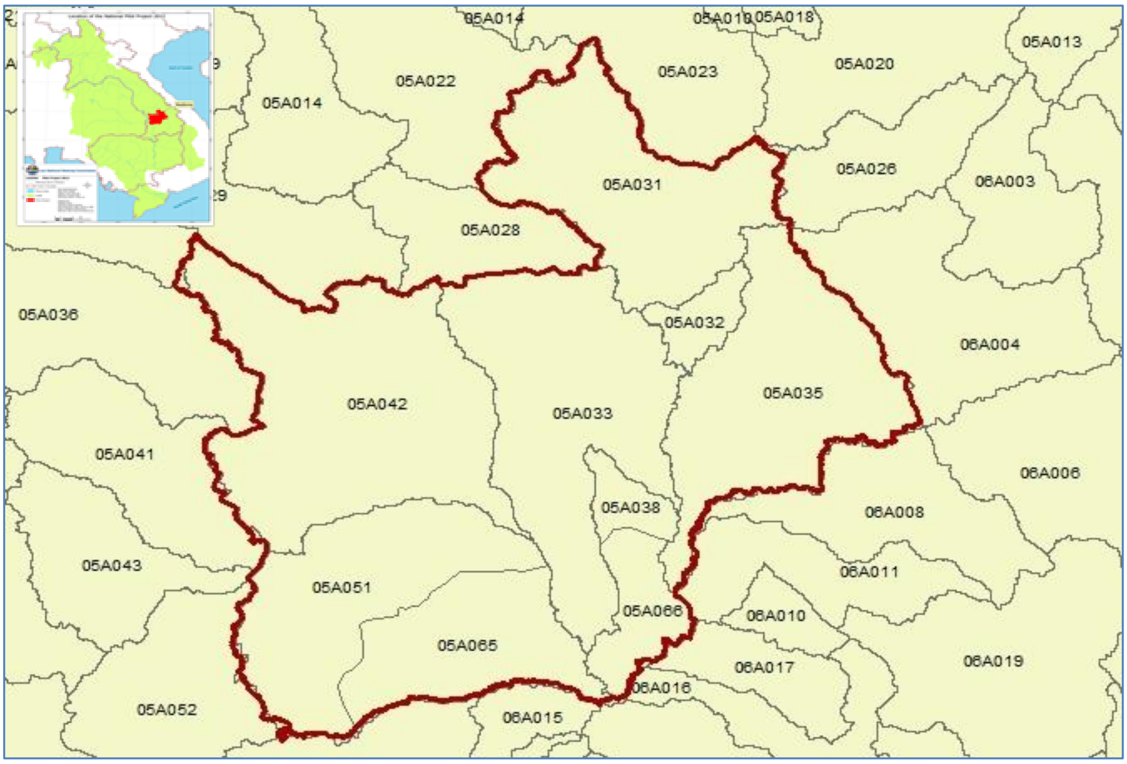

Figure 4.2 Mekong SWAT sub-basins configuration with the Xedone area.

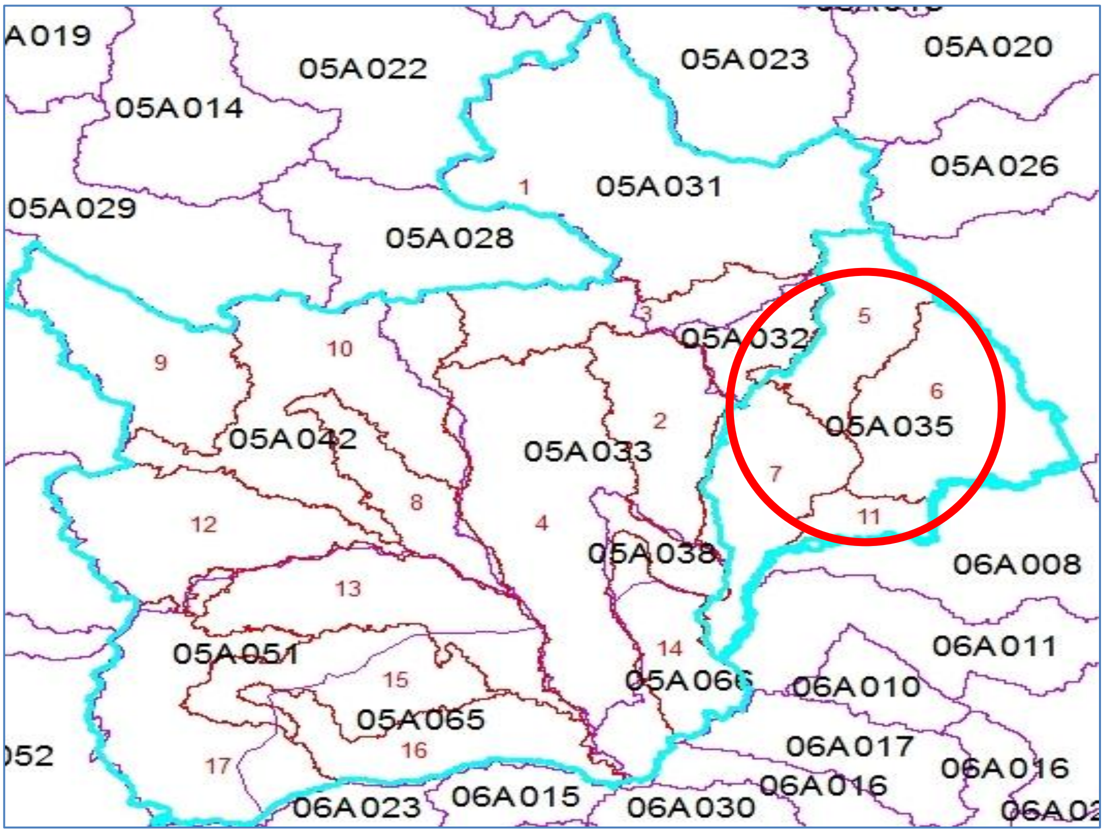

Figure 4.3 Narrow downs to the Xedone sub-basin.

Table 4.5 Mekong River sub-basin and Xedone sub-basin matching.

MRC SWAT Sub-basin	Xedone Sub-basin Numbers
05A031	1
05A032	3
05A033	2, 4
05A035	5, 6, 7, 11
05A038	Esc
05A042	8, 9, 10, 12
05A051	13, 17
05A065	15, 16
05A066	14

Table 4.6 Climate Change Factors RFINC of Geophysical Fluid Dynamics Laboratory (GFDL-cm3 2030)

Sub basin	Jan	Feb	Mar	Apr	May	Jun	Jul	Aug	Sep	Oct	Nov	Dec
1	1.010	1.044	1.200	0.937	1.053	1.017	0.964	1.046	1.119	1.017	1.128	1.056
2	1.014	1.045	1.213	0.934	1.049	1.019	0.964	1.045	1.118	1.017	1.129	1.056
3	1.010	1.046	1.203	0.935	1.050	1.018	0.963	1.045	1.117	1.017	1.125	1.056
4	1.014	1.045	1.213	0.934	1.049	1.019	0.964	1.045	1.118	1.017	1.129	1.056
5	1.012	1.046	1.197	0.934	1.049	1.018	0.964	1.043	1.113	1.018	1.123	1.055
6	1.012	1.046	1.197	0.934	1.049	1.018	0.964	1.043	1.113	1.018	1.123	1.055
7	1.012	1.046	1.197	0.934	1.049	1.018	0.964	1.043	1.113	1.018	1.123	1.055
8	1.018	1.042	1.228	0.937	1.049	1.019	0.962	1.047	1.123	1.017	1.135	1.058
9	1.018	1.042	1.228	0.937	1.049	1.019	0.962	1.047	1.123	1.017	1.135	1.058
10	1.018	1.042	1.228	0.937	1.049	1.019	0.962	1.047	1.123	1.017	1.135	1.058
11	1.012	1.046	1.197	0.934	1.049	1.018	0.964	1.043	1.113	1.018	1.123	1.055
12	1.018	1.042	1.228	0.937	1.049	1.019	0.962	1.047	1.123	1.017	1.135	1.058
13	1.027	1.041	1.227	0.935	1.046	1.020	0.965	1.045	1.116	1.019	1.138	1.058
14	1.021	1.044	1.207	0.932	1.046	1.019	0.966	1.042	1.110	1.019	1.129	1.055
15	1.027	1.041	1.219	0.933	1.045	1.020	0.966	1.044	1.112	1.020	1.135	1.057
16	1.027	1.041	1.219	0.933	1.045	1.020	0.966	1.044	1.112	1.020	1.135	1.057
17	1.027	1.041	1.227	0.935	1.046	1.020	0.965	1.045	1.116	1.019	1.138	1.058

Table 4.7 Climate Change Factors RFINC of NASA Goddard Institute for Space Studies (GISS-e2-r-cc 2030)

Sub basin	Jan	Feb	Mar	Apr	May	Jun	Jul	Aug	Sep	Oct	Nov	Dec
1	0.884	0.971	0.934	1.000	0.990	1.025	1.004	1.054	1.026	0.888	1.009	0.954
2	0.892	0.962	0.930	0.968	0.966	1.024	0.999	1.050	1.024	0.901	1.002	0.953
3	0.893	0.971	0.949	0.985	0.983	1.023	1.025	1.061	1.029	0.895	0.999	0.955
4	0.892	0.962	0.930	0.968	0.966	1.024	0.999	1.050	1.024	0.901	1.002	0.953
5	0.895	0.973	0.952	0.986	0.984	1.017	1.035	1.063	1.031	0.900	1.002	0.956
6	0.895	0.973	0.952	0.986	0.984	1.017	1.035	1.063	1.031	0.900	1.002	0.956
7	0.895	0.973	0.952	0.986	0.984	1.017	1.035	1.063	1.031	0.900	1.002	0.956
8	0.887	0.952	0.910	0.956	0.951	1.029	0.964	1.037	1.016	0.899	1.008	0.951
9	0.887	0.952	0.910	0.956	0.951	1.029	0.964	1.037	1.016	0.899	1.008	0.951
10	0.887	0.952	0.910	0.956	0.951	1.029	0.964	1.037	1.016	0.899	1.008	0.951
11	0.895	0.973	0.952	0.986	0.984	1.017	1.035	1.063	1.031	0.900	1.002	0.956
12	0.887	0.952	0.910	0.956	0.951	1.029	0.964	1.037	1.016	0.899	1.008	0.951
13	0.890	0.946	0.894	0.945	0.940	1.023	0.961	1.031	1.015	0.912	1.016	0.951
14	0.896	0.960	0.921	0.961	0.959	1.015	1.003	1.046	1.025	0.914	1.010	0.954
15	0.890	0.946	0.894	0.945	0.940	1.023	0.961	1.031	1.015	0.912	1.016	0.951
16	0.893	0.950	0.901	0.949	0.945	1.019	0.976	1.036	1.019	0.916	1.015	0.952
17	0.890	0.946	0.894	0.945	0.940	1.023	0.961	1.031	1.015	0.912	1.016	0.951

Table 4.8 Climate Change Factors RFINC of Institute Pierre-Simon Laplace (IPSL-cm5a-mr 2030)

Sub basin	Jan	Feb	Mar	Apr	May	Jun	Jul	Aug	Sep	Oct	Nov	Dec
1	1.059	0.900	0.810	0.825	0.981	1.043	1.008	1.039	1.065	1.292	1.052	1.266
2	1.061	0.879	0.795	0.828	0.985	1.046	0.988	1.035	1.059	1.288	1.056	1.306
3	1.066	0.886	0.803	0.826	0.984	1.045	1.001	1.041	1.062	1.280	1.060	1.282
4	1.061	0.879	0.795	0.828	0.985	1.046	0.988	1.035	1.059	1.288	1.056	1.306
5	1.012	1.046	1.197	0.934	1.049	1.018	0.964	1.043	1.113	1.018	1.123	1.055
6	1.012	1.046	1.197	0.934	1.049	1.018	0.964	1.043	1.113	1.018	1.123	1.055
7	1.012	1.046	1.197	0.934	1.049	1.018	0.964	1.043	1.113	1.018	1.123	1.055
8	1.060	0.875	0.794	0.828	0.985	1.047	0.978	1.031	1.061	1.314	1.051	1.339
9	1.060	0.875	0.794	0.828	0.985	1.047	0.978	1.031	1.061	1.314	1.051	1.339
10	1.060	0.875	0.794	0.828	0.985	1.047	0.978	1.031	1.061	1.314	1.051	1.339
11	1.012	1.046	1.197	0.934	1.049	1.018	0.964	1.043	1.113	1.018	1.123	1.055
12	1.060	0.875	0.794	0.828	0.985	1.047	0.978	1.031	1.061	1.314	1.051	1.339
13	1.045	0.869	0.784	0.831	0.985	1.046	0.966	1.024	1.050	1.292	1.053	1.342
14	1.045	0.874	0.787	0.832	0.984	1.044	0.979	1.030	1.051	1.262	1.059	1.296
15	1.042	0.870	0.783	0.832	0.984	1.045	0.968	1.025	1.048	1.276	1.056	1.324
16	1.042	0.870	0.783	0.832	0.984	1.045	0.968	1.025	1.048	1.276	1.056	1.324
17	1.045	0.869	0.784	0.831	0.985	1.046	0.966	1.024	1.050	1.292	1.053	1.342

4.6 Results and Discussions

The results of the three projection of river dischage at the Xedone River Basin under climate change scenarios were assessed by running the calibrated model for the period 1993-2008, and applied by climate change factors of (GFDL-cm3 2030), (GISS-e2-r-cc 2030), and (IPSL-cm5a-mr 2030), by keeping the DEM, soil map, slope map and land use/cover map and all parameters, to predicted surface runoff for the year 2030 which differences institutes researched climate change factor, such as the average monthly changes as Percentage differenced rank (-4.879 to 30.223) for the GDFL 2030 almost is increased flow, except July was -4.879% compared baseline, the average monthly change of GISS 2030 scenarios is resulted in Percentage differenced rank is (-6.218 to 19.006) and IPSL 2030 is (-37.155 to 23.135) respectively, these results are detailed in **Table 4.9**.

The comparison of the baseline and scenarios discharges (monthly) for the Souvanakhli station is shown in **Figure 4.5.** It is seen all of the scenario flows, it is started increase at mid-July until to mid-September while in the mid-August hydrograph is highest, this peak almost provides more than 450 m^3/s (Monthly average) after mid-September the hydrograph is straight down, except the scenario GISS 2030, where the peak of scenarios was high given flows beyond 500 m^3/s in August which present in **Figure 4.5**, the scenario of GISS 2030 is a higher baseline both wet and dry season. With the result of the IPSL 2030 given lower flows in the dry season (Feb-May) which lower than baseline while in the rainy season is beyond the baseline shown in **Figure 4.6**.

The results of the four climate change scenarios are compared with baseline conducted by SWAT model that included climate change factors applied to the original input baseline data are shown in **Figures 4.4** and **4.5**.

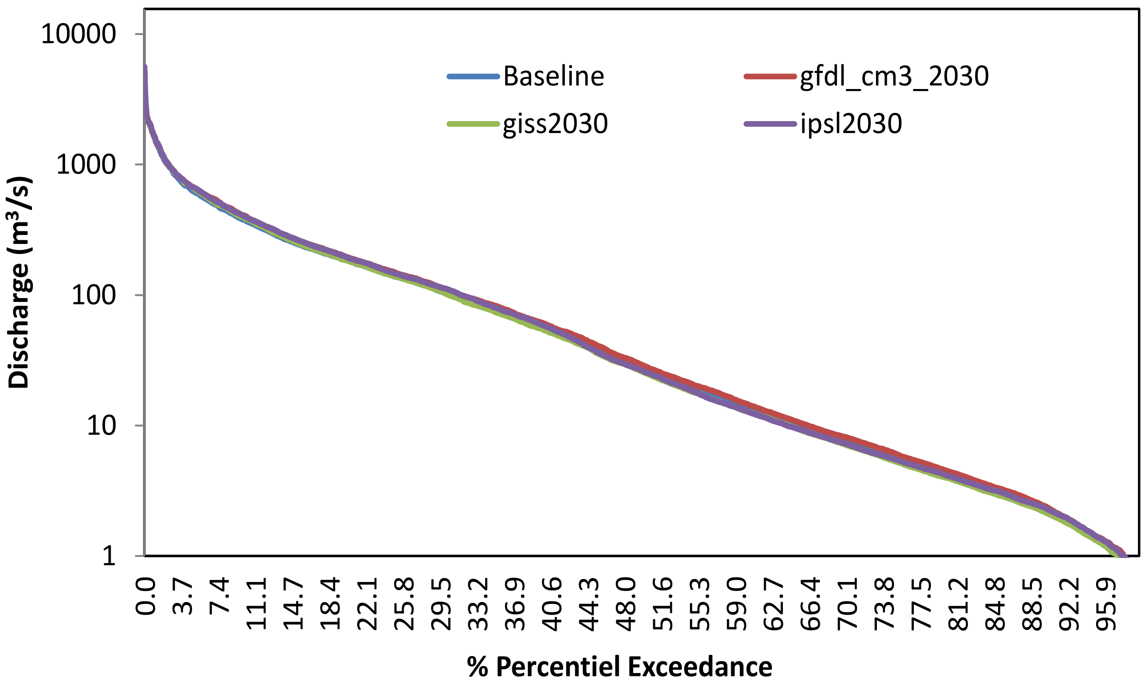

Figure 4.4 Comparison flow of the climate change scenarios with baseline scenario.

The Scenario IPSL 2030, GFDL 2030 and GISS 2030 were shown the flow in both seasons wet and dry. While the result of the IPSL 2030 has given lower flows in the dry season (Feb-May) than the baseline while on the end of the rainy season is beyond the baseline. The flows of climate change scenarios generated more than 400 m^3/s for the monthly in (July, August and September) with comparison of baseline at Souvannakhili station, reason peak flow during these months because in the southwest monsoon (wet season) normally affects the catchments from mid of May to early October and is predominant when atmospheric pressure is low over Asia, Laos is also affected from heavy rainfall by some studies: Virana. (2007); Västilä et al. (2008) and Eastham et al. (2008). The extreme change scenario is GISS 2030, as the volume of high monthly runoff, increase the duration of the high monthly runoff also increases and prolong until the first week of September. The comparison of the flow change is provided in Table **4.9** and **Figure 4.5.**

Table 4.9 Climate change scenarios, which effected in surface runoff.

Months	Monthly Scenarios Flow				Percentage Differences Compared to Baseline		
	Baseline Flow (m^3/s)	GFDL 2030 flow (m^3/s)	GISS 2030 flow (m^3/s)	IPSL 2030 flow (m^3/s)	% Difference of GDFL 2030	% Difference of GISS 2030	% Difference of IPSL 2030
Jan	3.60	3.85	3.72	4.13	6.33	3.02	12.76
Feb	4.30	4.68	4.29	4.01	8.14	-0.15	-7.29
Mar	6.73	9.65	8.31	5.28	30.23	19.01	-27.36
Apr	14.42	14.81	13.58	10.51	2.65	-6.22	-37.16
May	81.51	90.88	83.94	73.68	10.31	2.90	-10.62
Jun	155.63	163.96	167.13	162.92	5.08	6.89	4.47
Jul	427.34	407.47	410.23	420.49	-4.88	-4.17	-1.63
Aug	448.21	470.86	503.97	467.89	4.81	11.06	4.21
Sep	348.10	405.69	423.06	383.87	14.19	17.72	9.32
Oct	137.36	144.28	129.97	178.70	4.80	-5.69	23.14
Nov	32.30	36.15	35.25	36.53	10.64	8.36	11.57
Dec	8.06	8.64	8.46	9.02	6.71	4.80	10.67
Annually Scenarios Flow					**% Annually Change**		
Annually	138.96	146.74	149.33	146.42	5.30	6.94	5.09

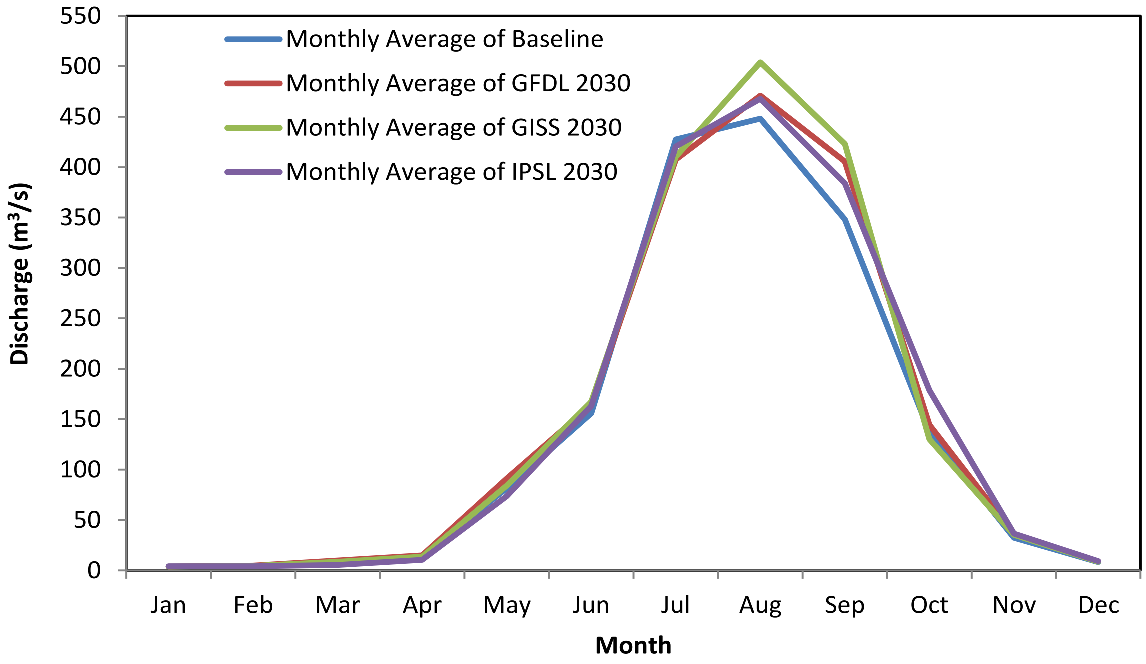

Figure 4.5 Comparison monthly changes in flow at Souvannakhli station of the climate change scenarios with baseline scenario.

From **Figure 4.6** and **Table 4.10,** it is seen that response the information in the beginning, which during the dry season water resources availability is very less thought out the years which flow lower than 5 m^3/s and severe drought is seen in the region but during the rainy season this area is under the water. From **Table 4.9** presented the river discharge of the Xedone River Basin for the year of 2030 through the future climate change factor of three institutes suggested stream flow considering climate change is effected as well as in normal condition.

Table 4.10 Monthly average of scenarios 2030 in the dry season of Souvannakhili station.

Dry season	Monthly Average Of BASELINE (m^3/s)	Monthly Average of GFDL2030 (m^3/s)	Monthly Average of GISS 2030 (m^3/s)	Monthly Average of IPSL 2030 (m^3/s)
Dec	8.06	8.64	8.46	9.02
Jan	3.60	3.85	3.72	4.13
Feb	4.30	4.68	4.29	4.01
Mar	6.73	9.65	8.31	5.28
Apr	14.42	14.81	13.58	10.51

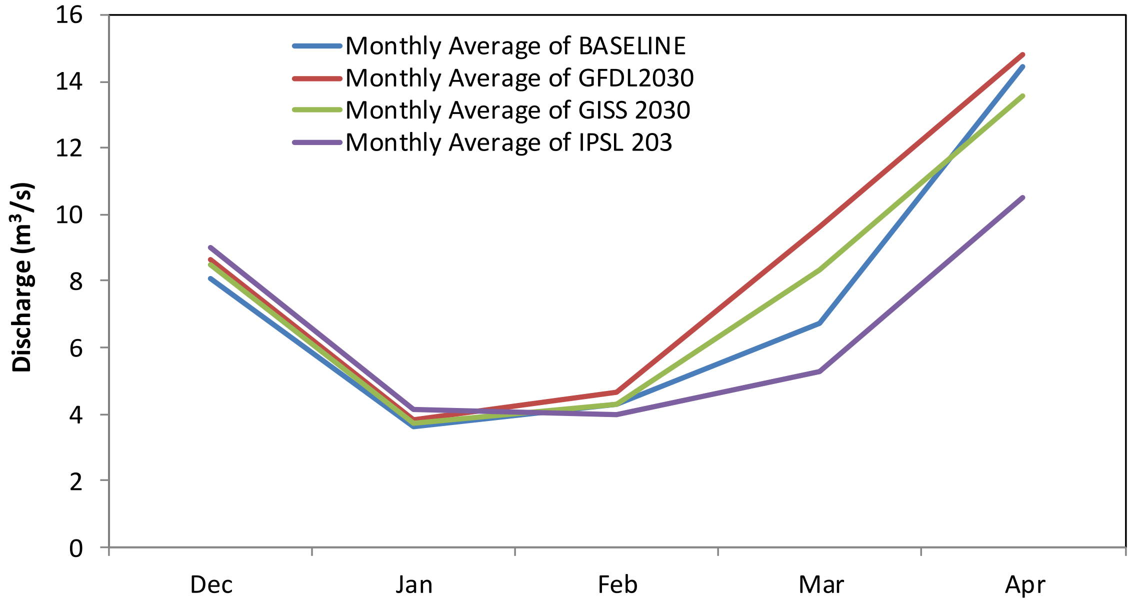

Figure 4.6 Monthly average plots in the dry season of all scenarios and baseline.

4.7 Summary

The climate change scenarios are successfully analyzed in this study by using the data set of exploratory climate change factors from MRC. MRC (2014) climate change information is used to input for the SWAT model in the Xedone River Basin. The results of the three climate change scenarios were assessed by running the calibrated model for the period 1993-2008, and applied by climate change factors of DFDL 2030, GISS 2030, and IPSL 2030, to predicted surface runoff for the year 2030. Differences institutes researched climate change factor, such as the average monthly changes as Percentage differenced rank (-4.879 to 30.223) for the GFDL 2030 almost is increased flow, except July was -4.879% compared baseline, the average monthly change of GISS 2030 scenarios is resulted in Percentage differenced rank is (-6.218 to 19.006) and IPSL 2030 is (-37.155 to 23.135) respectively. These results of climate change scenarios' model would be used for better information for water management and disaster prevention. Also, it can be used as the benchmark for future research on water quality analysis and sediment yield analysis. In addition, it can be implemented to the planning of flood disaster risk management, which is useful for the sustainable development of the Lao PDR.

References

Eastham, J., F. Mpelasoka, M. Mainuddin, C.Ticehurst, P. Dyce, G. Hodgson, R. Ali and M. Kirby, 2008. Mekong River Basin Water Resources Assessment: Impacts of Climate Change. CSIRO: Water for a Healthy Country National Research Flagship.

Giang, P. Q., Toshiki, K., Sakata, M., Kunikane, S., & Vinh, T. Q., 2014. Modelling climate change impacts on the seasonality of water resources in the Upper Ca River Watershed in Southeast Asia. ScientificWorldJournal, 2014, 279135. doi: 10.1155/2014/279135.

Jasparro, C., & Taylor, J., 2008. Climate Change and Regional Vulnerability to Transnational Security Threats in Southeast Asia. Geopolitics, 13 (2), 232-256. doi: 10.1080/14650040801991480.

Keskinen, M., Chinvanno, S., Kummu, M., Nuorteva, P., Snidvongs, A., Varis, O., & Västilä, K., 2010. Climate change and water resources in the Lower Mekong River Basin: putting adaptation into the context. Journal of Water and Climate Change, 1(2), 103. doi: 10.2166/wcc.2010.009.

Moriasi, D.N., Arnold, J.G., Van Liew, M.W., Bingner, R.L., Harmel, R.D., & Veith, T.L., 2007. Model Evaluation Guideline for Systemetic Quantification of Accuracy in Watershed Simulates. Journal of American Society of Agricultural and Biological Engineers ISSN 0001−235, 50 (3): 885−900.

MRC., 2014. Exploratory analysis of climate change factor ranges-Final Report. Revision 3.1, June2014.

Räsänen, T. A., & Kummu, M., 2013. Spatiotemporal influences of ENSO on precipitation and flood pulse in the Mekong River Basin. Journal of Hydrology, 476, 154-168. doi: 10.1016/j.jhydrol.2012.10.028.

Saleh, A. and Du, B., 2004. "Evaluation of SWAT and HSPF within BASINS program for the upper North Bosque River watershed in central Texas", Transactions of the American Society of Agricultural Engineering, 47 (4): 1039-1049.

Thompson, J. R., Green, A. J., & Kingston, D. G., 2014. Potential evapotranspiration-related uncertainty in climate change impacts on river flow: An assessment for the Mekong River Basin. Journal of Hydrology, 510, 259-279. doi: 10.1016/j.jhydrol.2013.12.010.

Västilä, K., Kummu, M., Sangmanee, C., & Chinvanno, S., 2010. Modelling climate change impacts on the flood pulse in the Lower Mekong floodplains. Journal of Water and Climate Change, 01 (1), 67. doi: 10.2166/wcc.2010.008.

Verona, S., 2007. Lao PDR's country flood report for 2007. National Flood Expert, National Flood Unit, Lao National Mekong Committee Secretariat Water Resources and Environment Administration, Vientiane, Lao PDR.

Chapter 5 Conclusions

The impact of climate change on hydrology of the Xedone River Basin, Lao PDR was analyzed by using hydrologic data and modeling. The analysis presented in different chapters cover statistical analysis at the inter-annual, season and event-based time scales. In chapter 1, and continuous long-term hydrologic simulation.

In chapter 2 trend analysis of precipitation and temperature in the Xedone River Basin, Lao PDR was conducted with annual and seasonal precipitation, and temperature data by using Mann-Kendall test and Inverse Distance Weighting (IDW) interpolation method in GIS software. The objective of the analysis was to find the impact of climate change and attempt to discuss a relationship with the recent increase of natural disasters. The precipitation increased trend of (annual daily maximum etc.) scale was found in the southeastern part of the Xedone River Basin at Nikhom34 station. The annual decreased trend precipitation of associated to drought risk was also found in the middle part of the Xedone River Basin at the LaoNgam station. The results of the analysis provide important information for water resource management in the region.

In chapter 3 SWAT model was successfully calibrated and validated in the Xedone River Basin by using an application algorithm called SUFI-2. Then is the sensitivity analysis of the model showed that the flow is sensitive not only parameter, but also to the HRU delineation thresholds followed by sub-basin discretization effect. The results suggested that 230 HRUs are appropriate in the whole basin. The SUFI-2 algorithm performed will be adjusted between and simulated flow in the Xedone River Basin. The model was calibrated and validated in the two periods: 1993-2000 and 2001-2008. The results of daily simulation values of R^2 and NSE were 0.821 and 0.819 during the calibration period, and 0.732 and 0.707 during the validation period. Results of monthly simulation R^2 and NSE were 0.927 and 0.925 during the calibration period, and 0.910 and

0.856 during the validation period. The SWAT model produced good simulation results of daily, monthly time steps, which are useful for water resources management in this basin. The calibrated model can be used for further analysis of the effect of climate and land use changes as well as other different management scenarios on river discharge.

In chapter 4 the calibrated model was run with climate change scenarios proposed by the Mekong River Commission (MRC). The three climate change scenarios were considered for running the model for the period of 1993-2008 with climate change factors of GFDL 2030, GISS 2030, and IPSL 2030, to project surface runoff for the period of year 2030. Different institutes researched climate change factor such as the Scenario GFDL 2030, GISS 2030 and IPSL 2030 and showed the flow in both seasons wet and dry. Which the result of IPSL 2030, flows in the dry season (Feb-May) becomes lower than the baseline while on the end of the rainy season is beyond the baseline. The flows of climate change scenarios generated more than 400 m^3/s for the months in July, August and September; baseline at Souvannakhili station. The reason for the peak flow during these months is the southwest monsoon, normally affects the catchments from mid of May to early October. It is predominant when atmospheric pressure is low over Laos and cause heavy rainfall (Virana. (2007); Västilä et al. (2008) and Eastham et al. (2008)). The extreme change was observed with the scenario of GISS 2030, which result in the high volume monthly runoff, increase the duration of the high monthly runoff and prolong the high runoff season until the first week of September. The model climate change scenarios simulate with the should be used for better information for future studies.

Overall, the results obtained in this thesis enhance the knowledge of climate change impacts on hydrology in Lao PDR. The results can be utilized to water management and disaster prevention. Furthermore, the research provides useful information for the planning of dam constructions and flood disaster risk management, which are vital for the sustainable development of the country.

References

Eastham, J., F. Mpelasoka, M. Mainuddin, C.Ticehurst, P. Dyce, G. Hodgson, R. Ali and M. Kirby, 2008. Mekong River Basin Water Resources Assessment: Impacts of Climate Change. CSIRO: Water for a Healthy Country National Research Flagship.

Västilä, K., Kummu, M., Sangmanee, C., & Chinvanno, S., 2010. Modelling climate change impacts on the flood pulse in the Lower Mekong floodplains. Journal of Water and Climate Change, 01 (1), 67. doi: 10.2166/wcc.2010.008.

Virana, S., 2007. Lao PDR's country flood report for 2007. National Flood Expert, National Flood Unit, Lao National Mekong Committee Secretariat Water Resources and Environment Administration, Vientiane, Lao PDR.

Appendix: Results of Mann-Kendall Test

Summary of Results

During the statistical calculations the summary table of the results in the Trend Statistics,. The results are given for each time series in the table below:

The columns in the table have the following meanings:

- **Time series:** the names of the time series are derived (from the Annual data)
- **First year:** starting year of each time series (from the Annual data)
- **Last year:** ending year of each time series (from the Annual data)
- **n:** the number of annual values in the calculation excluding missing values (from the Annual data).
- **Test S:** If ***n*** is 9 or less, the test statistic ***S*** is displayed. The absolute value of ***S*** is compared to the probabilities of the Mann-Kendall non-parametric test for trend to define if there is a monotonic trend or not at the level ***α*** of significance. A positive (negative) value of ***S*** indicates an upward (downward) trend. In ***n*** is larger than 9, this cell is empty.
- **Test Z:** If ***n*** is at least 10, the test statistic ***Z*** is displayed. The absolute value of ***Z*** is compared to the standard normal cumulative distribution to define if there is a trend or not at the selected level ***α*** of significance. A positive (negative) value of ***Z*** indicates an upward (downward) trend. If ***n*** is 9 or less, this cell is empty.
- **Signific:** the smallest significance level ***α*** with which the test shows that the null hypothesis of no trend should be rejected. If ***n*** is 9 or less, the test is based to the ***S*** statistic and if ***n*** is at least 10, the test is based to the ***Z*** statistic (normal approximation). For the four tested significance levels the following symbols are used in the template:

*** if trend at α = 0.001 level of significance

** if trend at α = 0.01 level of significance

* if trend at α = 0.05 level of significance

+ if trend at α = 0.1 level of significance

If the cell is blank, the significance level is greater than 0.1.

- **Sen's slope estimate *Q*:** the Sen's estimator for the true slope of linear trend i.e. change per unit time period (in this case a year)
- ***Qmin99*:** the lower limit of the 99 % confidence interval of ***Q*** (α = 0.1)
- ***Qmax99*:** the upper limit of the 99 % confidence interval of ***Q*** (α = 0.1)
- ***Qmin95*:** the lower limit of the 95 % confidence interval of ***Q*** (α = 0.05)
- ***Qmax95*:** the upper limit of the 95 % confidence interval of ***Q*** (α = 0.05)
- ***B*:** estimate of the constant ***B*** in equation "***f***(year)=***Q****(year-firstYear)+***B***" for a linear trend
- ***Bmin99*:** estimate of the constant ***Bmin99*** in equation "***f***(year)=***Qmin99****(year-firstYear)+***Bmin99***" for 99% confidence level of linear trend
- ***Bmax99*:** estimate of the constant ***Bmax99*** in equation "***f***(year)=***Qmax99****(year-firstYear)+***Bmax99***" for 99% confidence level of linear trend:
- ***Bmin95*:** estimate of the constant ***Bmin95*** in equation "***f***(year)=***Qmin95****(year-firstYear)+***Bmin95***" for 95% confidence level of a linear trend:
- ***Bmax95*:** estimate of the constant ***Bmax95*** in equation "***f***(year)=***Qmax95****(year-firstYear)+***Bmax95***" for 95% confidence level of a linear trend

A.1 Mann-Kendall Test of Total Annual Precipitation

Time series	First year	Last Year	n	Mann-Kendall trend: Test S	Test Z	Signific.	Sen's slope estimate: Q	Qmin99	Qmax99	Qmin95	Qmax95	B	Bmin99	Bmax99	Bmin95	Bmax95
Kongsedone	1960	2013	54		1.00		3.100	-6.811	11.835	-3.958	9.810	1739.90	1997.50	1500.22	1905.05	1545.44
LaoNgarm	1960	2013	54		-4.58	***	-16.919	-24.946	-8.324	-23.286	-10.615	2430.58	2639.47	2256.78	2582.58	2292.53
Pakse	1960	2013	54		-0.99		-3.367	-12.506	5.456	-10.202	3.466	2136.00	2331.16	1907.22	2272.92	1954.61
Saravan	1964	2013	50		-0.72		-3.219	-15.541	8.840	-12.744	5.613	2247.22	2514.89	1879.32	2451.38	1978.95
Selabam	1972	2013	42		0.20		1.886	-16.737	20.646	-12.192	16.676	1794.75	2401.93	1164.58	2256.06	1249.02
Nikhom 34	1980	2013	34		0.56		3.500	-16.138	22.720	-11.165	17.014	2245.50	3043.69	1558.42	2863.82	1735.15
Batieng	1990	2013	24		-1.14		-17.262	-53.243	27.267	-49.393	16.044	2952.00	4488.56	1197.54	4313.22	1614.45

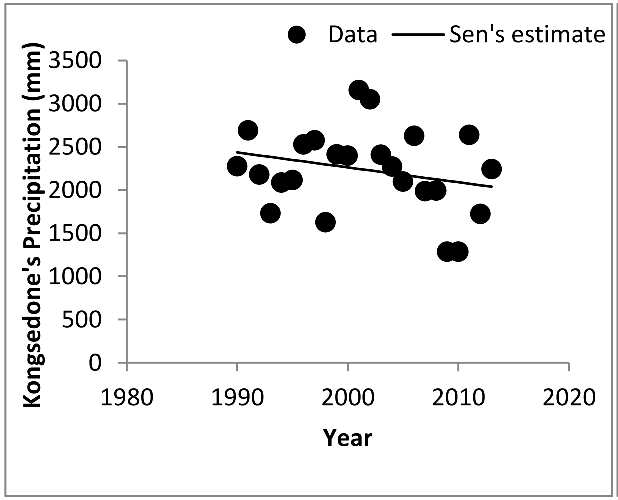

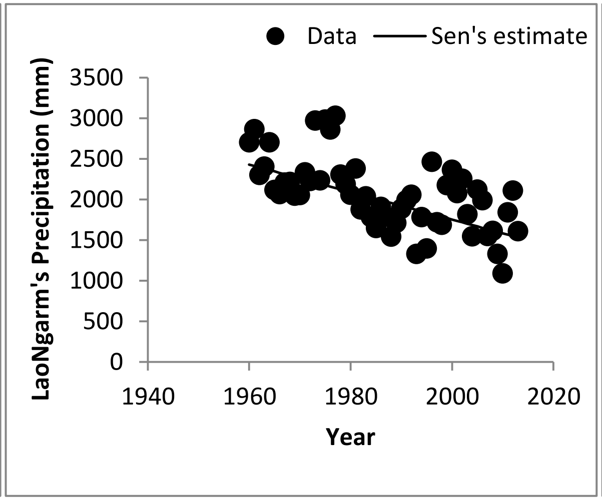

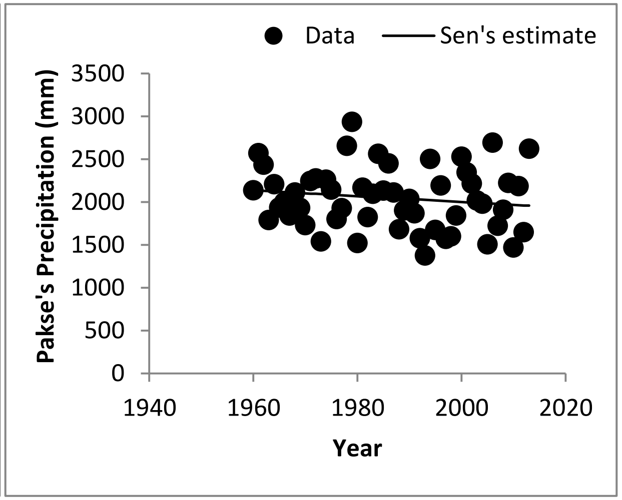

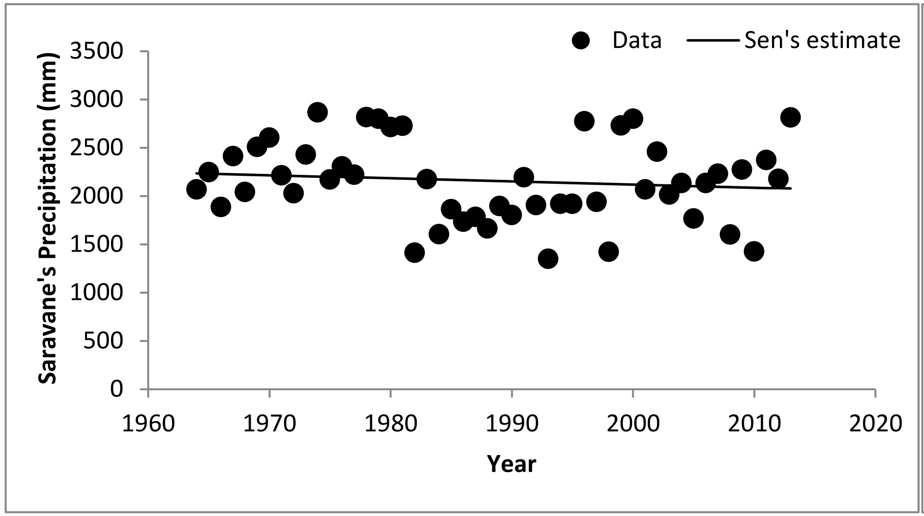
Data
Sen's estimate
Saravane's Precipitation (mm)
3500
3000
2500
2000
1500
1000
500
0
1960
1970
1980
1990
2000
2010
2020
Year

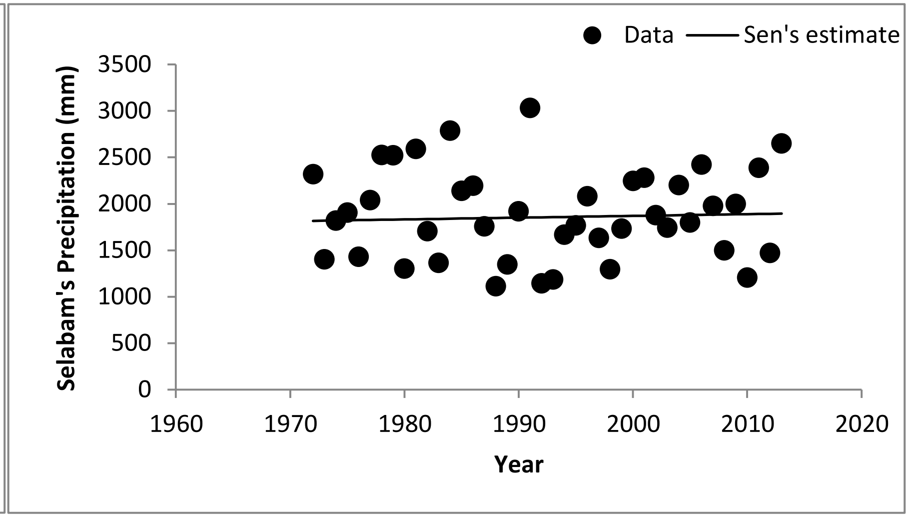
Data
Sen's estimate
Selabam's Precipitation (mm)
3500
3000
2500
2000
1500
1000
500
0
1960
1970
1980
1990
2000
2010
2020
Year

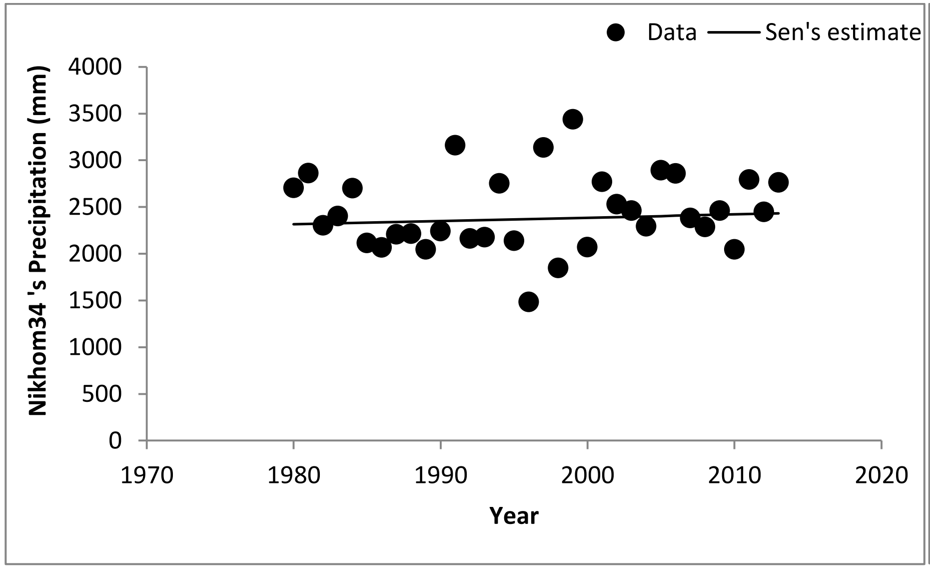
Data
Sen's estimate
Nikhom34 's Precipitation (mm)
4000
3500
3000
2500
2000
1500
1000
500
0
1970
1980
1990
2000
2010
2020
Year

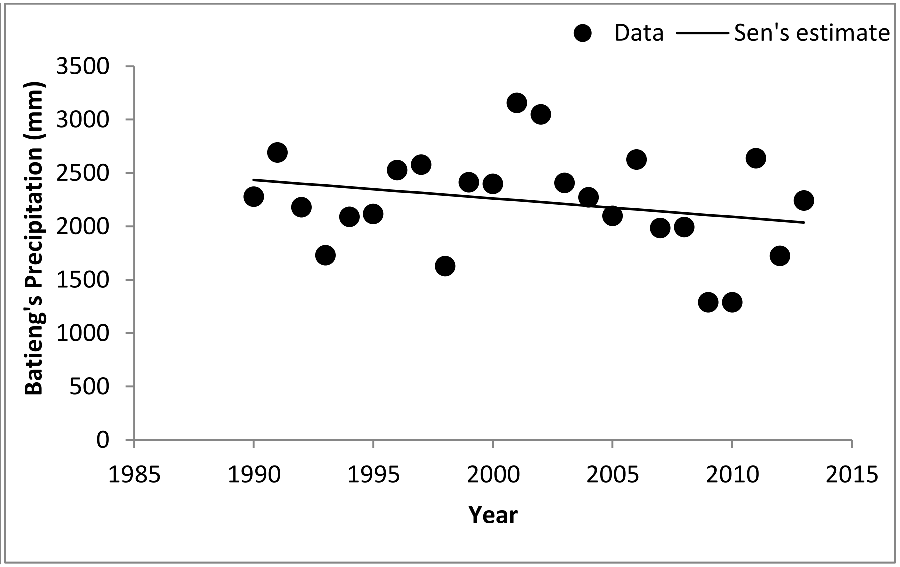
Data
Sen's estimate
Batieng's Precipitation (mm)
3500
3000
2500
2000
1500
1000
500
0
1985
1990
1995
2000
2005
2010
2015
Year

A.2 Mann-Kendall Test of Annual Maximum Daily Precipitation

Time series	First year	Last Year	n	Test S	Test Z	Signific.	Q	Qmin99	Qmax99	Qmin95	Qmax95	B	Bmin99	Bmax99	Bmin95	Bmax95
				Mann-Kendall trend			Sen's slope estimate									
Kongsedone	1960	2013	54		-1.51		-0.855	-2.386	0.538	-1.950	0.228	159.67	209.10	118.39	193.00	128.35
LaoNgarm	1960	2013	54		0.25		0.093	-1.180	1.286	-0.750	0.929	106.81	148.76	87.43	132.00	94.87
Pakse	1960	2013	54		0.01		0.000	-0.994	0.910	-0.700	0.683	111.50	139.80	87.79	130.39	94.25
Saravan	1964	2013	50		-0.08		-0.047	-1.500	1.267	-1.216	0.983	120.33	170.25	91.00	158.77	100.63
Selabam	1972	2013	42		-2.40	*	-1.333	-3.863	0.092	-3.320	-0.209	160.60	272.35	113.65	249.39	123.37
Nikhom34	1979	2013	34		0.85		0.333	-1.000	1.873	-0.614	1.360	82.33	134.50	32.36	118.92	56.72
Batieng	1990	2013	24		-1.09		-1.561	-6.063	2.783	-4.875	1.584	199.36	381.35	26.70	335.64	75.14

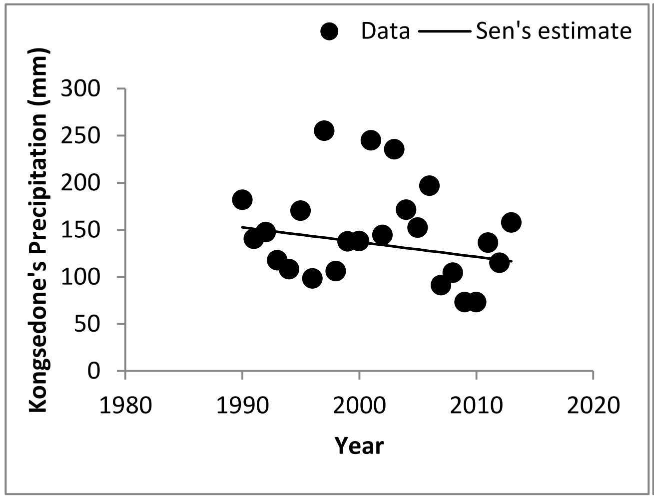

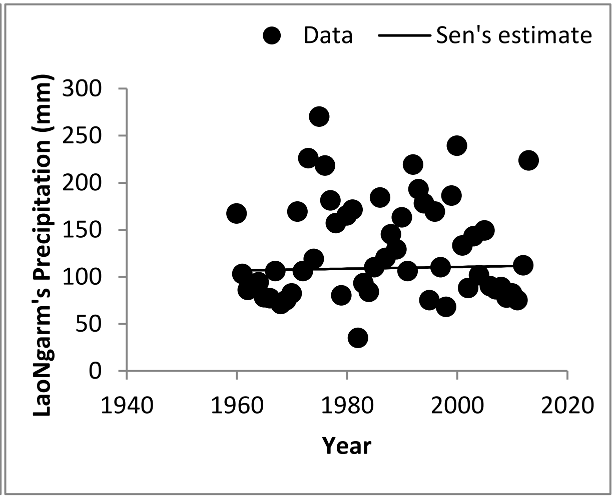

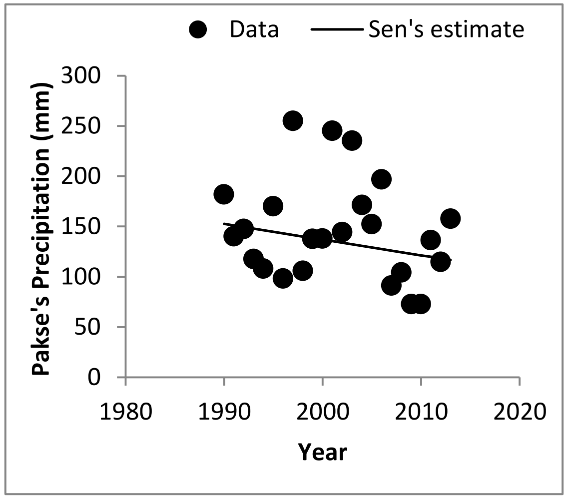

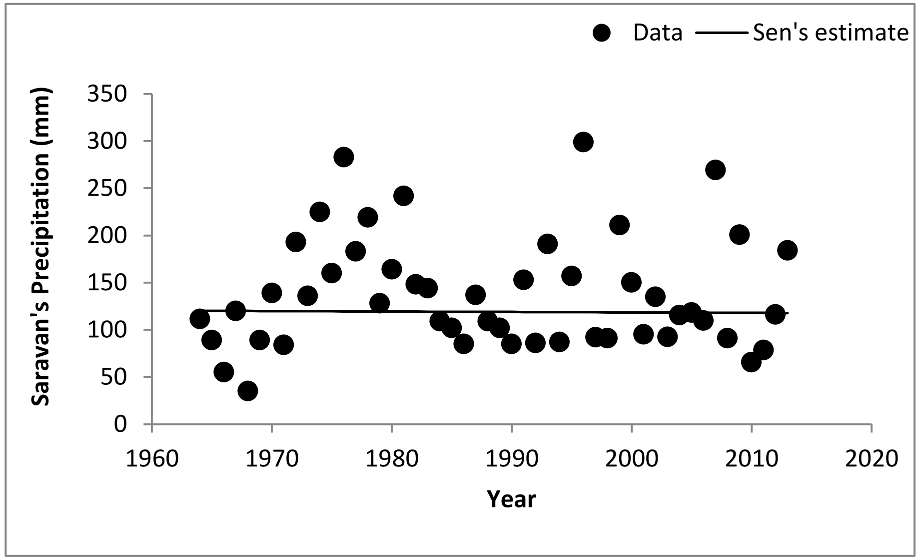
Data
Sen's estimate
Saravan's Precipitation (mm)
350
300
250
200
150
100
50
0
1960
1970
1980
1990
2000
2010
2020
Year

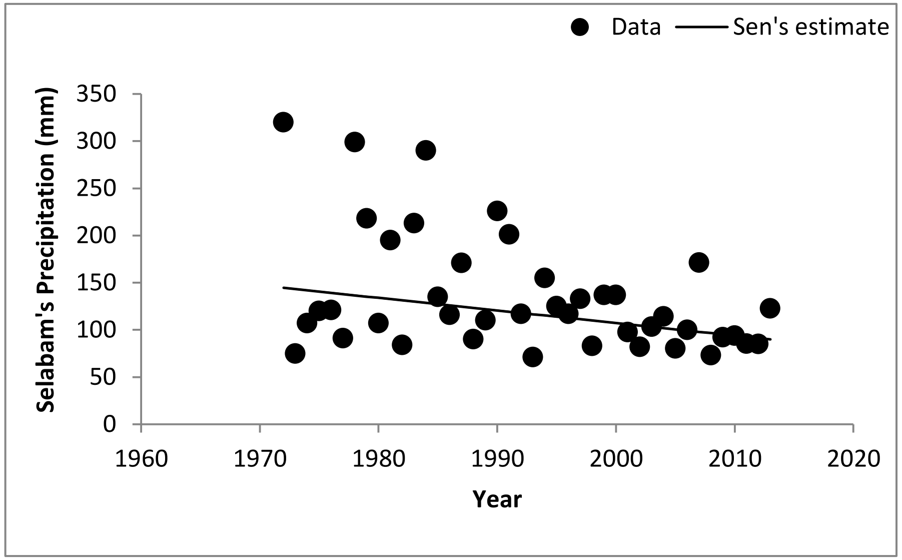
Data
Sen's estimate
Selabam's Precipitation (mm)
350
300
250
200
150
100
50
0
1960
1970
1980
1990
2000
2010
2020
Year

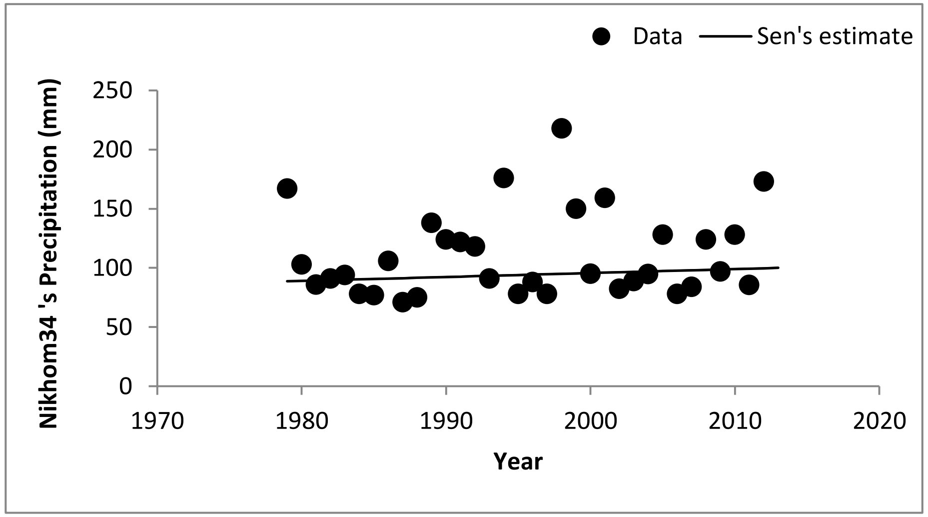
Data
Sen's estimate
Nikhom34 's Precipitation (mm)
250
200
150
100
50
0
1970
1980
1990
2000
2010
2020
Year

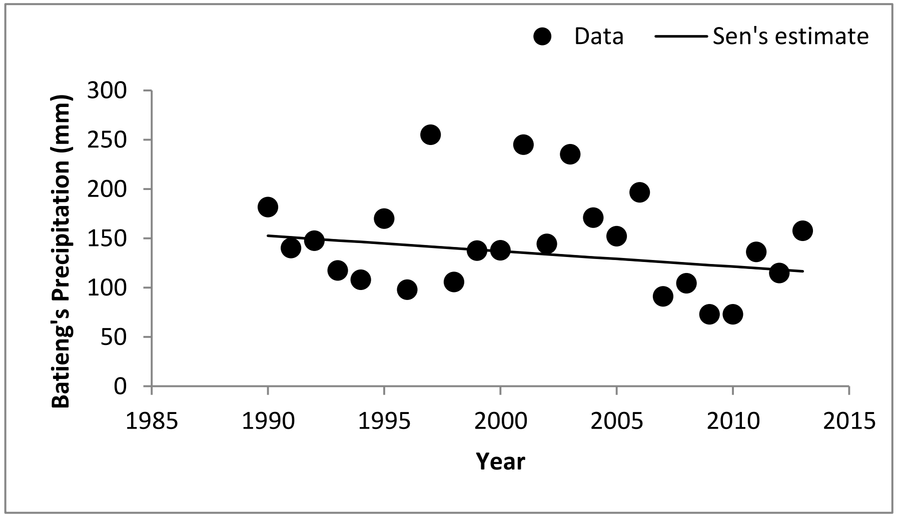
Data
Sen's estimate
Batieng's Precipitation (mm)
300
250
200
150
100
50
0
1985
1990
1995
2000
2005
2010
2015
Year

A.3 Mann-Kendall Test of Total Annual Precipitation in Rainy Season

Time series	First year	Last Year	n	Mann-Kendall trend: Test S	Test Z	Signific.	Sen's slope estimate: Q	Qmin99	Qmax99	Qmin95	Qmax95	B	Bmin99	Bmax99	Bmin95	Bmax95
Kongsedone	1960	2013	54		0.67		2.135	-6.073	11.741	-3.702	9.562	1638.73	1843.37	1342.89	1787.29	1374.18
LaoNgarm	1960	2013	54		-3.22	**	-9.525	-16.569	-2.217	-15.142	-3.677	1922.70	2081.16	1754.32	2028.21	1797.76
Pakse	1960	2013	54		-1.05		-3.875	-12.872	4.844	-10.584	2.803	1986.56	2201.40	1766.26	2155.50	1814.95
Saravan	1964	2013	50		0.69		2.566	-7.831	13.782	-4.968	10.593	1801.17	2049.95	1441.23	1987.28	1585.05
Selabam	1972	2013	42		0.23		1.400	-16.484	18.559	-12.205	15.468	1647.05	2275.22	1096.83	2136.32	1185.54
Nikhom34	1980	2013	34		0.18		1.322	-14.130	20.353	-9.065	16.622	1877.80	2399.36	1265.03	2221.12	1386.30
Batieng	1990	2013	24		-1.19		-18.365	-54.453	25.102	-50.083	15.085	2743.77	4337.32	1120.66	4161.34	1511.34

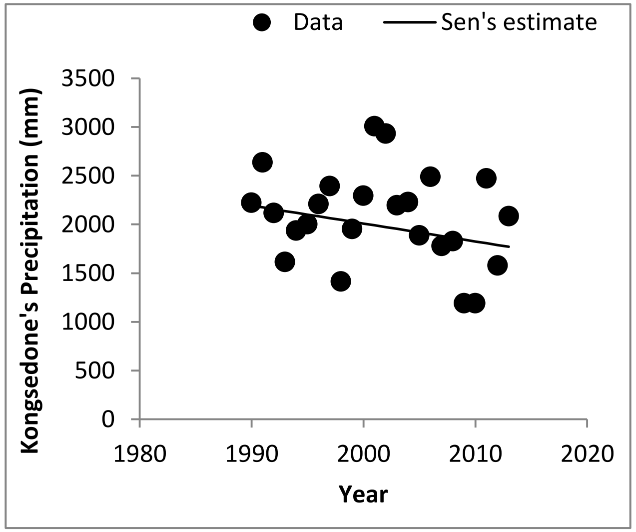

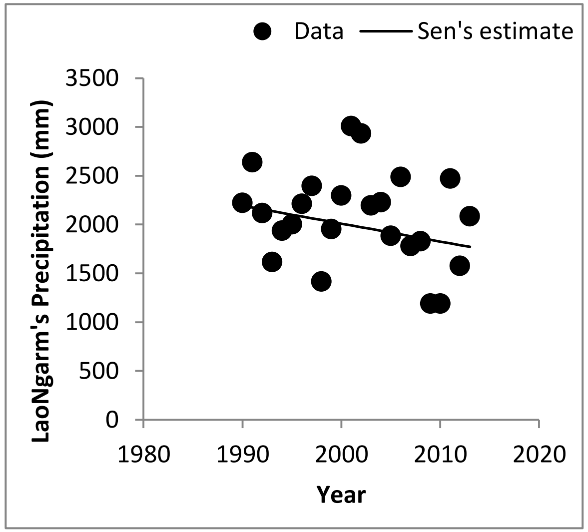

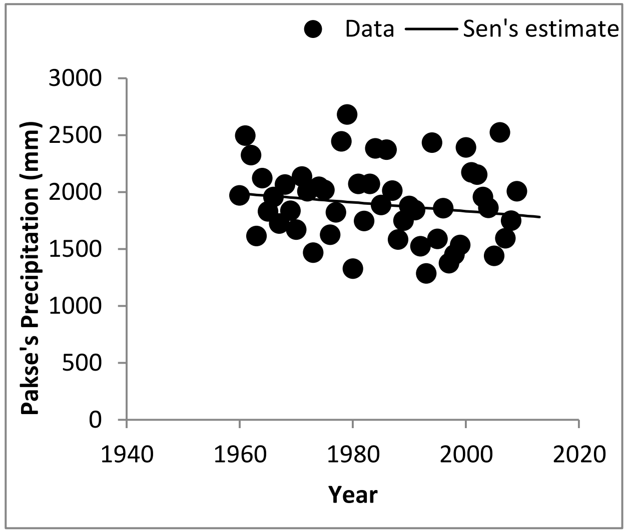

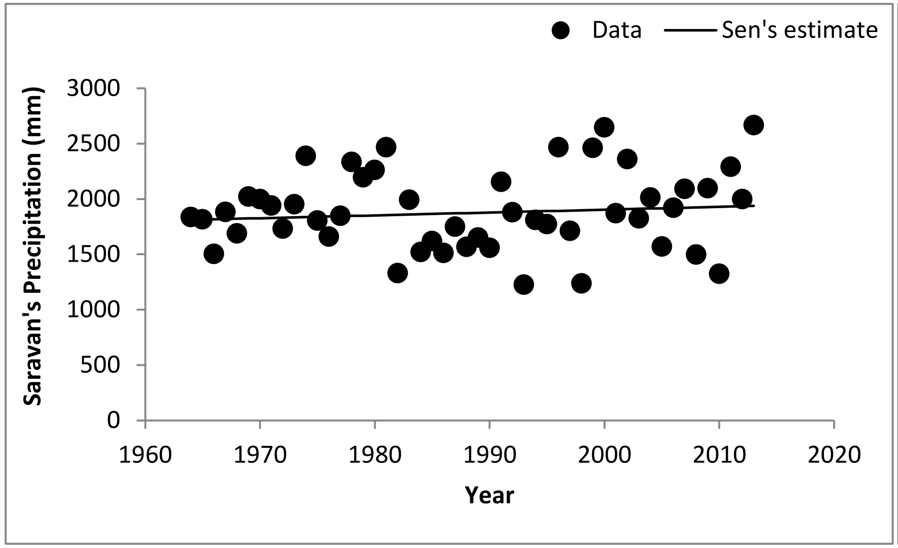
Data
Sen's estimate
Saravan's Precipitation (mm)
Year
0
500
1000
1500
2000
2500
3000
1960
1970
1980
1990
2000
2010
2020

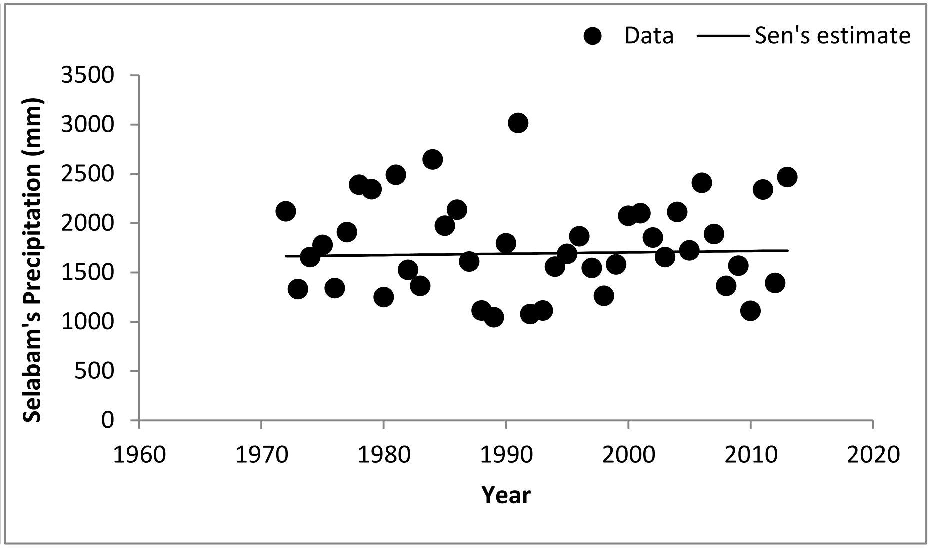
Data
Sen's estimate
Selabam's Precipitation (mm)
Year
0
500
1000
1500
2000
2500
3000
3500
1960
1970
1980
1990
2000
2010
2020

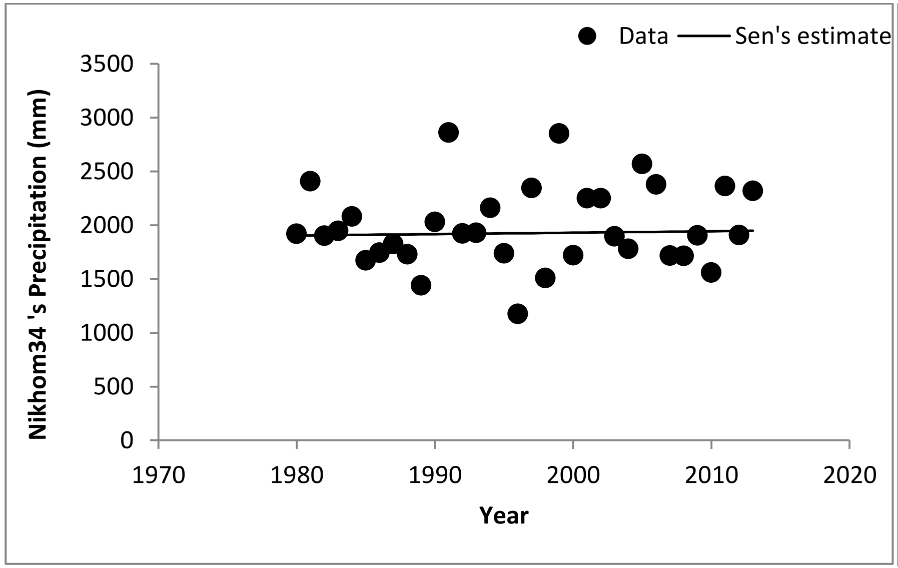
Data
Sen's estimate
Nikhom34 's Precipitation (mm)
Year
0
500
1000
1500
2000
2500
3000
3500
1970
1980
1990
2000
2010
2020

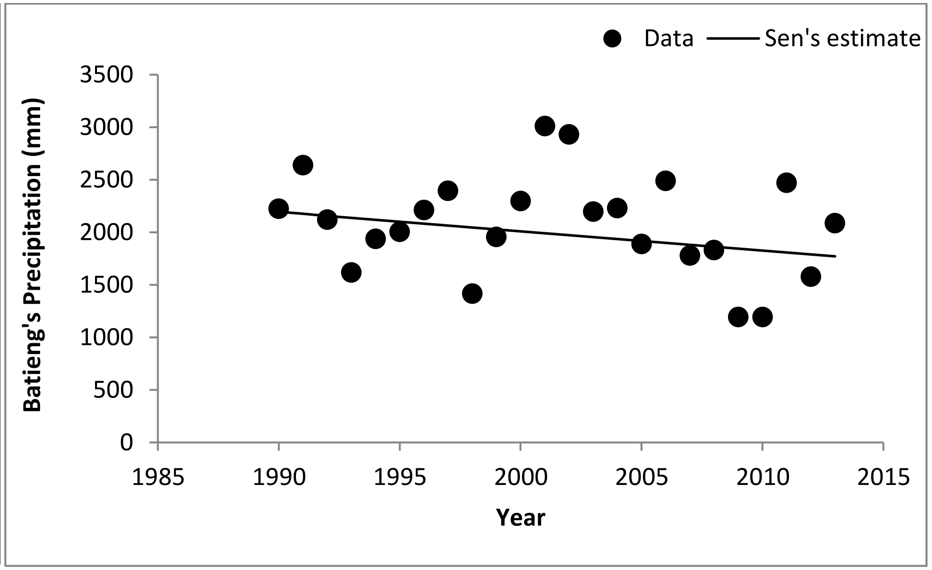
Data
Sen's estimate
Batieng's Precipitation (mm)
Year
0
500
1000
1500
2000
2500
3000
3500
1985
1990
1995
2000
2005
2010
2015

A.4 Mann-Kendall Test of Total Annual Precipitation in Dry Season

				Mann-Kendall trend			Sen's slope estimate									
Time series	**First year**	**Last Year**	**n**	**Test S**	**Test Z**	**Signific.**	**Q**	**Qmin99**	**Qmax99**	**Qmin95**	**Qmax95**	**B**	**Bmin99**	**Bmax99**	**Bmin95**	**Bmax95**
Kongsedone	1960	2013	54		0.22		0.337	-3.280	2.708	-2.425	2.338	135.57	244.65	84.26	222.83	90.29
LaoNgarm	1960	2013	54		-4.86	***	-7.600	-11.043	-4.166	-10.214	-5.186	534.20	616.50	447.74	601.89	471.40
Pakse	1960	2013	54		0.42		0.290	-1.241	1.750	-0.820	1.308	113.23	154.43	81.88	143.25	91.88
Saravane	1964	2013	50		-3.93	***	-6.719	-10.301	-2.585	-9.503	-3.578	445.41	551.18	301.56	528.06	338.08
Selabam	1972	2013	42		-0.86		-0.857	-3.500	1.914	-2.792	1.024	134.21	223.45	46.45	192.79	78.73
Nikhom34	1980	2013	34		0.06		0.371	-8.070	7.125	-6.014	5.556	450.77	755.07	217.05	708.82	275.59
Batieng	1990	2013	24		0.87		2.251	-4.800	9.174	-2.351	6.879	36.05	335.45	-235.24	233.93	-152.25

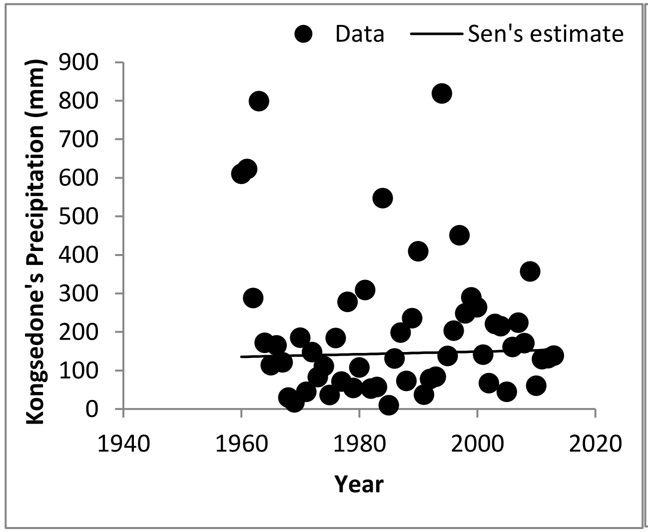

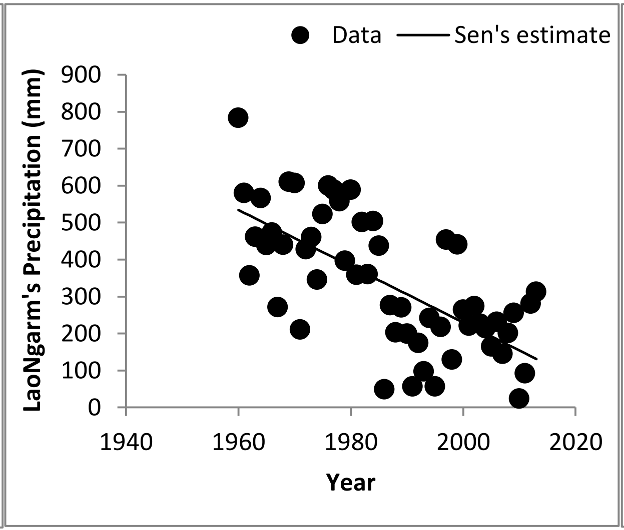

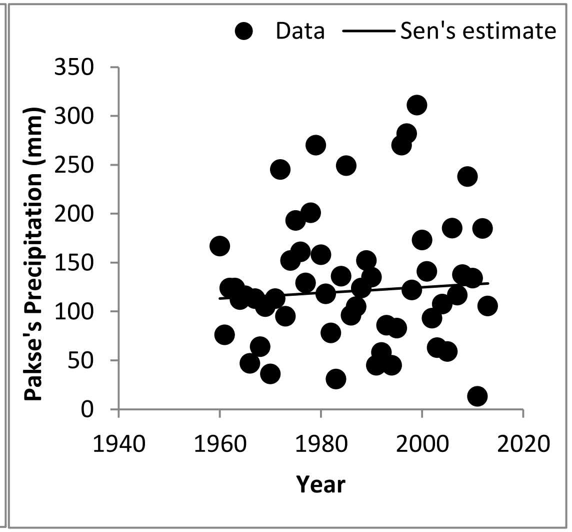

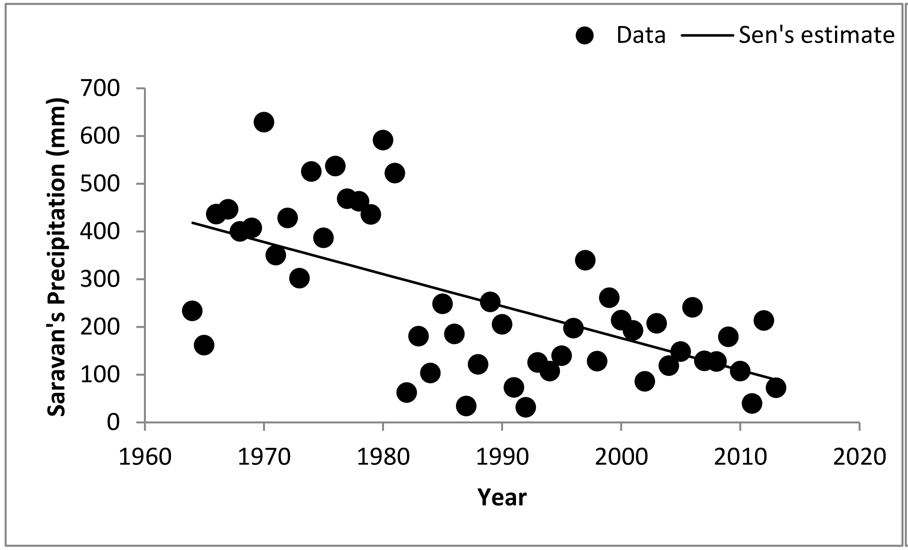
Data
Sen's estimate
Saravan's Precipitation (mm)
700
600
500
400
300
200
100
0
1960
1970
1980
1990
2000
2010
2020
Year

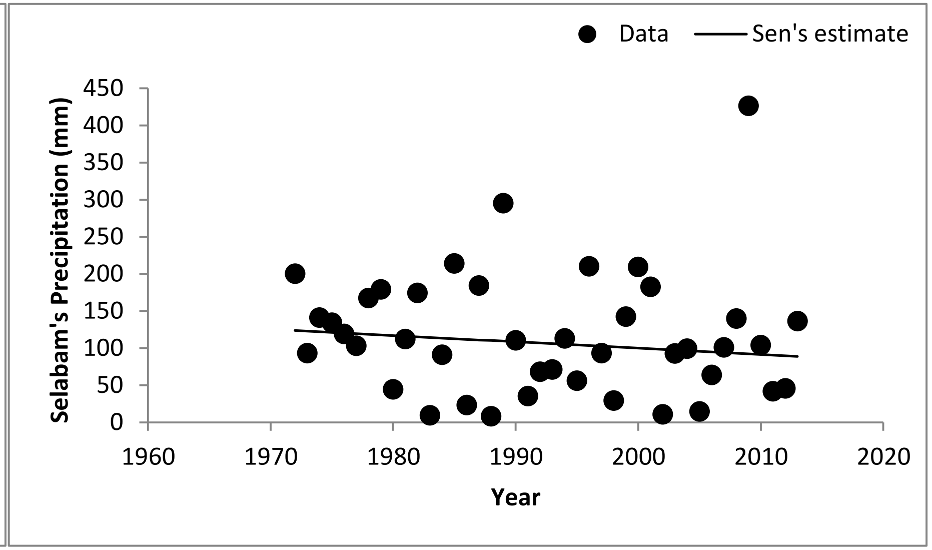
Data
Sen's estimate
Selabam's Precipitation (mm)
450
400
350
300
250
200
150
100
50
0
1960
1970
1980
1990
2000
2010
2020
Year

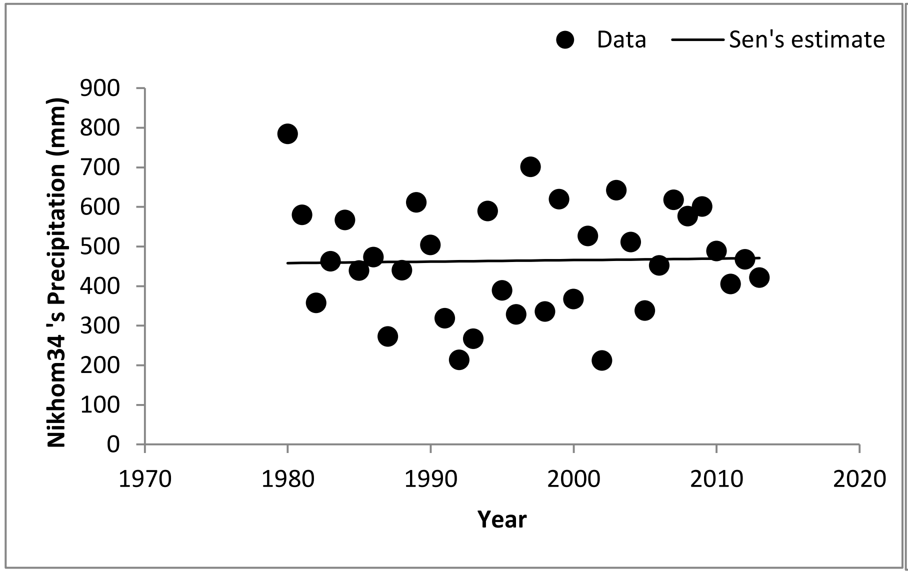
Data
Sen's estimate
Nikhom34 's Precipitation (mm)
900
800
700
600
500
400
300
200
100
0
1970
1980
1990
2000
2010
2020
Year

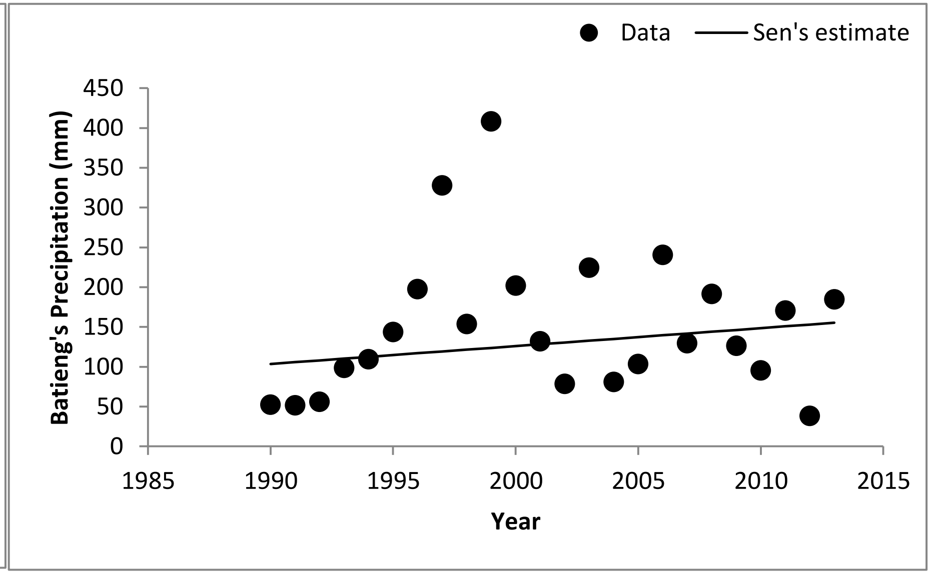
Data
Sen's estimate
Batieng's Precipitation (mm)
450
400
350
300
250
200
150
100
50
0
1985
1990
1995
2000
2005
2010
2015
Year

A.5 Mann-Kendall Test of Annual Mean Temperature

				Mann-Kendall trend			Sen's slope estimate									
Time series	First year	Last Year	n	Test S	Test Z	Signific.	Q	Qmin99	Qmax99	Qmin95	Qmax95	B	Bmin99	Bmax99	Bmin95	Bmax95
Saravanh	1990	2012	23		0.53		0.013	-0.028	0.060	-0.019	0.049	26.79	27.23	26.29	27.08	26.38
Kongsedone	1990	2012	23		0.21		0.005	-0.033	0.049	-0.024	0.039	27.29	27.68	26.81	27.62	26.95
Pakse	1990	2012	23		-2.09	*	-0.043	-0.112	0.007	-0.093	-0.002	28.70	29.60	28.03	29.37	28.16
Nikom34	1990	2012	23		0.37		0.018	-0.128	0.120	-0.096	0.098	18.95	19.98	18.03	19.76	18.18
Lao Ngarm	1990	2012	23		2.75	**	0.086	0.008	0.162	0.027	0.145	23.45	24.37	22.63	24.12	22.79
Paksong	1990	2012	23		-0.21		-0.005	-0.126	0.063	-0.078	0.047	19.29	20.78	18.69	20.18	18.84

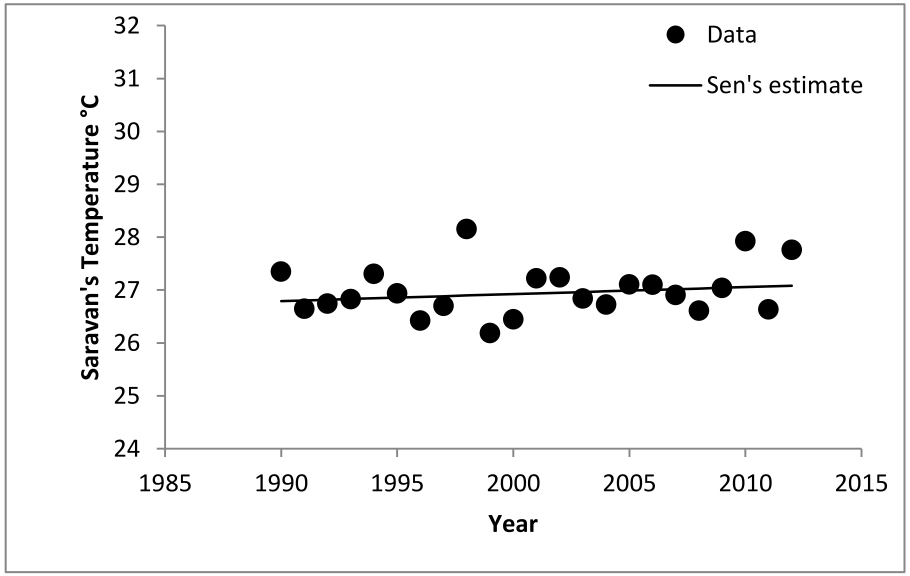

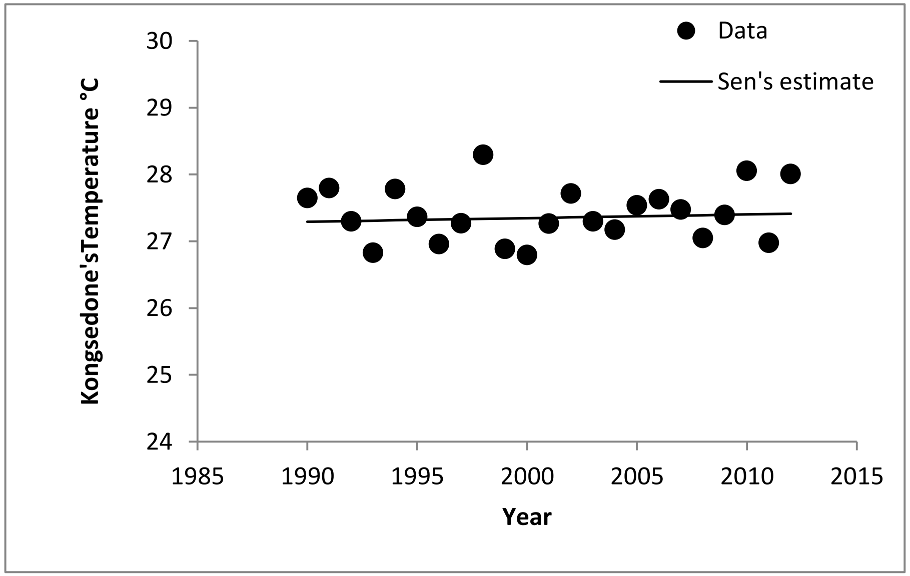

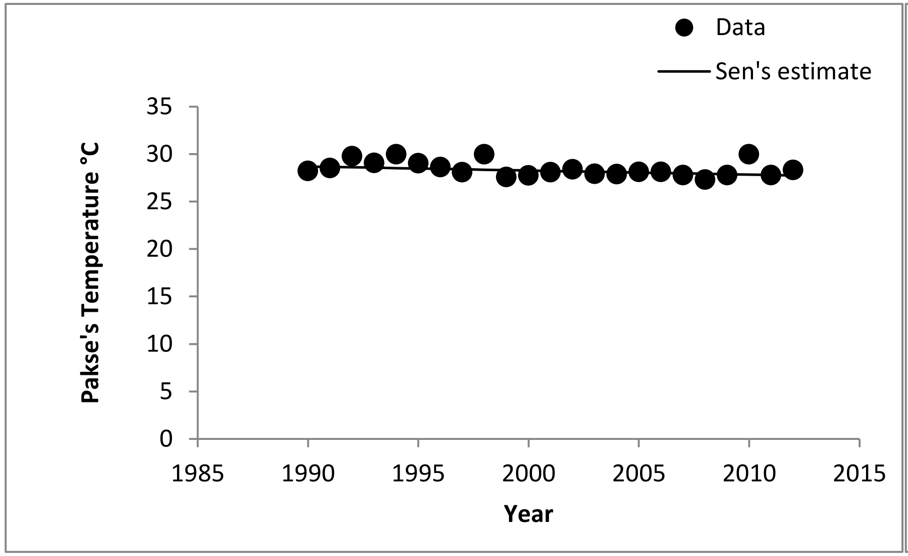
Data
Sen's estimate
35
30
25
20
15
10
5
0
Pakse's Temperature °C
1985
1990
1995
2000
2005
2010
2015
Year

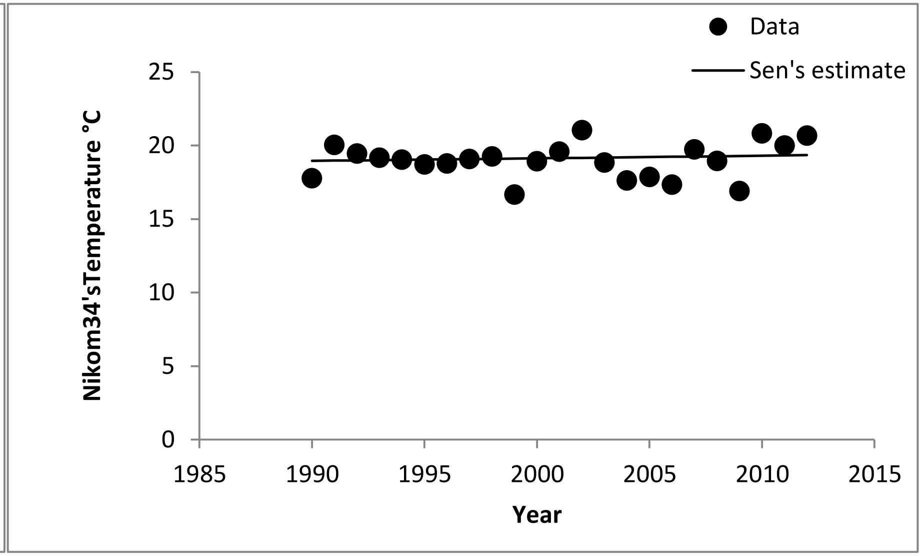
Data
Sen's estimate
25
20
15
10
5
0
Nikom34'sTemperature °C
1985
1990
1995
2000
2005
2010
2015
Year

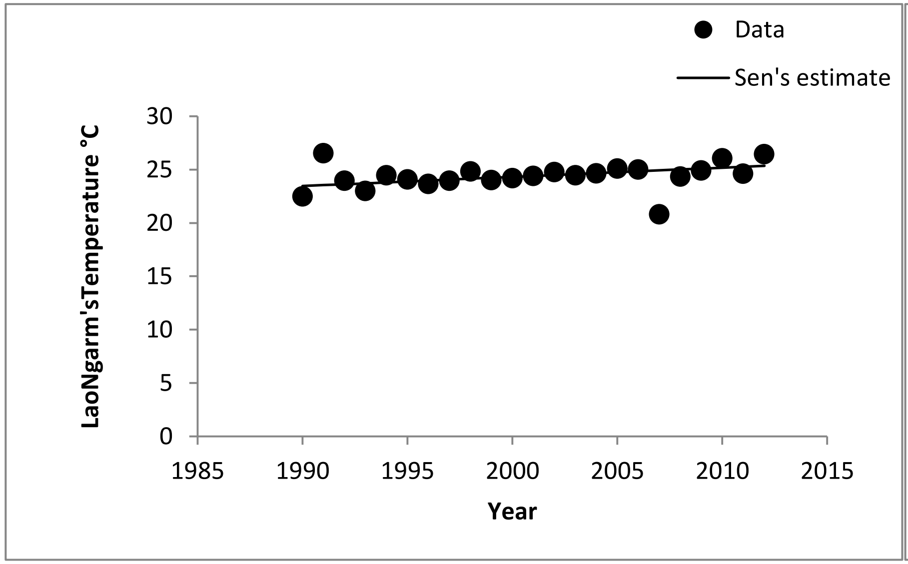
Data
Sen's estimate
30
25
20
15
10
5
0
LaoNgarm'sTemperature °C
1985
1990
1995
2000
2005
2010
2015
Year

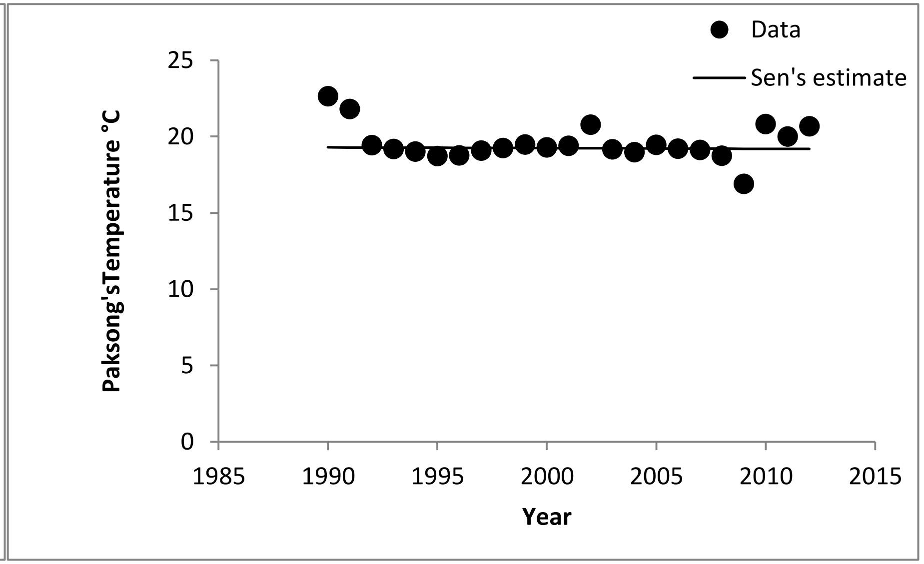
Data
Sen's estimate
25
20
15
10
5
0
Paksong'sTemperature °C
1985
1990
1995
2000
2005
2010
2015
Year

A.6 Mann-Kendall Test of Annual Daily Maximum Temperature

Time series	First year	Last Year	n	Test S	Test Z	Signific.	Q	Qmin99	Qmax99	Qmin95	Qmax95	B	Bmin99	Bmax99	Bmin95	Bmax95
				Mann-Kendall trend			Sen's slope estimate									
Saravan	1990	2012	23		-1.67	+	-0.052	-0.135	0.020	-0.110	0.001	39.33	40.27	38.98	40.19	39.00
Kongsedone	1990	2012	23		-3.21	**	-0.120	-0.211	-0.033	-0.183	-0.055	40.04	41.01	38.86	40.51	39.10
Pakse	1990	2012	23		-3.48	***	-0.333	-0.515	-0.005	-0.500	-0.127	45.00	46.28	40.06	46.00	41.52
Nikom34	1990	2012	23		2.35	*	0.056	0.000	0.135	0.000	0.116	29.06	29.70	28.43	29.70	28.65
Lao Ngarm	1990	2012	23		-1.84	+	-0.100	-0.200	0.016	-0.167	0.000	36.60	37.80	35.67	37.33	35.80
Paksong	1990	2012	23		-0.50		-0.027	-0.136	0.111	-0.100	0.067	29.61	30.69	28.22	30.30	28.53

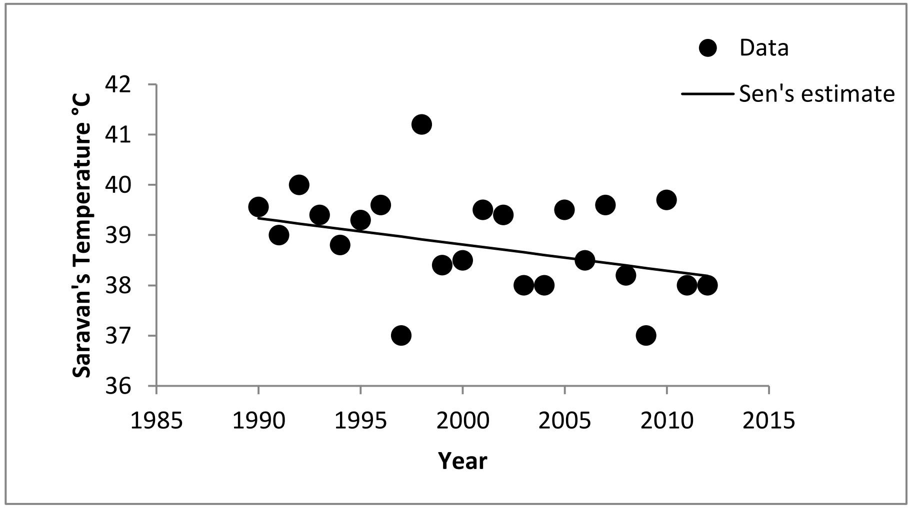

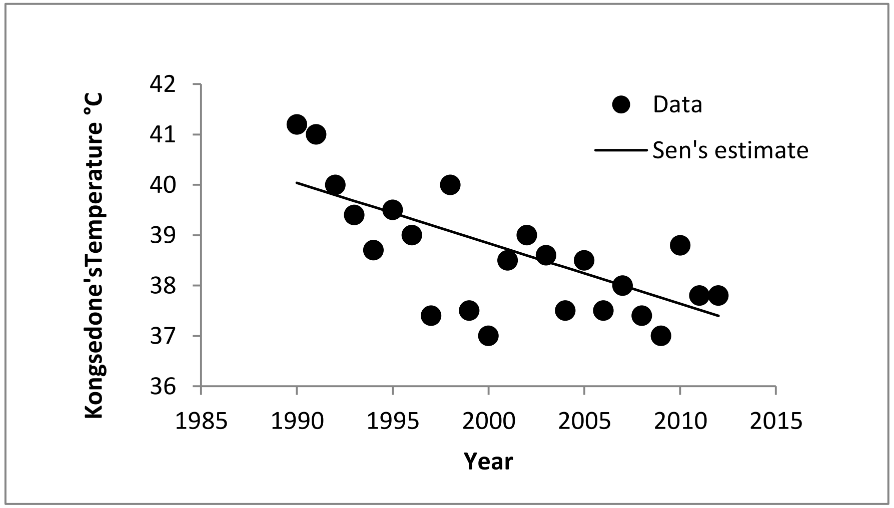

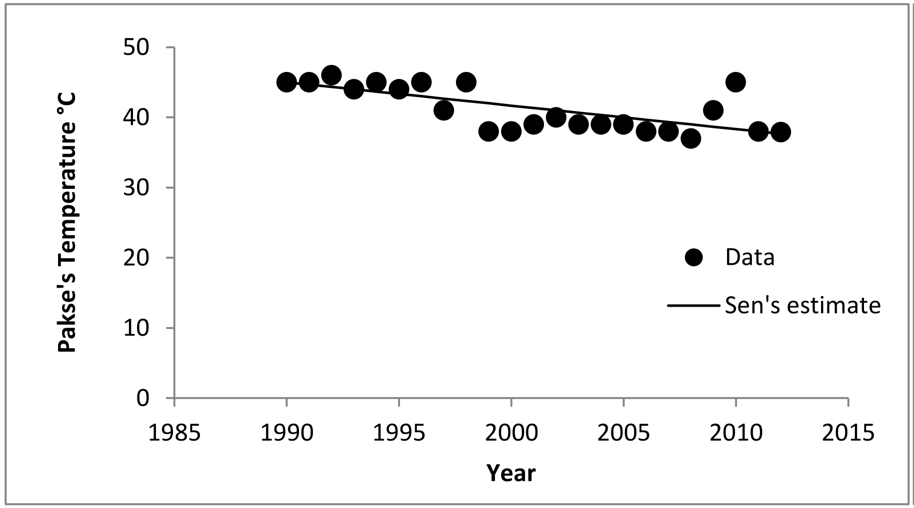
Pakse's Temperature °C
Year
Data
Sen's estimate

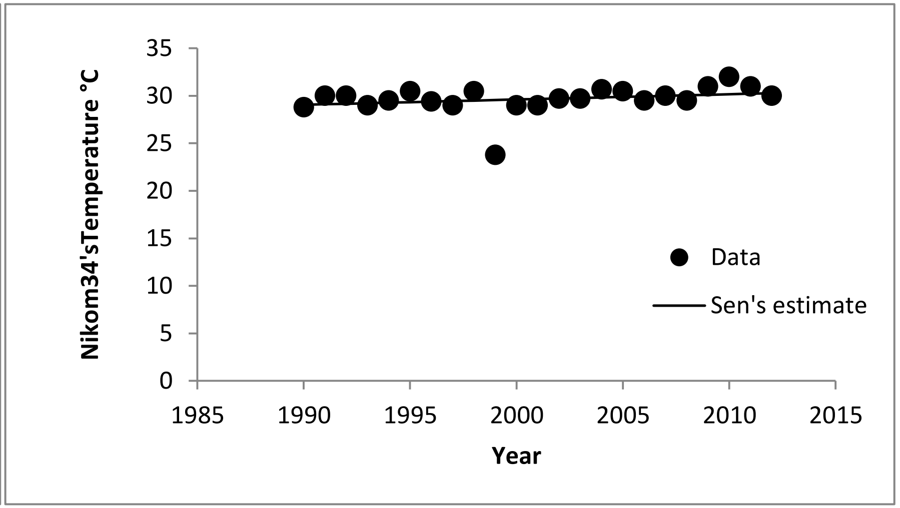
Nikom34'sTemperature °C
Year
Data
Sen's estimate

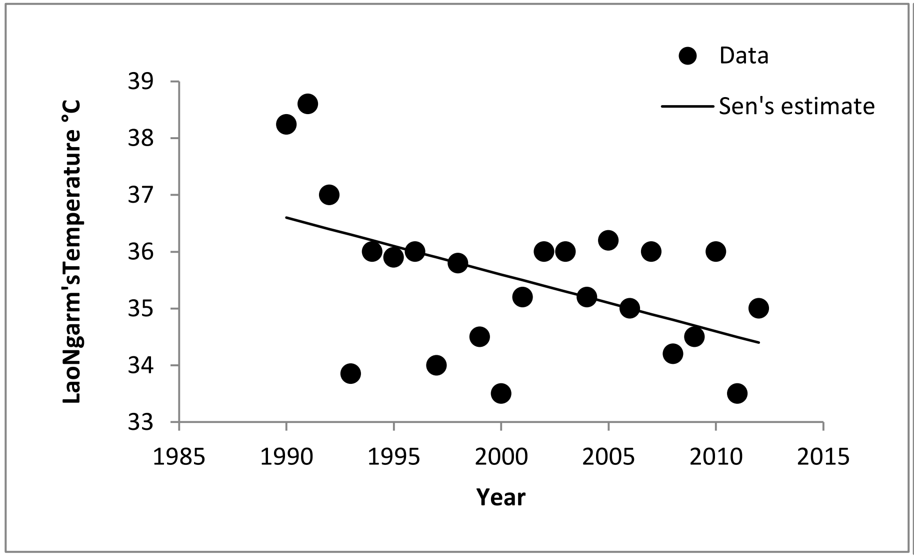
LaoNgarm'sTemperature °C
Year
Data
Sen's estimate

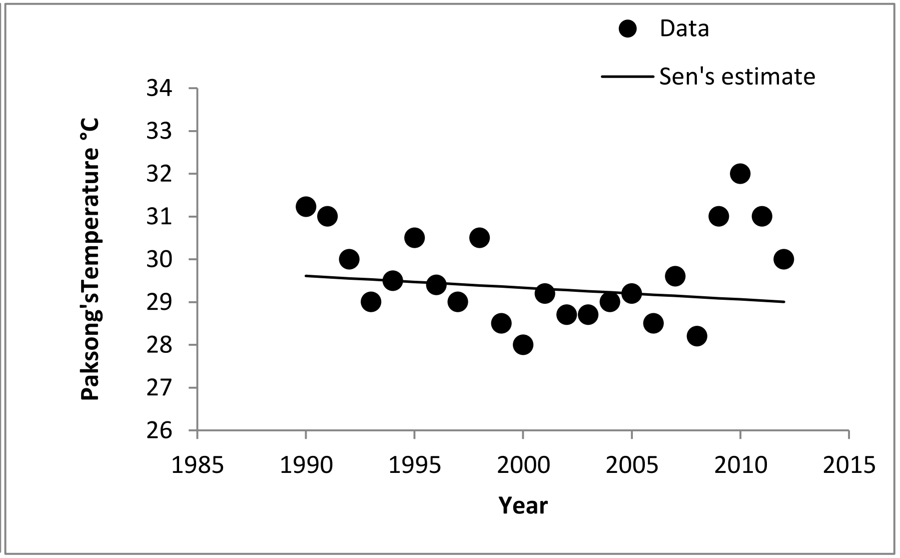
Paksong'sTemperature °C
Year
Data
Sen's estimate

A.7 Mann-Kendall Test of Annual Daily Minimum Temperature

Time series	First year	Last Year	n	Test S (Mann-Kendall trend)	Test Z	Signific.	Q (Sen's slope estimate)	Qmin99	Qmax99	Qmin95	Qmax95	B	Bmin99	Bmax99	Bmin95	Bmax95
Saravan	1990	2012	23		2.04	*	0.119	-0.022	0.250	0.000	0.200	9.63	11.00	8.25	10.80	8.80
Kongsedone	1990	2012	23		1.82	+	0.125	-0.054	0.310	-0.016	0.265	10.75	12.42	8.48	12.11	9.06
Pakse	1990	2012	23		2.60	**	0.063	0.000	0.143	0.000	0.116	13.81	15.00	12.71	15.00	13.03
Nikom34	1990	2012	23		1.10		0.036	-0.042	0.180	-0.010	0.136	0.36	1.19	-0.80	0.59	-0.41
Lao Ngarm	1990	2012	23		2.81	**	0.179	0.000	0.350	0.074	0.285	7.82	10.00	5.89	9.11	7.01
Paksong	1990	2012	23		1.93	+	0.122	-0.041	0.300	0.000	0.252	0.68	2.50	-1.10	1.80	-0.73

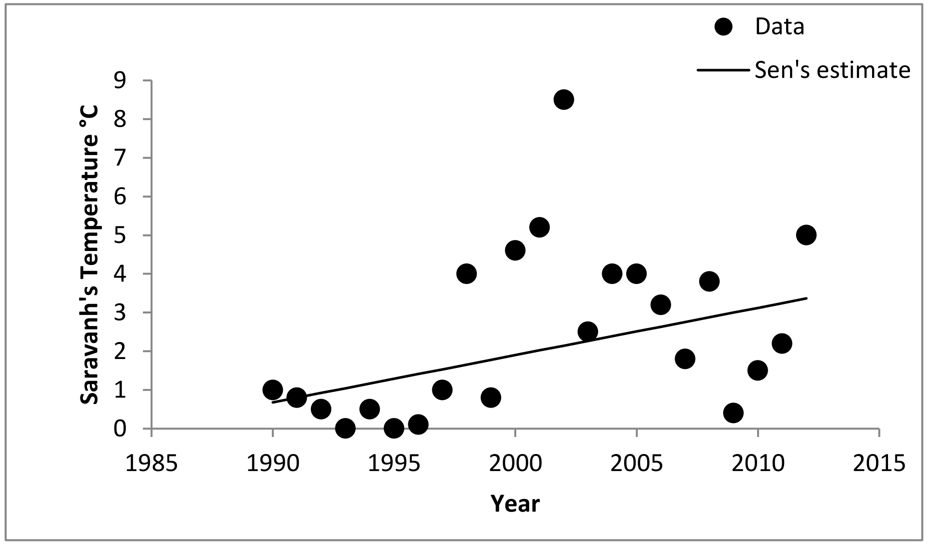

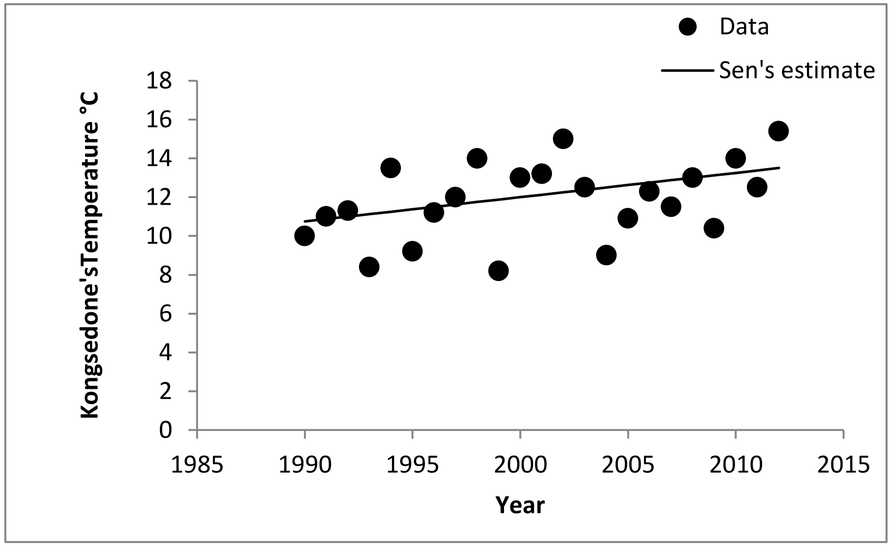

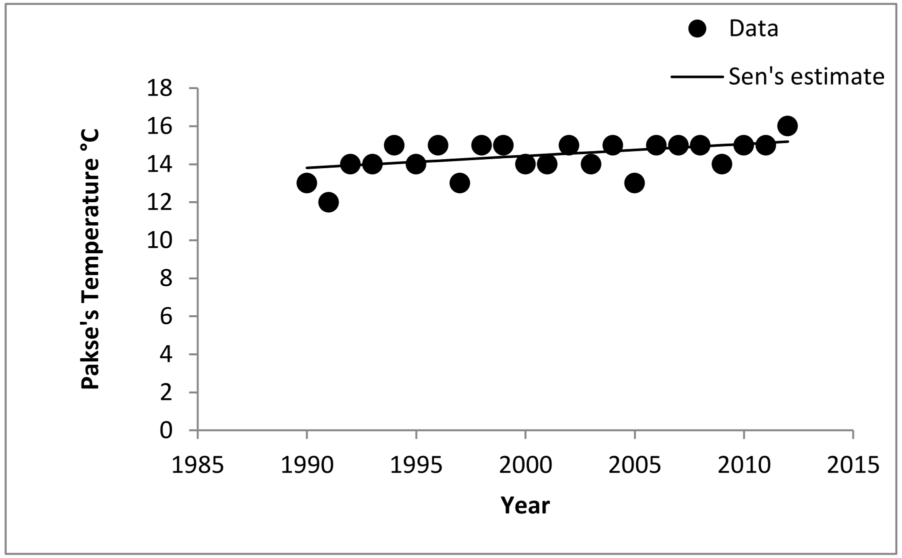
Data
Sen's estimate
Pakse's Temperature °C
Year
18
16
14
12
10
8
6
4
2
0
1985
1990
1995
2000
2005
2010
2015

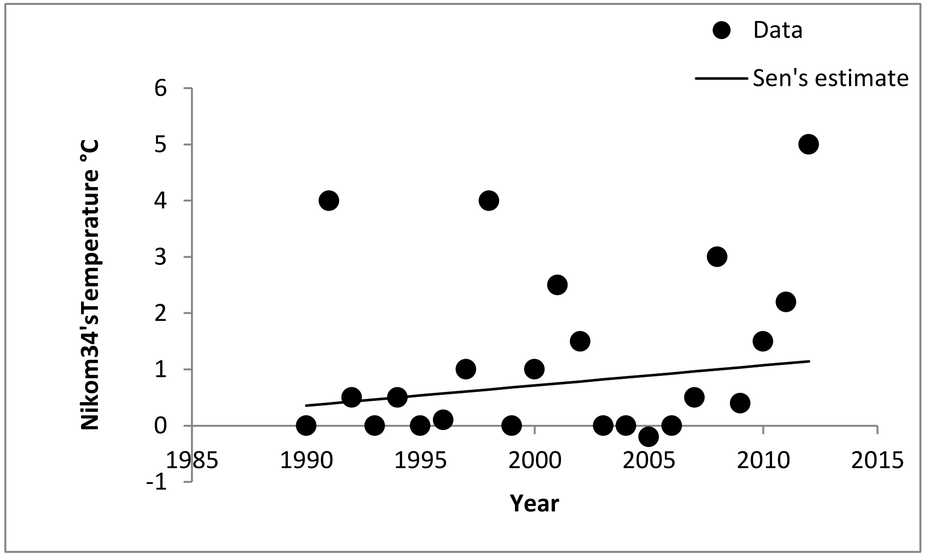
Data
Sen's estimate
Nikom34'sTemperature °C
Year
6
5
4
3
2
1
0
-1
1985
1990
1995
2000
2005
2010
2015

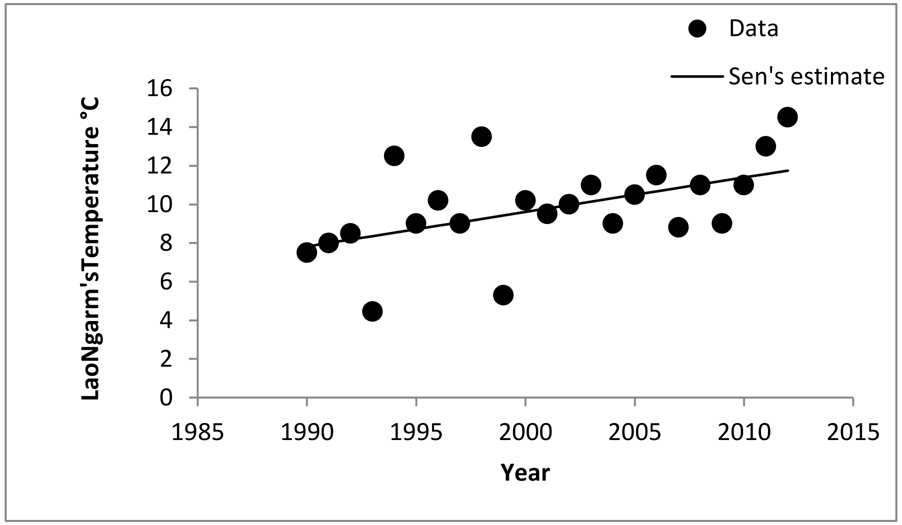
Data
Sen's estimate
LaoNgarm'sTemperature °C
Year
16
14
12
10
8
6
4
2
0
1985
1990
1995
2000
2005
2010
2015

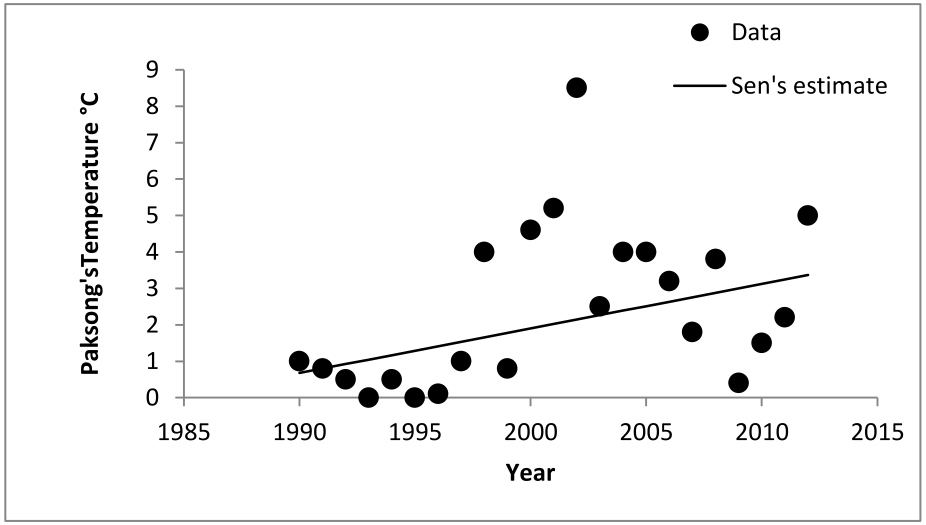
Data
Sen's estimate
Paksong'sTemperature °C
Year
9
8
7
6
5
4
3
2
1
0
1985
1990
1995
2000
2005
2010
2015